UNIVERSIDADE ESTADUAL DE CAMPINAS

INSTITUTO DE BIOLOGIA

DANIEL CARLOS FERREIRA LANZA

A proteína FEZ1: pouca organização estrutural, atividades associadas a elementos do citoesqueleto e formação do fenótipo "flower like"

Tese apresentada ao Instituto de Biologia para obtenção do Título de Doutor em Biologia Funcional e Molecular, na área de Bioquímica.

Orientador: Prof. Dr. Jörg Kobarg

Campinas 2009

FICHA CATALOGRÁFICA ELABORADA PELA
BIBLIOTECA DO INSTITUTO DE BIOLOGIA – UNICAMP

L297p

Lanza, Daniel Carlos Ferreira
A proteína FEZ1: pouca organização estrutural, atividades associadas a elementos do citoesqueleto e formação do fenótipo "flower like" / Daniel Carlos Ferreira Lanza. – Campinas, SP: [s.n.], 2009.

Orientador: Jörg Kobarg.
Tese (doutorado) – Universidade Estadual de Campinas, Instituto de Biologia.

1. Proteína intrinsicamente desenovelada. 2. Microtúbulos. 3. Leucemia. 4. Neurônios. 5. Fasciculação. I. Kobarg, Jörg. II. Universidade Estadual de Campinas. Instituto de Biologia. III. Título.

(rcdt/ib)

Título em inglês: FEZ1 protein: little organizational structure, activities related to elements of the cytoskeleton and generation of the "flower like" phenotype.
Palavras-chave em inglês: Intrinsically unfolded protein; Microtubules; Leukemia; Neurons; Fasciculation.
Área de concentração: Bioquímica.
Titulação: Doutor em Biologia Funcional e Molecular.
Banca examinadora: Jörg Kobarg, Kleber Gomes Franchini, Cláudio Chrysostomo Werneck, Marcelo Damário Gomes, Henning Ulrich.
Data da defesa: 27/08/2009.
Programa de Pós-Graduação: Biologia Funcional e Molecular.

Campinas, 27 de agosto de 2009

BANCA EXAMINADORA

Prof. Dr. Jörg Kobarg (Orientador) — Assinatura

Prof. Dr. Kleber Gomes Franchini — Assinatura

Prof. Dr. Claudio Chrysostomo Werneck — Assinatura

Prof. Dr. Marcelo Damário Gomes — Assinatura

Prof. Dr. Alexander Henning Ulrich — Assinatura

Prof. Dr. Celso Eduardo Benedetti — Assinatura

Prof. Dr. Mario Tyago Murakami — Assinatura

Profa. Dra. Adriana Franco Paes Leme — Assinatura

Não são as respostas que movem o mundo;
são as perguntas**.**

(Frase que eu ouvi na TV)

ÍNDICE

Dedico este trabalho

Aos meus amados pais

Maria José Tôrres Ferreira Lanza e Geraldo Carlos Moreira Lanza,

A minha e amada irmã

Karina Ferreira Lanza,

A minha amada esposa

Luciana Nunes Menolli Lanza.

Agradecimentos

Acredito que não devo agradecer aqui apenas aos que me ajudaram diretamente no desenvolvimento dos resultados científicos obtidos durante o meu doutorado. Claro que estes não são menos importantes, entretanto afirmo que estipular uma ordem de prioridade ou de significância para cada um é impossível.

O que seria de mim sem a "Lu querida" minha esposa, me dando apoio incondicional em todos os momentos? Estamos construindo nossa vida juntos e estou certo de que ela é imprescindível em todas as vitórias que estamos conquistando.

O que seria de mim sem a minha família? Muito obrigado à minha mãe, ao meu pai e à minha irmã, que entendem e apóiam em minhas decisões, às vezes inusitadas, como a de ficar a 700Km de casa por 7,5 anos para estudar (até agora), e me perdoam por ter que sacrificar muitos momentos em família em prol da minha formação. Agradeço aos meus tios, primos, e a meus queridos avós Maria José e José Justino, com os quais sempre pude contar. Espero que essa conquista seja uma pequena retribuição a todos.

O que seria de mim sem a ajuda do prezado orientador Dr. Jörg Kobarg? Sou muito grato pela oportunidade de integrar o seu grupo, além do apoio, ensinamentos e paciência durante todo o desenvolvimento do nosso trabalho, principalmente quando cheguei a Campinas. Agradecimento especial pela liberdade proporcionada para execução de idéias e dedicação em me ensinar a escrever artigos científicos. Não posso deixar de agradecê-lo também de forma especial por corrigir o meu inglês, e especialmente por me ensinar a administrar as emoções ao responder as cartas dos revisores. Esses ensinamentos serão importantíssimos para minha vida profissional.

O que seria de mim sem o amigo Dr. Gustavo Bressan? Nos meus primeiros anos em Campinas, sua ajuda foi essencial tanto em relação a minha moradia na república quanto no desenvolvimento de experimentos no laboratório. Muito obrigado meu caro, espero poder retribuir.

O que seria de mim sem os grandes companheiros de grupo, que me ajudaram no laboratório e fora dele? Muito obrigado a Gabriela, Daniel M.T., Marcos, Marcos S., Dr. Alexandre, Marcel, Kaliandra, Jéssica, Priscila Z. e é claro, à Maria Eugênia, uma pessoa muito importante para todos nós, e para o perfeito funcionamento do nosso grupo.

Agradeço muito ao Dr. Julio Silva e Dra. Iris Torriani, excelentes colaboradores que me ajudaram muito nos experimentos de SAXS.

Agradeço aos grandes companheiros Carlos Paier, José Jadsom, Luiz Gustavo e Tiago Antônio pelas inestimáveis conversas e convivência.

Agradeço muito ao Dr. José Andrés Yunes e seu grupo, pela ajuda em idéias e pelas horas extras de trabalho durante a execução de experimentos no Hospital Infantil Boldrini.

Agradeço ao, Dr. Nilson Zanchin, Dr. Celso Benedetti e Dr. João Alexandre Barbosa pela disponibilidade em me ajudar sempre que necessário. É claro que esse agradecimento e extensível a todos os componentes dos grupos dos referidos pesquisadores.

Agradeço ao grupo do Dr. Henning Ulrich da USP pela excelente recepção e ajuda em experimentos com células P19.

Não posso me esquecer de agradecer a todo *staff* técnico do CEBIME em especial à Adriana, Tereza, Givanil e Veruska que sempre se disponibilizaram a me ajudar, nos mais inusitados "acontecimentos" durante a execução dos experimentos.

E como não poderia deixar de ser, agradeço a todo suporte oferecido pelo LNLS e pela Unicamp, e ao suporte financeiro da FAPESP e do CNPq sem os quais seria impossível o desenvolvimento desse trabalho.

Lista de Abreviações

aPKC - Atypical Protein Kinase C (Proteína Cinase C Atípica)

ATLL - Acute T-Cell Leukemia Limphoma (Leucemia Aguda de Células T)

ATRA - All Trans Retinoic Acid (Ácido Retinóico All-trans)

BBS4 - Bardet- Biedl Syndrome Protein 4 (Proteína Vinculada a Síndrome Bardet-Biel)

BSA - Bovine Serum Albumin (Albumina do Soro Bovino)

CLASP1 - Clip Associated Protein 1 (Proteína Associada a Clip)

CLIPs - Cytoplasmic Linker Proteins

cPKC – Classical Protein Kinase C (Proteína Cinase C Clássica)

GABA - Aminobutyric Acid (Ácido Aminobutírico)

GAD67 - Glutamic Acid Descaboxylase (Descaboxilase do Ácido Glutâmico)

GST - Glutatione S Transferase (Glutationa S Transferase)

HIV - Human Immunodeficiency virus (Vírus da Imunodeficiência Humana)

HSN - Hermaphrodite Specific Neuron (Neurônio Hermafrodita Específico)

IL1 - Interleukin 1 (Interleucina 1)

JCV - John Cunningham Virus (Vírus John Cunningham)

JIP1 - c-Jun N-terminal kinase-interacting protein 1

JNK - c-Jun N-terminal kinase

KDa - Kilodalton

KHC - Kinesin High Chain (Cadeia pesada da Kinesina)

KLC - Kinesin Light Chain (Cadeia leve da Kinesina)

LB - Luria Bertani Medium (Meio Luria Bertani)

LIS1 - Human Lissencephaly protein (Proteína do Lisencéfalo Humano)

MAGE - Melanome Antigen Family

MAPK - Mitogen Activated Protein Kinase (Proteína Cinase Ativada por Mitógeno)

mg – Milligram (Miligrama)

MLV - Moloney Murine Leukemia Viruses

mRNA - Messenger RNA (RNA mensageiro)

MTOCS - Microtubule Organization Centers (Centros de Organização de Microtúbulos)

NFκB - Nuclear Factor Kappa B (Fator Nuclear Kappa B)

ng - Nanogram (Nanograma)

NGF - Nerve Growth Factor (Fator de crescimento neuronal)

NIMA - Never in Mitosis Gene A

nPKC - Novel PKC (Proteína Quinase C Nova)

NUDEL - Nuclear Distribution Element-like

PCR - Polimerase Chain Reaction (Reação em Cadeia da Polimerase)

PML - Progressive Multifocal Leucoencephalopaty (Leucoencefalopatia Multifocal Progressiva)

PWS - Prader Willi Syndrome (Síndrome de Prader Willi)

SDS - Sodium Dodecyl Sulfate (Dodecil Sulfato de Sódio)

SDS PAGE - SDS Polyacrilamide gel electrophoresis

SNARE - N-ethylmaleimide Sensitive Fusion Attachment Protein Receptor

SV40 - Simian Virus 40

TIRFM - Total Internal Reflection Fluorescence Microscopy

TNFα - Tumor Necrosis Factor Alpha (Fator Alfa de Necrose Tumoral)

UNC - Uncoordinated

µg - Microgram (Micrograma)

OBS: Os significados de outras abreviações estão apresentados na tabela 1.

RESUMO

A proteína FEZ1 foi caracterizada inicialmente como um ortólogo da proteína UNC76 de *C. elegans,* responsável pelo desenvolvimento e fasciculação neuronal nesse verme. Estudos subsequentes demonstraram sua atuação em processos de desenvolvimento neuronal, polarização celular, mecanismos de transporte associado à kinesinas e transporte de vesículas e mitocôndrias. Outros trabalhos demonstraram que a superexpressão de FEZ1 interfere no ciclo de vida de alguns tipos de vírus como HIV e JCV. FEZ1 é capaz de interagir com mais de 51 proteínas diferentes, e participa em muitos processos celulares. Observamos que FEZ1 apresenta ausência de estrutura molecular rígida, sendo pertencente à classe das *natively unfolded proteins*, e é capaz de formar dímeros em solução. Essa observação condiz com sua extrema capacidade de interagir com muitas proteínas diferentes. A capacidade de FEZ1 interagir com outras proteínas é influenciada pela fosforilação da sua região C-terminal por diferentes isoformas de PKC. FEZ1 interage e colocaliza com NEK1 e com CLASP2 em células de mamífero, em uma região candidata ao centrossomo. Essas interações são dependentes da região *coiled-coil* presente na parte C-terminal de FEZ1, e ocorrem em regiões *coiled-coil* de CLASP2 e NEK1. A interação com CLASP2 é rompida quando FEZ1 é fosforilada por PKC. A superexpressão de FEZ1 causa o fenótipo *flower like* observado em células de alguns tipos de leucemia. Nós observamos que FEZ1 interage e colocaliza com α e γ-tubulinas e que a formação desse fenótipo em células HEK293 ocorre devido a uma alteração na organização dos microtúbulos causada pelo excesso de FEZ1. A formação do fenótipo *flower like* é influenciada por ativação das vias de PKC e PI3K. Os dados obtidos durante o nosso trabalho indicam que FEZ1 é uma proteína intrinsecamente desenovelada, que atua em processos celulares associados ao citoesqueleto e centrossomo em conjunto com NEK1 e CLASP2, e que defeitos em sua regulação, possivelmente pelas vias de PKC ou PI3K, causam alteração da organização dos microtúbulos originando núcleos *flower like*.

ABSTRACT

FEZ1 was identified first as a orthologue of *C elegans* UNC-76 protein, that plays functions related to neuronal development in this worm. Subsequent studies, shows FEZ1 functions in neuronal development process, cell polarization, transport mechanisms associated to kinesins and vesicular and mitochondrial transports. Other works showed that FEZ1 super-expression interfere in the life cycle of some viral types such as HIV and JCV. FEZ1 is able to interact with more than 51 different proteins and participates in several cellular processes. We observed that FEZ1 has a mobile molecular structure, is a member of the natively unfolded protein class, and can form dimers in solution. This observation is in agreement with its capacity to interact with a large number of different proteins. The capacity of FEZ1 to interact with other proteins is influenced by different PKC isoforms phosphorylation in its C-terminal region. FEZ1 interacts and co-localizes with NEK1 and CLASP2 in a centrossomal candidate region of mammalian cells. These interactions are dependent of a coiled coil inside the C-terminal region of FEZ1, and occur in dependence of coiled coil regions of NEK1 and CLASP2. The interaction between FEZ1 and CLASP2 is abolished after FEZ1 phosphorylation by PKC. The FEZ1 over-expression causes the flower like phenotype observed in cells of some leukemias. We observed that FEZ1 interacts and co-localizes with α and γ-tubulins and that the phenotype formation in HEK293 cells is mediated by an atypical organization of microtubule spindles, caused by over-expression of FEZ1. The flower like phenotype formation is influenced by activation of PKC and PI3K pathways. The data generated by our work indicate that FEZ1 is an intrinsically unfolded protein, that works in cellular processes associated to the cytoskeleton in conjunct with NEK1 and CLASP2, and that defects in its regulation, maybe via the PKC or PI3K pathways, causes alterations in microtubule organization and formation of the “flower like” nuclei.

1- INTRODUÇÃO

1.1 - A proteína UNC76

Durante o seu desenvolvimento, os axônios do sistema nervoso central percorrem ambientes extracelulares variados até atingir a região final aonde desempenharão sua função principal [1]. Muitos axônios crescem associados a outros axônios formando os fascículos, fenômeno denominado fasciculação, fundamental para o desenvolvimento do sistema nervoso. *Screenings* genéticos em mutantes de *Caenohabiditis elegans* defectivos para fasciculação revelaram mutações em três genes, agrupados como genes UNC (*Uncoordinated*), que são: UNC34, UNC71 e UNC76 [2]. Entre mutantes com defeitos de fasciculação específicos, os mutantes UNC76 apresentam as anormalidades mais severas em locomoção e desenvolvimento do HSN (*Hermaphrodite Specific Neuron*) [3,4].

Três grupos de sequências humanas similares à sequência de UNC76 foram identificados e a família de proteínas relacionadas à UNC76 recebeu o nome FEZ (*Fasciculation and Elongation protein/zygin*) [2,5]. Os dois primeiros genes identificados na família foram denominados FEZ1 e FEZ2 [2]. A proteína FEZ1 apresenta 392 aminoácidos, três regiões *poly-glu* em sua região N-terminal, e um domínio *coiled-coil* predito em sua porção C-terminal.

Em outra abordagem, foi observado que UNC76 interage com Kinesina [6]. No mesmo trabalho, ensaios de imunofluorescência e análises genéticas demonstraram que a proteína UNC76 é fundamental em eventos de transporte axonal no sistema nervoso de *Drosophila*.

Os resultados desses trabalhos pioneiros associam UNC76 ao sistema nervoso e a mecanismos de transporte associado a proteínas motoras, apesar de não fornecerem subsídios para definir se UNC76 atua como reguladora ou adaptadora de cargas transportadas por kinesinas. A primeira isoforma da família das Kinesinas foi caracterizada no axoplasma de lulas, como uma proteína que causava o movimento de vesículas por um mecanismo dependente de ATP ao longo dos microtúbulos; atualmente essa é a família de proteínas motoras mais conhecida, amplamente relatada em trabalhos e revisões bibliográficas [7,8].

1.2 - FEZ1 no desenvolvimento do sistema nervoso

Inferências de que FEZ1 atua basicamente no sistema nervoso foram reforçadas por resultados que associam FEZ1 às proteínas DISC1 (*Disrupted in Schizophrenia Gene 1*) [9,10] e

PKCζ (*Protein Kinase C Zeta*) [11], durante a diferenciação neuronal e desenvolvimento do sistema nervoso.

Foi demonstrado que FEZ1 é substrato e interage com a região regulatória da PKCζ. O mRNA da PKCζ é abundante em cérebros, e PKCζ juntamente a outras aPKCs participa em processos de polarização celular associada a proteínas do complexo ternário PAR3 e PAR6, e de vias de ativação da NFκB (*Nuclear Factor Kappa B*), a partir da sinalização pelos receptores de TNFα (*Tumor Necrosis Factor Alpha*) IL1 (*Interleukin 1*) e NGF (*Nerve Growth Factor*) [12-16]. A inibição da fosforilação de FEZ1 pelo inibidor Staurosporina causa a retenção de FEZ1 na membrana plasmática em células COS-7. A importância desse mecanismo de regulação foi demonstrada pela co-expressão de FEZ1 e PKCζ, que aumentou em ~48% a taxa de diferenciação de células PC12 em neurônios. A taxa de diferenciação se mantém em ~18% quando PKCζ é expressa sozinha [11].

FEZ1 interage e colocaliza com a região C-terminal de DISC1 em cones de crescimento de neurônios hipocampais, em um complexo associado a F-actina [9]. Foi demonstrado que o desenvolvimento dos neuritos é aumentado pela superexpressão de DISC1 em células PC12, e que a interação entre DISC1 e FEZ1 é regulada positivamente na diferenciação neuronal [9]. O mRNA de FEZ1 é preferencialmente expresso no bulbo olfatório em neurônios corticais e hipocampais. Este mesmo padrão de expressão foi observado para o mRNA de DISC1 durante o desenvolvimento de ratos do período pré-natal até o nascimento [10].

A idéia de que FEZ1 atua no desenvolvimento inicial do sistema nervoso foi reforçada a partir de análises recentes, que mostram essa proteína expressa predominantemente no sistema nervoso central de camundongos [17]. O pico de expressão ocorre 10 dias após o nascimento, declinando gradualmente a partir desse ponto, sendo mantido até 5 meses de idade. FEZ1 foi observada em conjuntos de neurônios de várias regiões do cérebro incluindo o hipocampo, neocortex, *putamen-caudatus* e *núcleus accumbens*. Em todos os neurônios que continham FEZ1 também foi observada a presença da proteína GAD67 (*Glutamic Acid Descaboxylase*), enzima responsável pela síntese do neurotransmissor inibitório GABA (*Aminobutyric Acid*), indicando que FEZ1 é expressa predominantemente em neurônios inibitórios GABAérgicos [17].

1.3 - FEZ1, microtúbulos e mecanismos de transporte

O transporte axonal a longas distâncias via citoesqueleto, é essencial para o desenvolvimento e função neuronais. Em interações regulatórias, componentes individuais do citoesqueleto afetam ou controlam cascatas de sinalização, processo que é auxiliado por filamentos de actina que geralmente estão fisicamente ligados a microtúbulos [18-20]. Os microtúbulos são guiados até a periferia das células neuronais, crescendo associados aos feixes de actina no cone de crescimento [21]. Interações estruturais entre microtúbulos e filamentos de actina podem ser mediadas por diferentes classes de proteínas, incluindo proteínas motoras e complexos motores, além de proteínas convencionais associadas aos microtúbulos [22,23].

CLASP2 (*Clip Associated Protein 2*) interagiu com a região C-terminal de FEZ1 em um screening de duplo híbrido em levedura [24]. CLASPs e CLIPs (*Cytoplasmic Linker Proteins*) assim como outras proteínas *Tip*, são encontradas nas extremidades dos microtúbulos, e são fundamentais para mediar às interações envolvendo elementos do citoesqueleto no cone de crescimento neuronal [25]. As funções de CLASP2 e outras proteínas *Tip* como CLASP1 e E4B (UFD2A-*Ubiquitin Fusion Degradation Pathway 2a*) que interagem com ela, estão diretamente relacionadas à estabilização e regulação de feixes de microtúbulos durante a divisão e desenvolvimento celular, assim como de nucleação em MTOCs (*Microtubule Organization Centers*) [26-28]. CLASP2 interage com F-actina, e imagens TIRFM (*Total Internal Reflection Fluorescence Microscopy*) mostraram a movimentação retrógrada de CLASP2 associada à Actina em lamelipódios de fibroblastos embrionários de *Xenopus* [29].

A atuação de proteínas motoras como a Kinesina-1 é fundamental no tráfego de vesículas, moléculas e mitocôndrias para extremidades dos neuritos crescentes [8, 30]. Os mecanismos coordenadores da ligação de proteínas carga específicas às kinesinas, que convertem as Kinesinas a uma conformação ativa para o transporte direcionado a um compartimento celular [31], ainda não são plenamente conhecidos. Um padrão geral que rege a ligação de kinesinas às cargas se baseia na participação de proteínas adaptadoras (*scaffold proteins*) que podem se ligar diretamente a Kinesinas [32]. No caso da Kinesina-1 (chamada também de Kif5), a KLC (*Kinesin Light Chain*) se liga diretamente a JIP1 (*c-Jun N-terminal kinase–interacting protein 1*), JIP2 e JIP3/Syd que atuam como *scaffold proteins* [33-35]. JIPs são moléculas adaptadoras para sinalização que se ligam a JNK (*c-Jun N-terminal kinase*), a muitas MAPKs (*Mitogen Activated Protein kinase*) e também a KLC, mediando o transporte intracelular [36]. Já foi observado que

somente a ligação de JIP1 sozinha, não é suficiente para ativar Kinesina-1 e que FEZ1 e JIP1 atuam de forma cooperativa para ativação da Kinesina-1 *in vitro* e em células vivas [35]. No mesmo trabalho foi demonstrada a interação de FEZ1 com KHC. Mutantes de FEZ1 sem a região C-terminal, não são capazes de ativar a Kinesina-1 indicando a importância da região C-terminal de FEZ1 no desempenho dessa função.

Em *Drosophila* e *C. elegans*, mutantes para UNC-76/FEZ1 mostraram defeitos no transporte molecular, e resultados similares foram observados também em mutantes para Kinesina-1 no mesmo sistema [2,6]. A ligação de FEZ1 sozinha foi insuficiente para permitir a ligação de KHC aos microtúbulos, entretanto a recomposição do complexo, com a ligação de JIP1/KLC e de FEZ1/KHC atuando juntas, permitem que KHC se ligue a microtúbulos [35, 41].

A interação de FEZ1 com KIF3A e KIF3B, membros da famíla da kinesina 2, foi observada a partir de experimentos de imunoprecipitação [37,38]. KIF3A forma um heterodímero KIF3A/3B que apresenta atividade de deslizamento direcionada para a extremidade *plus* dos microtúbulos, dependente de ATP para o transporte anterógrado rápido em células altamente polarizadas [8, 39, 40]. KIF3A participa ativamente no tráfego de vesículas e de outros complexos protéicos, principalmente em células com morfologia altamente polarizada como células neuronais e ciliadas.

A supressão da expressão de FEZ1 por RNAi inibiu a polarização e a formação do axônio em neurônios hipocampais de rato [41]. A redução da expressão de FEZ1 também reduz a taxa do transporte anterógrado das mitocôndrias para o axônio, e altera a morfologia das mitocôndrias, que passam a se apresentar de forma mais alongada na ausência de FEZ1 [41].

Existem evidências de que FEZ1 também interage com β e γ tubulinas *in vivo* [38, 42] e ensaios de co-sedimentação com tubulina recombinante confirmaram sua interação direta com α-tubulina polimerizada, *in vitro* [37]. FEZ1 colocaliza com γ-tubulina em associação com as proteínas Necdin, MAGEL2 (*MAGE Like Protein 2*) e BBS4 (*Bardet-Biedl syndrome protein 4*) [42, 49]. Necdin e MAGEL2 são dois de quatro genes que estão inativados de forma individual na síndrome de Prader Willi (PWS) [50]. BBS4 é conhecida por transportar a proteína adaptadora PCM1 dos satélites centrossomais através de interações com dineína, permitindo a formação dos centros de organização dos microtúbulos [43].

Necdin atua na diferenciação e crescimento de neuritos em células PC12 estimuladas por NGF, e regula o desenvolvimento de neurônios liberadores de gonadotrofina [44, 45]. A presença

de Necdin e MAGEL2 diminui a degradação proteassômica de FEZ1 e FEZ2 [42]. FEZ1 e Necdin colocalizam em uma região pericentrossomal, coincidente com a localização do complexo formado pelas proteínas dineína, LIS1(*Human Lissencephaly Protein*), NUDEL (*Nuclear Distribution Element-like*), e DISC1 associadas ao transporte por Kinesina-1 [42-46]. Esses resultados suportam a hipótese de que a regulação positiva de Necdin/MAGEL2 em neurônios estabiliza FEZ1, que por sua vez atua junto ao citoesqueleto a partir do centrossomo, mediando à nucleação de centros de organização de microtúbulos e o transporte por kinesina.

FEZ1 interage com muitas proteínas relacionadas ao desenvolvimento neuronal e mecanismos de transporte, e sua capacidade multifuncional será discutida adiante. A FIGURA1 representa uma síntese do que já foi descrito sob o aspecto funcional de FEZ1, atuando em conjunto a elementos do citoesqueleto, elementos nucleares e formação do neurito durante o desenvolvimento neuronal.

1.4 - FEZ1 e vírus

Dois trabalhos relacionam FEZ1 a infectividade viral [37, 47]. Apesar de serem trabalhos independentes, que tratam de vírus com características diferentes, em ambos, a atuação de FEZ1 está intimamente relacionada ao transporte de moléculas virais.

A superexpressão de FEZ1 impede que o ciclo de desenvolvimento viral se complete. A participação de FEZ1 junto a outras proteínas associadas à SNARE (*N-ethylmaleimide Sensitive Fusion Attachment Protein Receptor*) já foi observada, e indica sua atuação no transporte vesicular [48]. Em concordância, foi observada atuação de UNC76 no transporte de vesículas sinápticas em *Drosophila* [6].

Curiosamente, foi observada superexpressão de FEZ1, uma proteína tipicamente neuronal, em linhagens mutantes resistentes a retrovírus. As duas linhagens resistentes, R4-7 e R3-2, isoladas a partir de fibroblastos Rat2, apresentam resistência cem vezes e mil vezes maior à infecção por MLV (*Moloney murine leukemia viruses*). A infecção em R4-7 é bloqueada antes do início da transcrição reversa. Na linhagem R3-2, observam-se níveis normais de síntese de DNA viral linear a partir de transcrição reversa, mas impedimento na formação de DNA circular viral e integração do provírus no núcleo [49,50]. As duas linhagens mutantes são também resistentes a infecção por pseudotipos do vírus HIV (*Human Immunodeficiency Virus*).

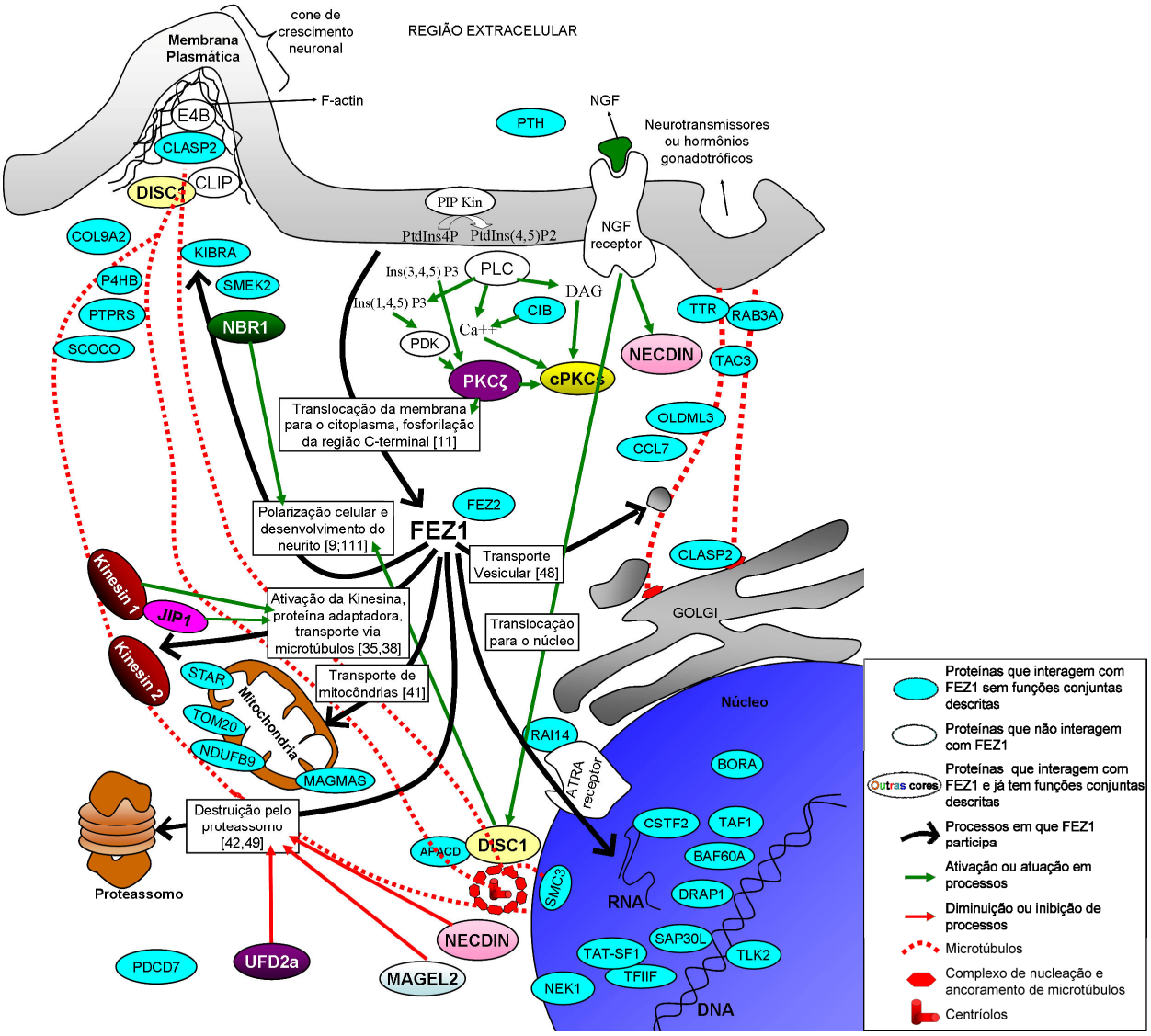

Figura 1 - Funções já descritas para FEZ1, associadas ao desenvolvimento neuronal. Polarização celular no cone de crescimento neuronal, transporte vesicular, ativação da Kinesina, transporte mitocondrial e participação conjunta com fatores de transcrição são eventos associados a atividade de FEZ1. A fosforilação por PKCζ causa a translocação de FEZ1 da membrana plasmática para o citoplasma, e disponibilização de FEZ1 para interação com elementos do citoesqueleto e outras interações. O mecanismo de sinalização que causa ativação/disponibilização de FEZ1 ainda não foi descrito, mas a ativação da PLC pelo PtdIns(4,5)P2, das PKCs clássicas por Ins (3,4,5)P3 e PKCζ por Ins (3,4,5)P3 possivelmente estão envolvidas. Apesar de várias proteínas nucleares interagirem com FEZ1, o fator que induz a migração de FEZ1 para o núcleo ainda não foi identificado. FEZ1 interage com proteínas reguladas pelas vias de sinalização de ATRA e NGF, e esse último causa aumento na expressão de FEZ1. Essas vias possivelmente atuam na sinalização de FEZ1 para entrada no núcleo. FEZ2, paráloga de FEZ1 possivelmente atua em processos similares aos de FEZ1 em células não neuronais.

A partir da comparação de genes super expressos em células R3-2 em relação à linhagem selvagem, foram identificadas pelo menos 5 proteínas tipicamente neuronais, dentre elas FEZ1, expressa pelo menos 30 vezes mais em relação ao controle [47]. Possivelmente, FEZ1 está relacionada ao transporte viral para o núcleo, via elementos do citoesqueleto. A superexpressão de FEZ1 na linhagem R3-2 exerce bloqueio na replicação de vários tipos de vírus pelo mesmo mecanismo, incluindo bloqueio ao HIV.

Experimentos controle mostraram que a supressão de FEZ1 na linhagem R3-2, resultou em aumento na susceptibilidade a infecção retroviral. Além disso, a super-expressão de FEZ1 em células parentais Rat2 e células humanas HEK293 conferiu resistência dezoito vezes maior contra infecção por HIV, o que indica que os mecanismos de resistência não estão associados à atuação conjunta de FEZ1 com outras proteínas diferencialmente expressas em linhagens resistentes [47, 55].

Em um segundo artigo publicado no mesmo ano, FEZ1 é associada ao Polyomavírus Humano JC vírus (JCV), agente causador da PML (*Progressive Multifocal Leucoencephalopaty*), a partir de sua interação com a Agnoproteína viral [37].

O genoma do JCV compreende uma molécula dupla fita circular de DNA que contém três regiões funcionais, os genes virais precoces e tardios e a região não codificadora regulatória [51,52]. A sequência líder de transcritos tardios codifica a Agnoproteína, uma proteína viral auxiliar que contém 71 aminoácidos [53]. A Agnoproteina, de SV40 (*Simian vírus 40*) que pertence à mesma família do JCV, contribui para vários estágios do ciclo lítico desse vírus. Mutações na Agnoproteína de SV40 resultam em defeitos no crescimento atribuído a rota de maturação viral [54,55]. Em um trabalho recente utilizando-se células CG-4 progenitoras, foi demonstrado que a expressão da Agnoproteína de JCV prejudica a diferenciação destas células em oligodendrócitos, e interfere na sobrevivência de células mielinizadas [56]. A deficiência da Agnoproteína causa liberação ineficiente de vírions SV40 a partir de células infectadas e prejudica a habilidade da propagação dos vírus em macacos. Outros trabalhos mostram que a supressão da Agnoproteína com iRNA impede a infecção pelo JCV [54,57]. A maioria das proteínas codificadas pelo genoma do JCV se localiza no núcleo em células infectadas, com exceção da Agnoproteína que está restrita a região citoplasmática perinuclear [66-69].

Em um ensaio de duplo híbrido em levedura foi identificada a interação da Agnoproteína com duas regiões de FEZ1, a região *poly-glu* N-terminal, e o domínio *coiled-coil* C-terminal [37].

Experimentos de co-precipitação e imunocitoquímica confirmaram a interação e colocalização entre Agnoproteína e FEZ1 principalmente na região perinuclear. A Agnoproteína colocaliza com microtúbulos na região perinuclear de células infectadas por JCV [37]. Também foi observada que a interação de FEZ1 com microtúbulos é rompida pela Agnoproteína, resultado de uma competição específica entre essas duas proteínas pela interação com o microtúbulo. Nesse mesmo trabalho foi observado que a expressão de FEZ1 inibe a propagação de JCV em linhagens gliais humanas [37].

A ligação da Agnoproteína ao domínio *coiled-coil* de FEZ1 tem importância fundamental no rompimento da interação entre FEZ1 e microtúbulos. A promoção do desenvolvimento de neuritos em células PC12 também é inibida pela Agnoproteína e ativada pela expressão de FEZ1 e PKCζ [11, 37]. A relação competitiva entre FEZ1 e Agnoproteína é clara. Visivelmente a razão positiva FEZ1/Agnoproteína na célula favorece o desenvolvimento neuronal.

A superexpressão de FEZ1 em células gliais humanas inibe a produção da Agnoproteína e da proteína VP1 de JCV, sem afetar a transcrição dos promotores do vírus. Os efeitos de FEZ1 na inibição da infecção aparecem tardiamente, aos sete dias após a infecção, o que sugere que a superexpressão de FEZ1 influencia na fase tardia da infecção com JCV, mas não afeta a fase primária, que inclui a entrada do vírus na célula e transcrição do genoma [37]. Entretanto nesse caso, diferentemente do observado para o HIV [47], os vírions do JCV entram e não conseguem sair de dentro do núcleo em células que estão super-expressando FEZ1. Esse fato interessante, condiz com análises de mutação na Agnoproteína de SV40 e estudos de iRNA da Agnoproteína de JCV, que mostram que essa proteína executa importante papel na liberação de vírions, provavelmente associada ao transporte vesicular anterógrado [34, 54, 57]. É possível que em presença de grande quantidade de FEZ1 na célula, o transporte anterógrado mediado pela Agnoproteína para eliminação dos vírions, seja parcialmente inibido ou sobreposto por sinais para transporte de elementos neuronais, inibindo a liberação dos vírions, conforme esquematizado na FIGURA 2. O fato de que FEZ1 apresenta a função de *scaffold prote*in atuando em conjunto com JIP1 na ativação de transporte mediado por Kinesina [35], reforça a hipótese de que ocorre uma "preferência" para transporte de elementos neuronais em presença de FEZ1. Interessantemente, a expressão de FEZ1 em linhagens celulares permissivas a JCV, tais como SVG-A ou IMR-32 é muito menor do que em células neuronais não permissivas tais como SH-SY5Y [58].

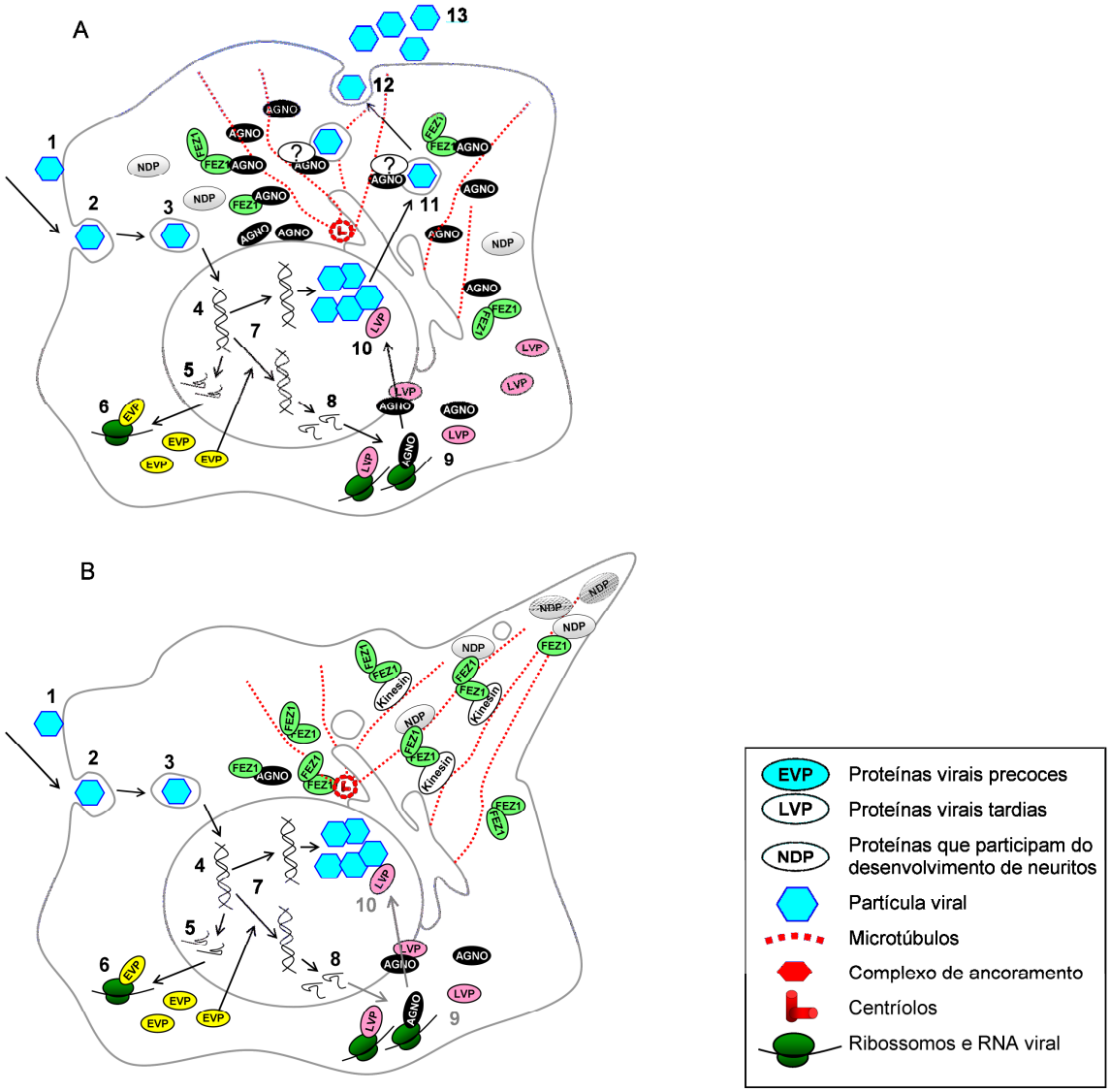

Figura 2 - O mecanismo competitivo entre FEZ1 e a Agnoproteína. FEZ1 interage com a Agnoproteína do JCV, e essa interação rompe a interação de FEZ1 com microtúbulos e impede a diferenciação neuronal. A infecção das células pelo JCV consiste dos seguintes passos: 1 – ligação do vírion ao receptor na membrana cellular externa 2 – endocitose 3 – transporte para o núcleo 4 – liberação do material genético do vírion, 5 – transcrição dos genes precoces, 6 – tradução das proteínas precoces antígeno T e antígeno t, 7 – replicação do DNA viral, 8 – transcrição da região tardia, 9 – tradução da Agnoproteína e das proteínas do capsídeo VP1, VP2 e VP3, 10 – montagem dos vírions, 11 – exportação do núcleo, 12 – liberação dos vírions, 13 – partículas virais infectivas. (A) Em uma célula que não tem expressão elevada de FEZ1 a Agnoproteína viral e outras proteínas virais dominam o transporte mediado por microtúbulos e ocorre a transcrição e produção de proteínas virais tardias e subsequente liberação das partículas virais. A polarização celular e desenvolvimento de neuritos é rompida nesse caso, e a diferenciação neuronal interrompida. (B) Em células que tem FEZ1 em quantidade suficiente, os passos 9 e 10 do ciclo de desenvolvimento viral são inibidos, e o transporte microtubular se torna disponível para o transporte de mitocôndrias, vesículas e outros elementos ou moléculas que devem atingir o cone de crescimento neuronal propiciando a diferenciação em neurônios. Figura construída a partir de dados já publicados [37].

1.5 - Uma proteína multifuncional

Dois estudos independentes foram realizados utilizando FEZ1 como isca em ensaios de duplo-híbrido de levedura. Um dos estudos, que utilizou várias iscas além de FEZ1, gerou uma rede de interações que conecta 1705 proteínas humanas via 3186 interações [59]. Entre as proteínas analizadas está FEZ1 (fragmento entre os aminoácidos 131-392) que interagiu com 21 proteínas. Paralelamente, no outro estudo utilizando a região C-terminal de FEZ1 (aminoácido 221 ao 392) como isca em um ensaio de duplo híbrido, nosso grupo observou 16 novas interações [24]. Como resultado desses trabalhos contabiliza-se 37 proteínas diferentes que interagem com FEZ1, as quais participam de processos que envolvem controle da transcrição e/ou organização da cromatina, organização dos microtúbulos/transporte e apoptose/tumorigênese, além da regulação de desenvolvimento neuronal.

A idéia tradicional do estudo de proteínas prevê a noção de "uma estrutura para uma função", e poderíamos associar uma função a uma ou poucas interações. No caso de FEZ1, pelo menos 50 proteínas diferentes interagem com ela, além de sua interação consigo mesma. Estas interações estão descritas na TABELA1.

TABELA1 – Proteínas que interagem direta e/ou indiretamente com FEZ1 já descritas.

Sigla	***Nome***	**Sinônimos**	**Número OMIM**	**Função**	**Identificação da interação**	**Região de FEZ1 (aa)**	**Ref**
N	*Agnoprotein*	N	N	Estagio lítico e liberação de vírions	Duplo híbrido em levedura; IP	32-392 192-392	[37]
APACD	*ATP Binding Protein Associated With Cell Differentiation*	TXNDC9	N	Dinâmica de microtúbulos e do centrossomo.	Duplo híbrido automatizado em larga escala; IP	N	[59]
BAF60a	*BRG1-Associated FACTOR 60A*	SMARCD1	601735	Controle transcricional, remodelagem da cromatina	Duplo híbrido em levedura; *pull down*	1-392 221-392 269-392	[24]
C13orf34	*Chromosome 13 Open Reading Frame 34*	FLJ22624; BORA	610510	Ciclo celular e entrada em mitose	Duplo híbrido automatizado em larga escala	N	[59]

CCL7	*Chemokine CC motif Ligand 7*	SCYA7; MCP3	158106	Ativação de linfócitos	Duplo híbrido automatizado em larga escala	N	[59]
CIB1	*Calcium and integrin binding protein*	KIP1, KIP	602293	Regulação do metabolismo de cálcio	Duplo híbrido em levedura	370-392	[111]
CLASP2	*Clip Associated Protein 2*	N	605853	Dinâmica de microtúbulos	Duplo híbrido em levedura; *pull down*	221-392	[24]
COL9A2	*Collagen type IX alpha 2*	DJ39G22.4 EDM2; MED	120260	Interação entre proteínas não colágenas e colágenas	Duplo híbrido automatizado em larga escala	N	[59]
CSTF2	*Cleavage Stimulation Factor*	3-Prime Pre-RNA Subunit 2, 64kD	600368	Processamento de RNA	Duplo híbrido automatizado em larga escala	N	[59]
DIS3L2	*DIS3 mitotic control homolog (S. cerevisiae)-like 2*	MGC4217 4	N	Regulação do desenvolvimento ósseo?	Duplo híbrido automatizado em larga escala	N	[59]
DISC1	*Disrupted in Schizophrenia 1*	N	605210	Desenvolvimento neuronal e atividade centrossomal	Duplo híbrido em levedura, IP	129-392 247-392	[9,79]
DRAP1	*DR1 Associated Protein 1*	NC2 Alpha	602289	Controle transcricional	Duplo híbrido em levedura; *pull down*	1-392 221-392	[24]
FEZ1	*Fasciculation and Elongation Protein Zeta 1*	Zygin1	604825	Desenvolvimento neuronal e transporte intracelular	Duplo híbrido em levedura; *pull down*	1-392 1-227 131-392 221-392 269-392	[24]
FEZ2	*Fasciculation and Elongation Protein Zeta 2*	Zygin2	604826	Desenvolvimento neuronal?	Duplo híbrido em levedura	131-392 221-392 238-392	[24]
FLJ13909	*Chromosome 16 open reading frame 59*	N	N	N	Duplo híbrido em levedura; *pull down*	221-392	[24]
FLJ20397	*hypothetical protein FLJ20397, isoform CRA_d*	N	N	N	Duplo híbrido automatizado em larga escala	N	[59]
HTATSF1	*HIV-1 TAT Stimulatory Factor 1*	TATSF1	300346	Ativação da proteina TAT do HIV e transcrição viral.	Duplo híbrido automatizado em larga escala	N	[59]
KIBRA	*Kidney and Brain Expressed Protein*	WWC1	610533	Desenvolvimento neuronal.	Duplo híbrido em levedura; *pull down*	1-392 221-392	[24]

Kinesin1	*Kinesin 1*	KIF5, KNS1	N	Transporte intracelular.	Duplo híbrido em levedura, *pull down*	1-392 1-308 163-393	[35]
Kinesin2	*Kinesin 2*	N		Transporte intracelular.	IP	1-392	[37,38]
MAGEL2	*MAGE Like 2*	N	605283	Desenvolvimento neuronal.	IP	1-392	[42]
Magmas	*N*	CGI136	N	Fator mitocondrial estimulador de linfócitos.	Duplo híbrido automatizado em larga escala	N	[59]
NBR1	*Neighbor of BRCA1*	N	166945	Morte celular?	Duplo híbrido em levedura	248-360 248-349 370-392	[111]
NDN	*Necdin*	N	602117	NGF signaling, neuronal development.	Duplo híbrido em levedura (FEZ2); IP	46-282 (FEZ2) 1-392	[42]
NDUFB9	*NADH Ubiquinone Oxidoreductase 1 Beta Subcomplex 9*	FLJ22885; UQOR22	601445	Cadeia de transporte de elétrons mitocondrial.	Duplo híbrido automatizado em larga escala	N	[59]
NEK1	*NIMA Related Kinase 1*	N	604588	Ciclo celular, desenvolvimento ciliar.	Duplo híbrido em levedura	124-392	[96]
OLDML3	*Olfactomedin-like*	OLF44	610088	Desenvolvimento embriônico e placentário.	Duplo híbrido automatizado em larga escala	N	[59]
P4HB	*Procollagen Proline, 2-Oxoglutarate-4-Dioxygenase Beta Subunit*	DSI; EBA2L; GIT; PDI; PDIA1; PO4DB; PO4HB; PROHB	176790	Biossíntese de colágeno.	Duplo híbrido automatizado em larga escala	N	[59]
PDCD7	*Programmed Cell Death 7*	N	608138	Morte celular.	duplo híbrido em levedura, duplo híbrido automatizado, *pull down*	221-392 269-392	[24, 59]
PKCζ	*Protein Kinase C Zeta*	PRKCZ	176982	Polarização celular, desenvolvimento neuronal.	duplo híbrido em levedura, IP	1-392	[11]
PTH	*Parathyroid Hormone*	N	168450	Homeostase de cálcio, hematopoiese.	Duplo híbrido automatizado em larga escala	N	[59]

PTPRS	*Protein-Tyrosine Phosphatase Sigma*	N	601576	Desenvolvimento neuronal.	Duplo híbrido automatizado em larga escala	N	[59]
RAB3A	*RAS Associated Protein*	N	179490	Transporte intra neuronal, liberação de neurotransmissores.	Duplo híbrido em levedura	221-392	[24]
RAI14	*Retinoic Acid Induced 14*	NORPEG; KIAA1334	606586	Apoptose.	Duplo híbrido em levedura; *pull down*	1-392 221-392 269-392	[24]
SAP30L	*SAP30 Like Protein*	N	610398	Controle transcricional.	Duplo híbrido em levedura; *pull down*	1-392 221-392 269-392	[24]
SCOCO	*Similar to Short Coiled Coil*	N	AAH16511	Desenvolvimento neuronal	Duplo híbrido em levedura	221-392	[24]
N	*Similar to OAT Like*	N	N	Atividade transaminase	Duplo híbrido em levedura	221-392	[24]
SMC3	*Structural Maintence of Chromosomes 3*	CSPG6; Bamacan	606062	Coesão de cromátides irmãns, dinâmica de microtúbulos.	Duplo híbrido em levedura; *pull down*	1-392 221-392	[24]
SMEK2	*MEK1 Supressor 2*	PP4R3B; PP4R3-BETA; KIAA1387	610352	Polarização celular, metabolismo de lipídios.	Duplo híbrido automatizado em larga escala	N	[59]
STAR	*Steroidogenic Acute Regulatory Protein*	STARD1	600617	Mobilização do colesterol na membrana mitocondrial.	Duplo híbrido automatizado em larga escala	N	[59]
TAC3	*Tachykinin 3*	NKB; NKNB; PRO1155; ZNEUROK1; NEUROMEDIN K	162330	Regulação da liberação de hormônios gonadotróficos.	Duplo híbrido automatizado em larga escala	N	[59]
TAF1	*Tata Box-Binding Protein Associated Factor 250kDa*	BA2R	313650	Controle transcricional, remodelagem da cromatina	Duplo híbrido em levedura	1-392 221-392	[24]
TFIIF	*Transcription Factor IIF Alpha Subunit*	GTF2F1; TF2F1; RAP74	189968	Controle transcricional	Duplo híbrido automatizado em larga escala	N	[59]
TLK2	*Tousled Like Kinase 2*	PKU-ALPHA	608439	Controle trasncricional, remodelagem da cromatina.	Duplo híbrido em levedura	221-392	[24]

TOM20	*Translocase of Outer Mitochondrial Membrane 20*	MAS20P; MOM19; TOMM20	601848	Receptor/translocase mitocondrial.	Duplo híbrido automatizado em larga escala	N	[59]
TTR	*Transthyretin*	HsT2651; PALB; TBPA; Prealbumin	176300	Carreadora de hormônios tireoidianos e retinol.	Duplo híbrido automatizado em larga escala	N	[59]
UFD2a	*Ubiquitin Fusion Degradation Pathway 2a*	E4B	N	Mecanismo de ubiquitinação Desenvolvimento neuronal	Duplo híbrido em levedura; IP	1-392	[112]
ZNF251	*Zinc finger protein 251*	N	N	Controle trasncricional?	Duplo híbrido em levedura	221-392 269-392	[24]
N	*Alpha Tubulin*	TUBA	191110	Constituição de microtúbulos	Ensaio de cossedimentação	192-392 297-392	[37]
N	*Beta Tubulin*	TUBB	191130	Constituição de microtúbulos	*Pull down*	163-393	[38]
N	*Gamma Tubullin*	TUBG-1	191135	Constituição de complexos de nucleação para microtúbulos	IP	1-392	[42]

aa = aminoácidos; IP= Imunoprecipitação; Ref = Referência em que a interação foi descrita; N= Não existe, não identificado ou omitido por conotação ambígua.

A noção de que o desenvolvimento neuronal não é um processo simples, condiz com a existência de mecanismos complexos que traduzem o fluxo de informação, iniciado na informação genética, a muitas ações no sistema. O fluxo da informação geralmente termina nas interações entre proteínas, que hoje, podem ser detectadas por técnicas que se difundiram nas últimas décadas [60-62]. A partir da análise da evolução de redes de interação em diferentes organismos, surge a definição de um elemento comum em todas as redes: proteínas *Hub* ("nó") [63-65]. Proteínas *Hub,* por definição, são proteínas se ligam ou interagem com um grande número de proteínas diferentes. Essas proteínas estão em menor número quando comparado ao número de proteínas não *Hub* em redes de interactoma elaboradas para todos os organismos já estudados [63, 64]. Poderíamos traduzir de outra forma, como uma proteína em que o fluxo de informação se ramifica.

Proteínas com grande conectividade apresentam maior probabilidade de serem essenciais ao sistema, sendo caracterizadas como alvos de maior eficiência para o desenho de drogas [64, 66, 67].

Em *S. cerevisiae* foram propostas duas classificações para *Hubs*: os estáticos (*Party Hubs*) e os dinâmicos (*Date Hubs*) [63]. Os *Party Hubs* são encontrados em complexos estáticos aonde interagem com muitas proteínas ao mesmo tempo, enquanto os *Date Hubs* se ligam a parceiros de interação em diferentes espaços de tempo ou localização. Os *Party Hubs* estão relacionados à centralidade em complexos funcionais enquanto os *Date Hubs* atuam como organizadores e conectores entre módulos semi-autônomos com funções diferentes no sistema. Estruturalmente, os *Party Hubs* interagem consigo mesmos, e realizam maior número de interações com proteínas relacionadas estruturalmente. Os *Date Hubs*, apresentam regiões desordenadas mais longas que viabilizam maior flexibilidade de interações com proteínas diferentes, influenciando em processos diferentes [68].

Com base no número de interações já identificadas para FEZ1, podemos propor sua inserção no grupo das proteínas *Hub.* A conservação genética e mecanística de FEZ1 em diferentes eucariotos, principalmente ao ser comparada com UNC76, também reproduz uma das principais características observadas em *Hubs*: a conservação na distribuição filogenética [69].

Ao inserir FEZ1 no centro de um mapa com todas as interações já descritas demonstradas simultaneamente, observamos que FEZ1 interage com muitas proteínas, e muitas dessas parceiras de interação também apresentam o "comportamento promíscuo" de *Hubs* (FIGURA 3). Nossa ilustração permite observar que FEZ1 é o "ponto de conexão" entre muitas proteínas que executam funções diferentes, de forma similar aos *Date Hub* já descritos para levedura. Com base em todos os dados descritos, observamos que FEZ1 extrapola o sistema neuronal, possivelmente participando em âmbito mais geral em diferentes processos e tipos celulares.

1.6 - Muitas funções, muitas interações... muitas estruturas?

A visão clássica prevê que uma proteína sem estrutura definida não é funcional. Entretanto aumentam as evidências de que uma fração significativa das proteínas eucarióticas, aproximadamente 30%, sejam intrinsecamente desenoveladas (*natively unfolded proteins*) [70]. Entende-se por intrinsecamente desenovelada aquela proteína que apresenta a maior parte de sua cadeia polipeptídica desenovelada em estado nativo. *Hubs* geralmente se apresentam como proteínas intrinsecamente desenoveladas [71,72].

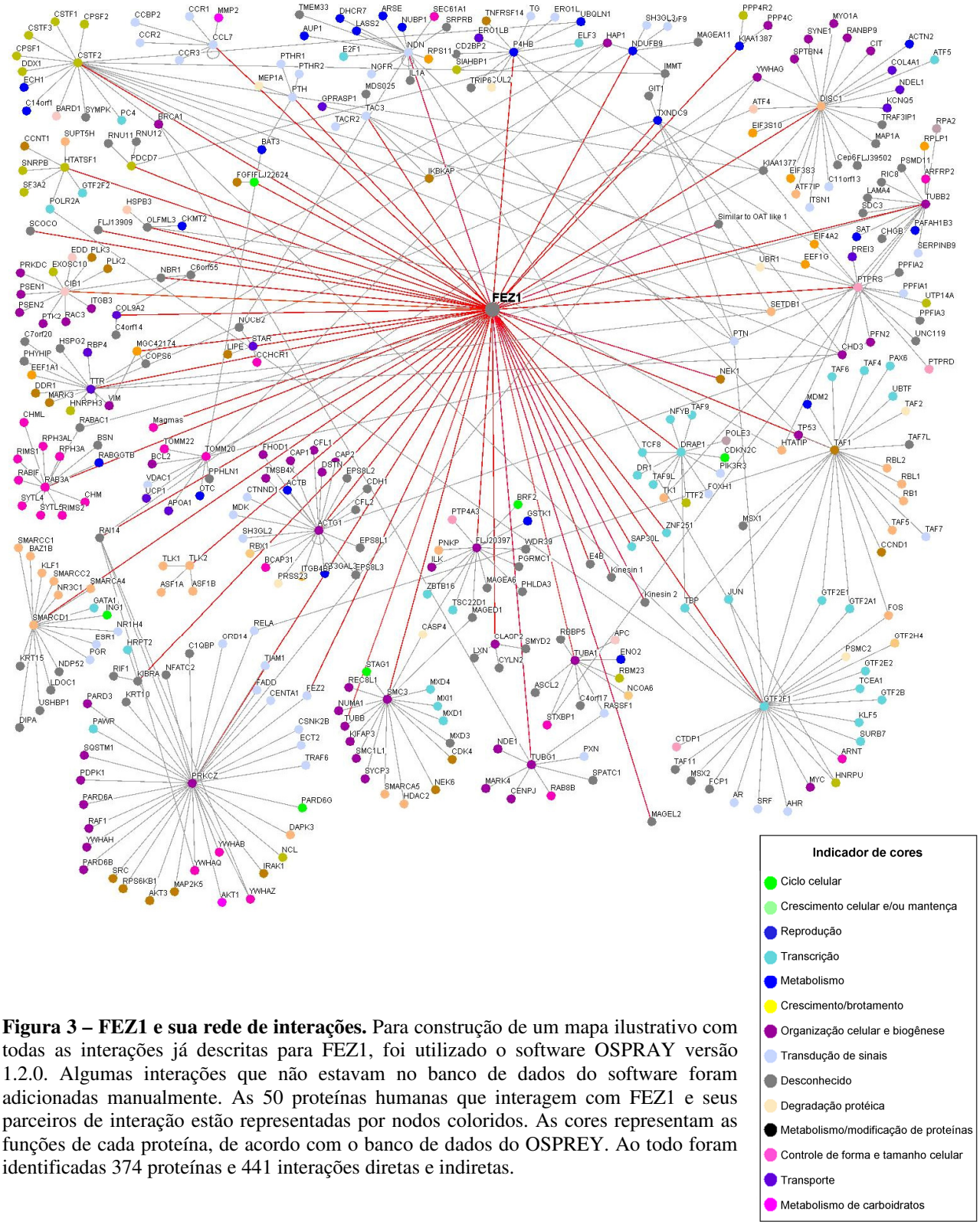

Figura 3 – FEZ1 e sua rede de interações. Para construção de um mapa ilustrativo com todas as interações já descritas para FEZ1, foi utilizado o software OSPRAY versão 1.2.0. Algumas interações que não estavam no banco de dados do software foram adicionadas manualmente. As 50 proteínas humanas que interagem com FEZ1 e seus parceiros de interação estão representadas por nodos coloridos. As cores representam as funções de cada proteína, de acordo com o banco de dados do OSPREY. Ao todo foram identificadas 374 proteínas e 441 interações diretas e indiretas.

O número de proteías intrinsecamente desenoveldas aumenta com a complexidade do organismo, e essas proteínas geralmente se enquadram como *Hubs* em redes de interação [73-75]. Tendo como base essas e outras informações podemos substituir o termo "ausência de estrutura" ao termo "potencial para assumir diversas estruturas".

Uma proteína desestruturada em seu estado nativo é diferente de uma proteína desorganizada ou desnaturada, no sentido funcional. Em uma estrutura móvel a interface para interações é cerca de 2 a 3 vezes maior, o que porporciona uma valiosa "economia evolutiva" de espaço em nível de DNA, proteína, e consequentemente em tamanho celular, aumentando em paralelo a eficiência do fluxo de informação [76].

A existência de proteínas capazes de se "moldar" de acordo com diferentes ligantes adotando estruturas diferentes é o tema central de muitas revisões de literatura, em muitos casos já foram resolvidas estruturas diferentes para uma mesma proteína com diferentes ligantes [83,86,88] .

1.7 - FEZ1 e doenças

Alguns trabalhos sugerem que FEZ1 pode estar relacionada direta ou indiretamente ao desenvolvimento de algumas doenças, principalmente doenças genéticas relativas ao desenvolvimento do sistema nervoso. FEZ1 está envolvida em mecanismos de transporte intracelular e sabe-se que defeitos ou ausência de elementos transportadores axonais causam várias doenças humanas relacionadas a sistema nervoso [77,78]. A seguir algumas informações que vinculam FEZ1 a algumas doenças.

1.7.1 - Esquisofrenia

A interação de FEZ1 com DISC1 é necessária para o desenvolvimento e a extensão de neuritos [9]. O rompimento dessa interação pela translocação (1:11) (q42:q14.3) é tida como uma das causas genéticas para o surgimento da esquisofrenia [9,79]. A esquisofrenia é uma doença associada a defeitos no desenvolvimento e função neuronais [80-83]. O mecanismo molecular da

possível relação entre FEZ1 e DISC1 no surgimento da esquisofrenia é proposto em uma revisão, em associação a via de sinalização por NGF (*Nerve Growth factor*) [79].

Após a estimulação com NGF, células PC12 param a proliferação e começam a extensão de neuritos, mas a translocação (1:11) (q42:q14.3), já identificada em pacientes de esquisofrenia, resulta na perda da região C-terminal de DISC1, que passa a não interagir mais com FEZ1. Com isso a cascata de sinalização é rompida inibindo o crescimento e maturação dos neurônios [79].

Camundongos deficientes em FEZ1 apresentam hiperatividade e maior sensibilidade a psicoestimulantes, sintomas correlatos aos observados em pacientes acometidos por esquisofrenia [34]. A hiperatividade do sistema dopaminérgico mesolímbico está implicada na patofisiologia da doença, e a deficiência de FEZ1 resulta em aumento da transmissão dopaminérgica no *nucleus accumbens* causando variações no comportamento [17].

FEZ1 foi observada em neurônios GABAérgicos inibitórios [17]. As funções cerebrais são executadas através de um balanço de sinais excitatórios e inibitórios em circuitos neurais, e neurônios GABAérgicos são muito ativos na regulação desse balanço. Mudanças na atividade de neurônios GABAérgicos podem ser a explicação para hiperatividade em camundongos deficientes em FEZ1. Anormalidades em transmissões GABAérgicas estão associadas ao surgimento da esquisofrenia [84].

1.7.2 - Síndrome de Prader–Willi

As proteínas Necdin e MAGEL2 interagem com FEZ1, impedindo sua degradação pelo complexo proteassômico e favorecendo o desenvolvimento neuronal [42]. A inativação de Necdin e MAGEL2 está associada ao surgimento da Síndrome de Prader-Willi (PWS), caracterizada por uma profunda neotonia, perda de desenvolvimento, hipoventilação, começo de hiperfagia obesidade e hipogonadismo [42,85,86]. Os sintomas da doença sugerem que seu início advém de um atraso na maturação dos circuitos neuronais, e anormalidades adicionais incluem elevados níveis de metabólitos de serotonina e dopamina no fluido cerebroespinhal e insensibilidade periférica a dor [86]. Necdin e MAGEL2 são partes de uma família multiproteína com um domínio homólogo MAGE. Esta família também inclui MAGED1 (NRAGE) que interage com o receptor para neurotrofina p75 e facilita apoptose mediada por NGF através da rota dependente de Jun quinase. [87]. A expressão de MAGEL2 murina é aumentada em

neurônios durante o desenvolvimento do hipotálamo. A Necdin murina é expressa em muitos neurônios após os estágios de diferenciação e também em músculo pele e cartilagem [88].

1.7.3 - AIDS e PML

A superexpressão de FEZ1, está associada a mecanismos de resistência a infecção por HIV. Fibroblastos R3-2 resistentes a infecção viral apresentam FEZ1 em quantidade pelo menos 30 vezes superior a observada em células susceptíveis [47] . O mecanismo de resistência se baseia no bloqueio do ciclo viral após a transcrição reversa mas antes da entrada do vírus no núcleo indicando associação com atividades de FEZ1 associadas ao citoesqueleto, conforme já descrito no tópico 1.4.

A replicação do HIV necessita de ativação das células T através de uma série de sinais intracelulares complexos, incluindo a via de sinalização por PKC e mobilização de cálcio e sinais induzidos por citoquinas, que culminam na ativação de proteínas que atuam na replicação viral [89]. A proteína TAT é uma das primeiras proteínas expressas após a entrada do HIV na célula, e é requerida no início da transcrição viral para progressão da doença [89]. FEZ1 interagiu com os fatores de transcrição humanos HTAT-SF1 e TFIIF, fatores fundamentais para ativação da transcrição e elongamento do RNA de TAT [59,90].

A PML se caracteriza como uma doença desmielinativa do sistema nervoso central, que resulta da reativação do JCV principalmente em pacientes imunocomprometidos [52,91,92]. JCV é encontrado em todo o mundo, cerca de 80% da população mundial apresenta infecção assintomática e aproximadamente 85% de todos os casos de PML ocorrem de forma oportunista após a infecção por HIV [92].

Os sintomas clínicos e sinais da PML não são específicos. Em cerca de 25% dos casos, PML é a doença inicial, utilizada para diagnosticar AIDS. O sintoma mais comum é a fraqueza dos membros, em 52% dos casos seguido por defeitos cognitivos em 45% dos casos. Apenas 10% dos casos apresentam sintomas sensoriais [92].

FEZ1 interage com a Agnoproteína viral, e compete com ela pela interação com microtúbulos. A superexpressão de FEZ1 inibe a liberação de vírions do JCV, que ficam retidos no núcleo da célula. A Agnoproteína, um polipetídeo de 71 aminoácidos, contribui em vários estágios do ciclo lítico do vírus, incluindo transcrição do genoma viral, tradução das proteínas

tardias e liberação de vírions. Em células do hospedeiro, inibe o crescimento celular e provoca atraso na transição G2/M no ciclo celular [93].

A relação entre HIV e JCV já foi amplamente relatada. Sabe-se que em astrócitos contendo os dois vírus uma pequena vantagem é conferida ao JCV em decorrência da interação da Agnoproteína com a proteína TAT do HIV, e consecutiva supressão da replicação do HIV [91,94]. Existem evidências de que a proteína TAT do HIV é capaz de ativar a transcrição de JCV em células gliais [91,95]. A ativação do promotor tardio de JCV pela proteína TAT de HIV pode indicar o motivo pelo qual ocorre grande incidência de PML em pacientes com AIDS, e FEZ1, por estar associada tanto a função de TAT quanto a função da Agnoproteína é um fator alvo para o estudo da progressão e controle dessas doenças.

1.7.4 - Doença Policística do Rim

FEZ1 interage com NEK1, uma proteína quinase associada a eventos centrossomais, mitose, reparo de DNA e desenvolvimento cilar [96-101] . Estudos em camundongos mutantes Kat e Kat2J mostram que mutações espontâneas no gene que codifica NEK1 estão diretamente envolvidas na etiologia da Doença Policística do Rim (PKD) [104]. A PKD é a nefropatia hereditária mais comum em humanos. É caracterizada por alargamento massivo do rim associado ao crescimento de cistos intrarrenais [102].

O cílio é a organela ancestral mais conservada em eucariotos, e se projeta a partir da superfície celular. O cílio primário está envolvido em diversas funções sensoriais e, concomitantemente, disfunções no cílio primário estão implicadas em doenças [103-105]. Nesse âmbito a doença mais estudada é a PKD. Muitos estudos mostram que as proteínas mutadas em modelos humanos e murinos para PKD estão localizadas no cílio ou no corpo basal [102,106,107]. Perda do cílio, disfunção do transporte intra-flagelar ou defeitos na regulação da sinalização do cílio, causam a proliferação celular e formação de cistos característicos da PKD.

NEK1 está localizada na região centrossomal e corpo basal ciliar [98,101]. Em células MEF e Kat2J o número de cílios é reduzido dramaticamente indicando que condições de superexpressão ou ausência de NEK1 inibem o desenvolvimento ciliar [101]. NEKs de *Trypanossoma, Clamydomonas* e *Tetraymena* estão localizadas no corpo basal e inibem a formação de flagelos quando suprimidas ou superexpressas [108-109]. Os mecanismos de

atuação das NEKs no cílio são relativamente conservados, e geralmente estão associados a dinâmica ciliar e ciclo celular, sendo portanto, importantes alvos a serem investigados em doenças que se caracterizam por mal funcionamento destes mecanismos, como a PKD [110].

2 - OBJETIVOS

2.1 - Objetivo Geral

Estudar a estrutura molecular e elucidar funções da proteína humana FEZ1.

2.1 - Objetivos específicos

1. Expressão da proteína FEZ1 humana em sistemas procariotos e purificação em larga para estudos de interação, espectroscópicos e biofísicos.
2. Obter dados sobre a estrutura molecular de FEZ1 a partir de estudos estruturais por meio da técnica de SAXS (*Small Angle X Ray Scattering*).
3. Elucidar possíveis funções de FEZ1 em células eucarióticas a partir de experimentos de superexpressão em linhagens celulares de mamíferos.
4. Análise da localização sub-celular de FEZ1 endógena, FEZ1 inteira e truncada em fusão com GFP.
5. Estudar a fosforilação de FEZ1 por diferentes isoformas de PKC e identificar as regiões de ocorrência dos sítios de fosforilação.
6. Estudar a influência do status de fosforilação de FEZ1 na interação com outras proteínas previamente identificadas por duplo híbrido em levedura [24].
7. Mapear as regiões de FEZ1 que interagem com NEK1 e CLASP2.
8. Elucidar a atuação de FEZ1 com outras proteínas principalmente com NEK1.

3-RESULTADOS

Artigo 1

Human FEZ1 has characteristics of a natively unfolded protein and dimerizes in solution

Lanza DC, Silva JC, Assmann EM, Quaresma AJ, Bressan GC, Torriani IL, Kobarg J.

Proteins (2009) 74(1):104-121.

Received 29 October 2007;
Revised 18 April 2008
Accepted 28 April 2008
Published online 9 July 2008 in Wiley InterScience.

doi: 10.1002/prot.22135
pISSN: 0887-3585 (Print)
eISSN: 1097-0134 (Electronic)
NLM ID: 8700181

Human FEZ1 has characteristics of a natively unfolded protein and dimerizes in solution

Daniel C. F. Lanza,[1,2] Julio C. Silva,[1,3] Eliana M. Assmann,[1] Alexandre J. C. Quaresma,[1,2] Gustavo C. Bressan,[1,2] Iris L. Torriani,[1,3] and Jörg Kobarg[1,2]*

[1] Laboratório Nacional de Luz Síncrotron, Campinas, SP, Brasil

[2] Instituto de Biologia, Universidade Estadual de Campinas, Campinas, SP, Brasil

[3] Instituto de Física "Gleb Wataghin", Universidade Estadual de Campinas, Campinas, SP, Brasil

ABSTRACT

The fasciculation and elongation protein Zeta 1 (FEZ1) is the mammalian orthologue of the *Caenorhabditis elegans* protein UNC-76, which is necessary for axon growth. Human FEZ1 interacts with Protein Kinase C (PKC) and several regulatory proteins involved in functions ranging from microtubule associated transport to transcriptional regulation. Theoretical prediction, circular dichroism, fluorescence spectroscopy, and limited proteolysis of recombinant FEZ1 suggest that it contains disordered regions, especially in its N-terminal region, and that it may belong to the group of natively unfolded proteins. Small angle X-ray scattering experiments indicated a mainly disordered conformation, proved that FEZ1 is a dimer of elongated shape and provided overall dimensional parameters for the protein. *In vitro* pull down experiments confirmed these results and demonstrated that dimerization involves the N-terminus. *Ab-initio* 3D low resolution models of the full-length conformation of the dimeric constructs 6xHis-FEZ1(1-392) and 6xHis-FEZ1(1-227) were obtained. Furthermore, we performed *in vitro* phosphorylation assays of FEZ1 with PKC. The phosphorylation occurred mainly in its C-terminal region, and does not cause any significant conformational changes, but nonetheless inhibited its interaction with the FEZ1 interacting domain of the protein CLASP2 *in vitro*. The C terminus of FEZ1 has been reported to bind to several interacting proteins. This suggests that FEZ1 binding and transport function of interacting proteins may be subject to regulation by phosphorylation.

Proteins 2009; 74:104–121.

Key words: SAXS; spectroscopy; protein-protein interactions; microtubular transport; circular dichroism; limited proteolysis; axonal transport.

INTRODUCTION

The fasciculation and elongation protein Zeta-1 (FEZ1) was initially identified as an orthologue of the *Caenorhabditis elegans* protein UNC-76, which is necessary for the formation and extension of the worms axons.[1] In rats it was later shown that FEZ1 mRNA is abundantly expressed in early stages of the developing brain at the onset of neurogenesis.[2]

In a yeast two-hybrid assay the FEZ1 protein was identified as a prey interacting with the N-terminal domain of PKCζ.[3] Co-expression of PKCζ and FEZ1 cells alters the sub-cellular localization of the latter in COS-7 and increases the rate of differentiation to neurons in PC12 cells. Several other independent yeast two-hybrid studies employing different, and at first sight, seemingly unrelated proteins as baits, all resulted in the identification of FEZ1 as a prey. These include the nuclear protein DISC1 (Disrupted-In-Schizophrenia 1), the murine E4B U-box-type ubiquitin ligase and the agnoprotein of the human polyoma JC virus.[4–6] In the latter study a functional association of FEZ1 with microtubule was demonstrated. By co-precipitation studies it was demonstrated that FEZ1 binds to the microtubule and that the viral agnoprotein can block this interaction. Based on this activity the agnoprotein is furthermore capable of inhibiting neurite outgrowth in PC12 cells.

The involvement of FEZ1 in transport processes has clear implications for its role in neuronal differentiation and axon growth. Several recent articles explored the potential role of FEZ1 in microtubule associated transport. In rat hippocampal neurons it was

Abbreviations: CC region, coiled-coil region; CLASP2, clip-associated protein; DISC1, disrupted-in-schizophenia 1; GST, glutathione-S-transferase; FEZ1/2, fasciculation and elongation factor 1/2; KIF3A, kinesin family member 3A; NEK1, NIMA related kinase 1; PKC, protein kinase C.

Grant sponsors: Fundação de Amparo à Pesquisa do Estado São Paulo (FAPESP), projects SmolbNet, CEPID, grant number: 05/00235-1, Conselho Nacional de Pesquisa e Desenvolvimento (CNPq), the LNLS.
*Correspondence to: Jörg Kobarg, Laboratório Nacional de Luz Síncrotron, Centro de Biologia Molecular Estrutural, Rua Giuseppe Máximo Scolfaro 10.000, C.P. 6192, 13084-971 Campinas - SP, Brasil. E-mail: jkobarg@lnls.br
Received 29 October 2007; Revised 18 April 2008; Accepted 28 April 2008
Published online 9 July 2008 in Wiley InterScience (www.interscience.wiley.com).
DOI: 10.1002/prot.22135

shown that inhibition of endogenous FEZ1 protein expression by iRNA-mediated gene silencing, leads to inhibition of axonal polarization and slower transport rates of mitochondria along microtubule.[7] Another recent study identified FEZ1 as a Kinesin heavy chain interacting protein and demonstrates further that FEZ1 collaborates with JIP1 (JNK-interacting protein) in order to activate the molecular motor protein Kinesin-1.[8]

After FEZ1 frequent detection as an interacting prey protein, its C-terminal region was recently explored also as a bait in yeast two-hybrid assays in order to identify additional interacting proteins and to get new clues on the possible cellular roles of FEZ1.[9,10] A total of 36 new interacting proteins were identified that can be grouped as follows: associated to microtubular transport (including CLASP2), neuronal cell development (including FEZ1 itself, RAB3, KIBRA, HNOEL-iso, *tachykinin,* and PTPRS), apoptose (Programmed Cell Death 7), mitochondrial function (including MAGMAS, KIAA1387, TOMM20), proteins with extracellular functions (Transthyretrin, P4HB, Parathyroid hormone, COL9A2), and the regulation of transcription or other nuclear functions (including DRAP1, SAP30L, BAF60a, HTAT-SF1, TFII2F).

Proteins that interact with more than 30 other protein are frequently called hubs and the chance that they are essential for the cells functions is three times larger than that of proteins with fewer functional links.[11] Interestingly, an analysis revealed that hub proteins have been described to contain a high surface charge content, and disordered domains, which allow them to interact with a multitude of proteins.[12]

Here we describe theoretical predictions and results from spectroscopic studies and limited proteolysis experiments, all of which suggest that FEZ1 could belong to the class of natively unfolded proteins. It is already known that proteins with multiple functions have frequently a disordered intrinsic structure.[13–18] It is well known that high resolution structures of proteins with a low degree of compactness are hard to obtain and small angle X-ray scattering (SAXS) is the most adequate technique to obtain dimensional parameters and low resolution 3D conformational models of very large or partially unstructured molecules. This technique was applied to unstructured proteins such as synucleins, prothymosine alpha and P53.[19–21] The SAXS analysis in solution of 6xHis-FEZ1(1-392) and 6xHis-FEZ1(1-227) confirmed both the dimerization of FEZ1 as well as its open extended shape, compatible with a largely unfolded protein. Finally, we show that FEZ1 interaction with the microtubule proteins CLASP2 is inhibited by its phosphorylation *in vitro*. Together, our results suggest that FEZ1 presents a dimeric conformation and that its phophorylation status may regulate its interaction with other regulatory proteins or transported cargoes.

METHODS

FEZ1 secondary structure prediction and sequence analysis

Prediction of disorder in FEZ1 was performed using the program PONDR (Prediction of Natural Disordered Regions, http://www.pondr.com) using the default predictor VL-XT.[22,23] This predictor integrates the three neural networks: the VL1 predictor and N- and C-terminal predictors, which use the disordered regions identified from missing electron density in X-ray crystallography and nuclear magnetic resonance (NMR) studies. Access to PONDR is provided by Molecular Kinetics Indianapolis (www.molecularkinetics.com). Further disorder predictions were performed using the Fold Index software (http://bip.weizmann.ac.il/fldbin/findex) that predicts if a given protein sequence is intrinsically unfolded implementing the algorithm of Uversky and coworkers, which is based on the average residue hydrophobicity and net charge of the sequence.[24–26] Additional analyses were performed using 12 prediction programs: DisEMBL TM,[27] DRIPPRED,[28] DISpro,[29] GlobPlot,[30] IUPred,[31] PreLink,[32] RoNN,[33] SPRITZ,[34] FoldUnfold,[35,36] VL2,[37] VL3H,[38] VSL2,[39] available in a Database of protein disorder DISPROT (www.disprot.org/predictors.php). For coiled coil predictions we used the COILS (http://www.ch.embnet.org/software/COILS_form.html) and Multicoil (http://groups.csail.mit.edu/cb/multicoil/cgi-bin/multicoil.cgi) programs.[40,41]

Plasmid constructions

To express full-length FEZ1(1-392) or truncated FEZ1(1-227) fused to a 6xHis-tag, the corresponding nucleotide sequences were amplified by PCR and inserted into a modified version of the bacterial expression vector pET28a (Novagen/EMD Biosciences, San Diego, CA) as described.[10] pET-TEV-28a has as the main difference the substitution of the thrombin cleavage site which follows the 6xHis-tag by a TEV protease cleavage site. The fusion protein constructs of both FEZ1 protein versions have the initiating Methionine encoded by the vector, followed by an additional 31 amino acids: Gly, 6xHis-tag, 7 amino acids from the TEV cleavage site and 16 poly-linker encoded amino acids. In the case of both fusion protein constructs of FEZ1 the natural first Met residue was left out to prevent its usage as an additional translation initiation site. These protein constructs have been called 6xHis-FEZ1(1-392) or FEZ1(1-392) and 6xHis-FEZ1(1-227) or FEZ1(1-227), respectively (throughout the article). We also cloned the C-terminus of FEZ1(221-392) into pET28a, but it only showed little expression and was almost exclusively found in the insoluble fraction of the bacterial lysate. This precluded further comparative studies with the full-length and N-terminal constructions, both of which expressed very well and were very soluble.

For expression of different constructs coding indicated protein fragments fused to GST, the corresponding nucleotide sequences were cloned into a modified vector pET28a-GST that codifies GST protein upstream of the protein to be inserted. The cDNAs encoding the proteins or protein fragments identified to interact with FEZ1 in the yeast two-hybrid assay were sub-cloned from the pACT2 vector (Clontech) into bacterial expression vector pGEX-4T-2 (GE Healthcare, Waukesha, WI) as described.[10] This way full length SAP30L(1-183) and DRAP1(1-205), as well as the interacting protein fragments CLASP2(1046-1251), RAI 14 isoform(720-983), KIBRA(869-1113) and SMC3(881-1217), all fused to GST were expressed as described below.

Protein expression and purification

Soluble FEZ1 (complete 1-392, or deletion 1-227), fused to an N-terminal 6xHis-tag like described above, was purified from 1 L of culture of *E. coli* BL21 (DE3) cells that were induced for 2.5 h to protein expression at 30°C using 0.5 m*M* isopropyl 1-thio-β-D galactopyranoside. 6xHis-FEZ1(1-392) or 6xHis-FEZ1(1-227) proteins used in this study were purified using a HiTrap chelating column in an ÄKTA™ FPLC™ (GE Healthcare) as follows. Cells were harvested by centrifugation at 4500*g* for 10 min, and the cell pellet was resuspended and incubated for 30 min with 10 volumes of lysis buffer (137 m*M* NaCl, 2.7 m*M* KCl, 10 m*M* Na_2HPO_4, 1.8 m*M* KH_2PO_4, pH 7.4, 1 mg/mL lysozyme, 1 m*M* phenylmethylsulfonyl fluoride, and 0.05 mg/mL DNase). After three cycles of sonication, soluble and insoluble fractions were separated by centrifugation at 28,500*g* for 30 min at 4°C. The cleared supernatant was then loaded onto a HiTrap chelating column (GE Healthcare) preequilibrated with lysis buffer (lacking lysozyme and DNase), followed by extensive wash of the column with the same buffer. Bound proteins were eluted in a gradient of 0–100% of elution buffer (137 m*M* NaCl, 2.7 m*M* KCl, 10 m*M* Na_2HPO_4, 1.8 m*M* KH_2PO4, 1 m*M* phenylmethylsulfonyl fluoride, and 500 m*M* imidazole, pH 7.4). Aliquots of each eluted fraction obtained were analyzed by SDS-PAGE, and peak fractions containing FEZ1 fusion protein were dialyzed with PBS buffer (137 m*M* NaCl, 2.7 m*M* KCl, 10 m*M* Na_2HPO_4, 1.8 mM KH_2PO_4, pH 7.4). The proteins fused to GST were induced for expression and *E. coli* cells were lysed and processed as described above for 6xHis fusion proteins. The resulting cleared supernatant was incubated with glutathione-Uniflow resin (Clontech) and used for *in vitro* binding assays.

Circular dichroism and fluorescence spectroscopy

Circular dichroism (CD) measurements were done using a Jasco J-810 spectropolarimeter with a temperature of 25°C, controlled by a Peltier-type system PFD 425S. 6xHis-FEZ1 proteins were re-suspended in 20 m*M* Tris-HCl, pH 7.5 with 10 m*M* $MgCl_2$. Data were collected at a scanning rate of 50 nm/min with a spectral bandwidth of 1 nm using a 0.1 mm path length cell. In the TFE assay the sample concentrations were 8.1 μ*M* for 6xHis-FEZ1 (1-392) and 24.2 μM for 6xHis-FEZ1(1-227) and for the phosphorylation assays the sample concentration was 3.7 μ*M* for 6xHis-FEZ1(1-392) and 3.56 μ*M* for 6xHis-FEZ1(1-227) in 20 m*M* Tris-HCl and 10 m*M* $MgCl_2$ buffer, pH 7.5. All buffers used were of analytical grade and were filtered before use to avoid light scattering by small particles. Graphics were generated by Origin 7.5 software. Fluorescence measurements were performed at 25°C with a FP-6500 spectrofluorimeter (Jasco, Inc., Easton, MD). Intrinsic fluorescence spectra were taken between 310 and 400 nm, with excitation at 283 nm. Buffer contributions were subtracted from the raw fluorescence data to give corrected spectra.

SAXS experiments

The two protein samples were submitted to DLS (dynamic light scattering) analysis before the SAXS experiments. DLS data of two samples (6xHis-FEZ1, 1-392 and 6xHis-FEZ1, 1-227) showed narrow, single peaks and predicted masses and percentage of poly-dispersivity indicative of solutions of dimers in a monodisperse solution. The SAXS experiments were performed at the D02A-SAXS2 beamline of the Laboratório Nacional de Luz Síncrotron (LNLS, Campinas, Brazil). Measurements were performed with a monochromatic X-ray beam with a wavelength of $\lambda = 1.488$ Å. The X-ray patterns were recorded using a two-dimensional position-sensitive MARCCD detector. The sample-to-detector distances were set at 1374.4 mm and 1788.8 mm, resulting in a scattering vector range of $0.009\ \text{Å}^{-1} < q < 0.25\ \text{Å}^{-1}$, where q is the magnitude of the $\boldsymbol{q}$-vector defined by $q = (4\pi/\lambda)\sin\theta$ (2θ is the scattering angle). The samples of 6xHis-FEZ1(1-392) and 6xHis-FEZ1(1-227) in PBS buffer, were centrifuged for 30 min in an ultracentrifuge, at 356.000*g*, at 4°C to remove any aggregates or particles and then placed on ice. For SAXS measurements protein samples were placed in a 1-mm path length cell with mica windows, temperature-controlled ($T = 20$°C) via water circulation.[42] Three successive frames of 300 s each were recorded for each sample. The buffer scattering data were recorded before and after the sample scattering data for 300 s each and thereafter averaged. The scattering curves were individually corrected for the detector response and scaled by the incident beam intensity and the samples absorption. The average buffer scattering was subtracted from the corresponding sample scattering. The resulting curve was carefully inspected to check for possible radiation-induced damage, but no such effects were observed. The scattering patterns were recorded at

two different concentrations for each sample: 4.99 mg/mL and 2.57 mg/mL for 6xHis-FEZ1(1-392) and 9.17 mg/mL and 2.57 mg/mL for 6xHis-FEZ1(1-227). After scaling for concentration, the scattering data of both samples were analyzed to investigate concentration dependence. This effect was not observed. A 4.59 mg/mL bovine serum albumin (BSA, 66 kDa) solution, in the same buffer of the samples, was used as a standard sample to determine the molecular masses of the 6xHis-FEZ1 proteins. The molecular mass of each 6xHis-FEZ1 sample was inferred from the ratio of the extrapolated value of the intensity at the origin $I(0)$.[43]

SAXS data analysis

The radius of gyration was first evaluated using the Guinier approximation.[44–46] It is worth noting that in the case of an unstructured protein, the Guinier approximation holds true on a very restricted q range corresponding to $q < 1/R_g$. Such a very narrow range contains a small number of experimental points, thereby limiting the accuracy of the R_g determination. In that case, a more accurate determination of the radius of gyration can be obtained by Debye's equation,[47–51] which adequately describes the scattering in the domain $q < 1.4/R_g$ by:

$$\frac{I(q)}{I(0)} = \frac{2}{x^2}(x - 1 + e^{-x}) \qquad (1)$$

where $x = q^2R_g^2$.

Moreover, R_g was also evaluated from the pair distance distribution function $p(r)$ which was calculated using the indirect transform package GNOM.[52] The $p(r)$ function represents the histogram of all distances within a molecule and provides the maximum dimension D_{max} of the molecule where its value reaches zero.[22,23]

To analyze the natively unfolded conformation of 6xHis-FEZ1(1-227) and 6xHis-FEZ1(1-392) chains, a particularly useful representation of the SAXS intensity was used: the so-called Kratky Plot ($q^2I(q)$ vs. q). This plot is usually applied to study unstructured proteins because it provides information about the compactness of a molecule. For compact and structured proteins, the Kratky representation presents a bell-shaped plot with a well-defined maximum, because the scattering function satisfies Porod's law for large q values (i.e. $I(q)$ is proportional to $1/q^4$). Conversely, the Kratky representation of an ideal Gaussian chain,[47] (equivalent to a random coil in the case of an infinitely thin chain) presents a plateau at high q-values because $I(q)$ is proportional to $1/q^2$. Finally, in the case of a persistence length chain model, where short-range interactions between adjacent chain segments produce stiffness of the chain, the Kratky plot also displays a plateau over a specific q-range followed by a monotonic increase at still higher q-values.[50,51]

Ab initio modeling

Although the "shape" of naturally unfolded proteins is per se hard to define, we restored the low resolution average conformations of 6xHis-FEZ1(1-392) and 6xHis-FEZ1(1-227) from the experimental SAXS curves by the following *ab initio* approach. To obtain an overall view from the conformational space occupied by the proteins, the program DAMMIN,[53] was used. In this approach, each protein was represented as an assembly of densely packed spherical beads (dummy atoms) of radius $r_0 \ll D_{max}$ inside a sphere of diameter D_{max}, which was directly determined from the scattering data using the GNOM routine. Using simulated annealing, the program DAMMIN starts from a random configuration of beads and searches for a configuration that fits the experimental scattering pattern. Ten calculations were performed. The normalized spatial discrepancies (NSD) were evaluated using the DAMAVER suite,[54] and the most typical model (with lowest NSD value) were considered as close descriptions of the possible conformations of the molecule.

Limited proteolysis

Limited proteolysis with thrombin was performed by incubating 1 μg of thrombin (Sigma) with 100 μg of purified 6xHis-FEZ1(1-392) or 6xHis-FEZ1(1-227) in PBS buffer at 30°C. This corresponds to molar ratios of 1/55 and 1/83 protease/protein for the two different forms, respectively. Aliquots were collected in time intervals and reactions were stopped by adding sample buffer (50 m*M* Tris-HCl, pH 6.8, 2 m*M* EDTA, 1% sodium dodecyl sulfate (w/v), 1% β-mercaptoetanol, 8% glycerol, 0.025% bromophenol blue (w/v), 2 m*M* PMSF) and boiling for 5 min. The cleaved products were analyzed by SDS-PAGE on a 12.5% acryl amide gel. For proteolysis with proteinase K we utilized 100 ng of proteinase K for 5 μg of recombinant 6xHis-FEZ1(1-392) and 6xHis-FEZ1(1-227) as described.[55] For endogenous FEZ1 proteolysis, we used 400 ng of proteinase K which were added to the lysates of Hek293 cells.[55]

In vitro phosphorylation

For *in vitro* phosphorylation 5 μg of purified 6xHis-FEZ1(1-392) or (1-227) were incubated in 25 μL of the reaction mixture (20 m*M* Tris, 10 m*M* $MgCl_2$, 50 nm PMA; 20 m*M* ATP, pH 7.5) with 50 ng of PKC-Pan (a mixture of α, β, γ with lesser amounts of ζ and δ isoforms, purified from rat brain) or recombinant isoforms PKC α, δ, ζ (Calbiochem). After addition of 55 kBq of [γ-^{32}P]ATP (~220 TBq/mmol), the mixture was incubated at 30°C for 30 min. Samples were analyzed by SDS PAGE (10% acryl amide) and subsequent autoradiography. For spectroscopic analysis and protein–protein pull-down experiments nonradioactively labeled phospho-

6xHis-FEZ1 protein samples were prepared accordingly by leaving out the radioactive ATP. In case of the pull-down experiments FEZ1 was previously phosphorylated by PKC-Pan, and in the CD and fluorescence experiments with PKC-ζ.

In vitro binding assays and western blotting

Purified 6xHis-FEZ1 proteins were allowed to bind to 25 µL of Ni-NTA sepharose in PBS for 1 h at 4°C. After incubation, the beads containing bound recombinant proteins were washed three times with PBS at 4°C. GST or GST-fusion proteins were added to the supernatants of the protein coupled beads and incubated in 0.1 mL of PBS for 1 h at 4°C to allow protein–protein interactions to occur. The beads were then washed three times with 0.5 mL of PBS, followed by 10 washes with 1 mL NP40 buffer (1% NP-40, 0.15*M* NaCl, 50 m*M* Tris-HCl, pH 7.2, 2 m*M* EDTA), and three additional washes with 1 mL of PBS. Resin-bound proteins were run out by 10% acrylamid SDS-PAGE and transferred to PVDF membranes by electro blotting. After saturation with a solution of 5% dry milk in TBS-T (0.15*M* NaCl, 20 m*M* Tris-HCl, 0.05% Tween 20, pH 7.2), membranes were incubated either with a mouse anti-4xHis monoclonal antibody (1:5000, Qiagen) or with a mouse monoclonal anti-GST antibody 5.3.3 (hybridoma supernatant 1:5) for 1 h.[10] Alternatively, for detection of endogenous FEZ1 from Hek293 cells, we used a specific polyclonal rabbit antiserum that had been generated by four subsequent immunizations of rabbits with 1 mg 6xHis-FEZ1(131-392) fusion protein. After three washes with TBS-T (0.15*M* NaCl, 20 m*M* Tris-HCl, 0.05% Tween 20, pH 7.2), the membranes were incubated with the secondary horseradish peroxidase conjugated anti-rabbit IgG antibody (1:5000; Santa Cruz Biotechnology) for 1 h and washed again three times with TBS. The membranes were developed by chemi-luminescence using the reagent Luminol (Santa Cruz Biotechnology) for detection of His-tagged or GST fusion proteins. Interaction assays with proteins that interacted with FEZ1 in the two hybrid assay were performed as described.[10]

RESULTS

FEZ1 secondary structure prediction

A bioinformatics analysis of the amino acid sequence of human FEZ1 with the computer programs Fold Index and PONDR predicted a large contend of potentially unstructured regions [Fig. 1(A)]. PONDR predicts disordered regions throughout the whole sequence of FEZ1 but especially in the N-terminal and central regions of the protein sequence. Only at the C-terminus a short structured region was predicted. These predictions are at large in agreement with those obtained by the Fold index software. Additional analysis by 13 different predicting softwares at large confirmed these data that FEZ1 presents basically two unfolded regions with great probability in the N-terminal (regions between amino acids, 1-69 and 110-229) and a higher probability of structuring at the C-terminal (data not shown).

Using the software COILS and a window size of 28, we identified one region with a high probability to form coiled coils in the region between amino acids 230–265 (∼96% probability). The software MULTICOILS identified (window 28) more or less the same region (233–261, probability ∼54%). One additional region identified only by COILS but of high probability is located further C-terminal (278–306, probability ∼63%) and three regions of low probability at the N-terminus of FEZ1. The MultiCoil software furthermore predicted that the coiled coil region has a higher probability to form dimer than trimer coils.

Circular dichroism spectropolarimetry

To address the prediction of a largely disordered structure for FEZ1 experimentally we performed CD spectropolarimetry experiments. The spectrum of 6xHis-FEZ1(1-392) has an pronounced minimum at 205 nm as well as in the regions 208 and 222 nm [Fig. 1(B)]. 6xHis-FEZ1(1-227) has a pronounced minimum at 205 nm region. Disordered proteins or unfolded proteins are characterized by minima in their far UV CD spectra around 200 and 205 nm.[56] Therefore the spectra of full-length and even so more that of 6xHis-FEZ1(1-227) show clear characteristics of largely disordered proteins. This is in agreement with the theoretical secondary structure prediction by 12 softwares on the NPS@ server (http://npsa-pbil.ibcp.fr), which indicated an average of 48.7% of alpha helix, 41.13% of random coil and 4.73% of ambiguous regions in the amino acid sequence of FEZ1. Interestingly, the CD spectrum of full-length 6xHis-FEZ1 and 6xHis-FEZ1(1-227) showed a change in profile upon addition of 5% of TFE [Fig. 1(B,C)]. The change in the shape of the spectrum of full length FEZ1 suggests that there is a visible global gain of mainly α-helical content. This could suggest that FEZ1, although intrinsically disordered, can gain structure not only upon addition of TFE but also upon encountering with interacting proteins. The low signal intensity in this experiment may be explained by a certain aggregation of FEZ1 at higher concentrations, although we did not observe any precipitation during the experiments. Additional CD analyses, however, revealed a gain of signal in lower concentrations of FEZ1 (data not shown).

SAXS measurements

The corrected and normalized experimental SAXS curves for 6xHis-FEZ1(1-227) and 6xHis-FEZ1(1-392)

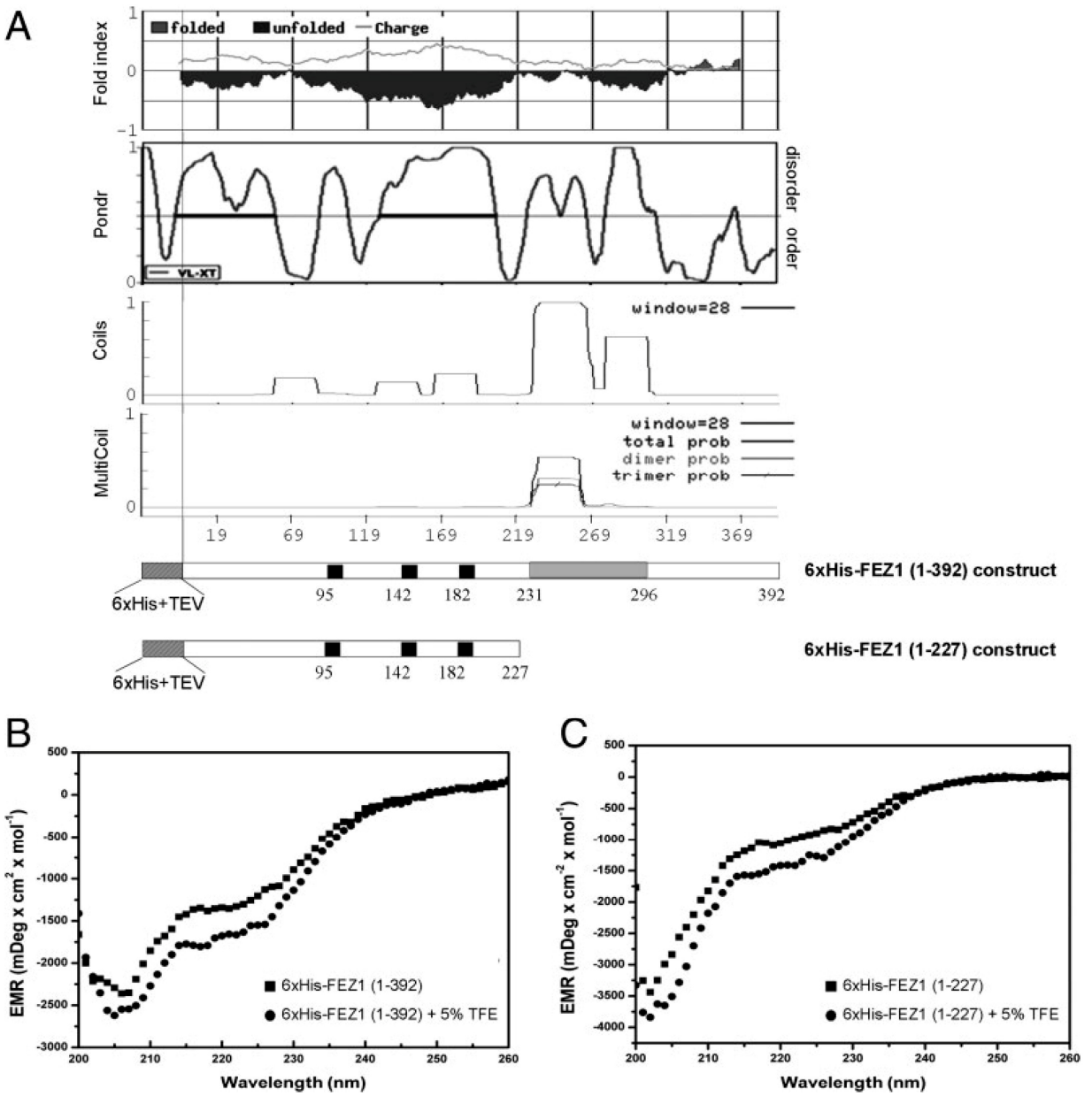

Figure 1

FEZ1 has features of a natively unfolded protein. (**A**) Unstructured and coiled-coil regions were predicted in the amino acid sequence of the fusion protein 6xHis-FEZ1(1-392) expressed from the plasmid peT28a. The y axes represent structure probability scores in the "Fold index" and "PONDR" softwares or coiled-coil probability in the "Coils" and "MultiCoil" programs. The x axis represents the amino acid sequence of human FEZ1. The fusion protein constructs of both FEZ1 protein versions have the initiating Methionine encoded by the vector, followed by an additional 31 amino acids: Gly, 6xHis-tag, 7 amino acids from the TEV cleavage site and 16 poly-linker encoded amino acids. In the case of both fusion protein constructs of FEZ1 the natural first Met residue was left out, to prevent usage of an additional translation initiation site. Schematic representations of the full-length human FEZ1(1-392) and the N-terminal fragment FEZ1(1-227) constructs are shown. At its N-terminal region FEZ1 contains three motifs rich in glutamic acid residues (black boxes). At its C-terminal region it contains an extensive coiled- coil region (grey box) of up to 65 amino acids. The indicated amino acid numberings refer to the native complete FEZ1 amino acid sequence. (**B**) Circular dichroism (CD) measurements indicate a secondary structure composition consisting mainly of random coil regions and alpha helices in 6xHis-FEZ1(1-392). A small but significant gain in alpha helix content is observed upon addition of 5% TFE in the CD spectrum of 6xHis-FEZ(1-392). (**C**) 6xHis-FEZ1(1-227) shows predominantly random coil content. Small change in the alpha-helical signal of 6xHis-FEZ1(1-227) was observe upon addition of 5% TFE.

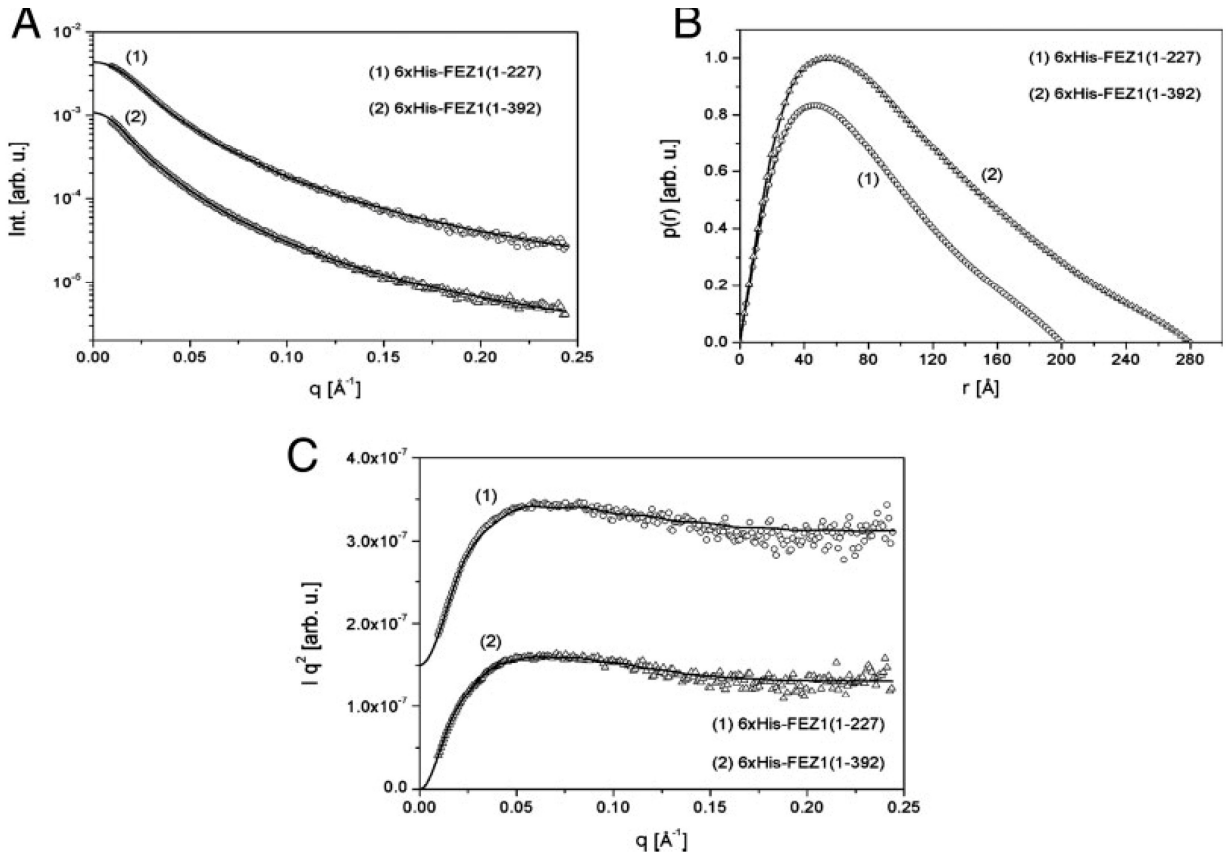

Figure 2

Experimental SAXS curves for human 6xHis-FEZ1(1-392) and 6xHis-FEZ1(1-227) in solution and the results of the fitting procedures. (**A**) Experimental scattering curve of 6xHis-FEZ1(1-227) (open circles) and 6xHis-FEZ1(1-392) (open triangles) and the theoretical fitting (solid lines) of data by using the program GNOM. (**B**) Pair distance distribution functions p(r). (**C**) Kratky Plots. In (A) and (C) the curve of 6xHis-FEZ1(1-392) was dislocated by a constant factor to allow better visualization and comparison.

are displayed in Figure 2(A), together with the individual GNOM curve fittings (solid lines). The $p(r)$ functions resulting from these calculations are shown in Figure 2(B). The maximum dimension values obtained for the molecules were 200 Å for 6xHis-FEZ1(1-227) and 280 Å for 6xHis-FEZ1(1-392). The R_g values derived from Guinier's law, Debye's law [see Eq. (1) above] and the $p(r)$ functions were respectively 62 ± 2 Å, 62.9 ± 0.3 Å, and 61.6 ± 0.6 Å for 6xHis-FEZ1(1-227), and 80 ± 2 Å, 84.6 ± 0.2 Å, and 83 ± 1 Å for 6xHis-FEZ1(1-392). The most reliable R_g value for each molecule is that obtained from the $p(r)$ function because it takes into account the complete experimental curve. However, all these values are in close agreement. It is interesting to compare the hydrodynamic radii estimated by DLS: 40 Å for 6xHis-FEZ1(1-227) and 47 Å for 6xHis-FEZ1(1-392) with those radii of gyration determined by SAXS (∼62 and ∼83 Å, respectively). The resulting ratios R_g/R_h are 1.55 and 1.77, respectively for the two constructs of FEZ1. Interestingly, ratios of this magnitude are frequently observed for proteins with extended shape. R_g/R_h ratios are reported to vary from 0.78 for homogeneous spheres, up to values nearing 2 for extended coils and prolate ellipsoids.[57]

Using BSA as reference sample, the molecular masses for FEZ1 proteins were obtained from SAXS results by comparison with the BSA scattering data. The values of ∼60 kDa for 6xHis-FEZ1(1-227) and ∼95 kDa for 6xHis-FEZ1(1-392) indicate that both the full length protein and the N-terminal construct exist in a dimeric state in solution, since the values obtained are approximately twice the theoretically values (calculated from the primary sequence using ProtParam)[58]: 29.7 kDa for 6xHis-FEZ1(1-227) and 48.6 kDa for 6xHis-FEZ1(1-392). These overall parameters suggest that both molecules have relatively elongated shapes, which is also evidenced by the

corresponding asymmetric and characteristic shapes of the p(r) functions. The Kratky plots of the two proteins are shown in Figure 2(C). Both representations are similar and they display a plateau for $q > 0.15$ Å^{-1}. The absence of a maximum clearly indicates that both the 6xHis-FEZ1(1-227) and 6xHis-FEZ1(1-392) present flexible chains and do not adopt compact conformations. These data suggest that both the full-length protein and the N-terminal construct are dimeric molecules with a largely open conformation.

Ab initio shape determination of human FEZ1

The low resolution *ab-initio* shapes of human 6xHis-FEZ1(1-227) and 6xHis-FEZ1(1-392) were restored from the experimental data using the approach described in "Experimental procedures". The low resolution structure models were derived from the experimental data without imposing any symmetry constrains for the dimers. As already mentioned in a previous section, in the absence of a unique solution for the *ab initio* calculations, several runs were performed for each protein with similar results. The obtained models from *ab-initio* calculations for 6xHis-FEZ1(1-227) and 6xHis-FEZ1(1-392) are shown in Figure 3(A,B), respectively. The NSD values for the set of 10 DAMMIN models ranged from 0.87 to 1.00. The low resolution of this representation only shows that the conformations of both proteins are extended. Inspection of the shapes obtained for 6xHis-FEZ1(1-227) [Fig. 3(A)] and 6xHis-FEZ1(1-392) [Fig. 3(B)], reveals a close resemblance of the conformations obtained for both proteins. The ratio between the DAMIN predicted volumes of 6xHis-FEZ1(1-392) and 6xHis-FEZ1(1-227) equals 1.52. This value is fairly close to ratio 1.65 of the number of amino acids of the two protein constructs.

Limited proteolysis of FEZ1

Natively unfolded proteins are due to their intrinsic flexibility more susceptible to proteolytical cleavage in comparison to more structured globular proteins which are more resistant.[59] Therefore, we submitted FEZ1 to proteolytical cleavage by thrombin and proteinase K [Fig. 4(A–D)]. We observed that when we incubated both 6xHis-FEZ1(1-392) and 6xHis-FEZ1(1-227) with thrombin a stable fragment of about 36 kDa appeared at 15 min and showed no further degradation up to 48 h. Other fragments are observed, which disappear until 48 h of digestion, indicating that they are intermediate products of cleavage. It is important to mention that both FEZ1 proteins, probably due to their high content of charged amino acids, show an anomalous mobility in SDS-PAGE: 6xHis-FEZ1(1-392) runs like a protein of about 70 kDa, although predicted to have a molecular mass of 48.6 kDa. 6xHis-FEZ1(1-227) runs like a protein of about 45–50 kDa, inspite a theoretical prediction of 29.7 kDa. The aberrant electroporetic mobility is a typical feature of intrinsic unstructured proteins and was observed for other proteins with intrinsically disordered regions and charged regions. Proteolysis with proteinase K generated similar results, giving rise to a prominent band of about 40 kDa in the case of both types of proteins [Fig. 4(C,D)]. However, this band is only stable up to 10 min, after which time point we can no longer detect 6xHis-FEZ1 in the SDS-PAGE. Next, we analyzed the same samples by anti-4xHis Western blot and were able to detect the same stable ~40 kDa band [Fig. 4(E,F)]. This indicates that both the full length and the N-terminal construct of 6xHis-FEZ1(1-227) still maintained their 6xHis-containing N-terminus and suggests that proteolysis occurs from the direction of the C-terminus inwards to the central region of the protein.

Finally, we submitted also endogenous FEZ1, from a Hek 293 cell extract, to limited proteolysis [Fig. 4(G)]. By Western blot, we found again a stable band of about 40 kDa, which maintained stability up to 30 min of incubation with proteinase K. Interestingly, this band was already present before incubation with proteinase K, suggesting that FEZ1 may suffer cleavage or proteolytical degradation either already *in vivo* or immediately after lysate preparation. Incubation of the control protein BSA for up to 40 min *in vitro* with proteinase K [Fig. 4(H)] did not show any signs of degradation. This demonstrates the capacity of the performed reactions to distinguish between globular (BSA) and open/unfolded proteins (FEZ1).

In summary, these results suggest that FEZ1 behaves like a natively unfolded protein with an open and flexible conformation which is susceptible to a significant amount of proteolysis under conditions that did not result in any cleavage in the globular control protein BSA. On the other hand we observe the accumulation of a relatively stable N-terminal fragment of about 40 kDa, which still contains the 6xHis-tag, and which is probably stabilized by the formation of the dimer (see Fig. 3).

Phosphorylation of FEZ1 by PKC at its C-termius *in vitro*

It was already known that FEZ1 interacts with PKCζ and that FEZ1 is phosphorylated.[3] A prediction of phosphorylated amino acids using the NetPhos software (http://www.cbs.dtu.dk/services/NetPhos/), showed that FEZ1 has possible Ser and Thr phosphorylation sites with varying probability of phosphorylation throughout its whole amino acid sequence (not shown). Using the program NetPhosK (http://www.cbs.dtu.dk/services/NetPhosK/) and defining a minimum score of 50% for PKC phosphorylation sites, we were able to identify six possible PKC sites (score ranging from 50.3–85.5), all of which are located in the C-terminal region of FEZ1 [Fig. 5(B,C)], right after the first predicted coiled-coil region

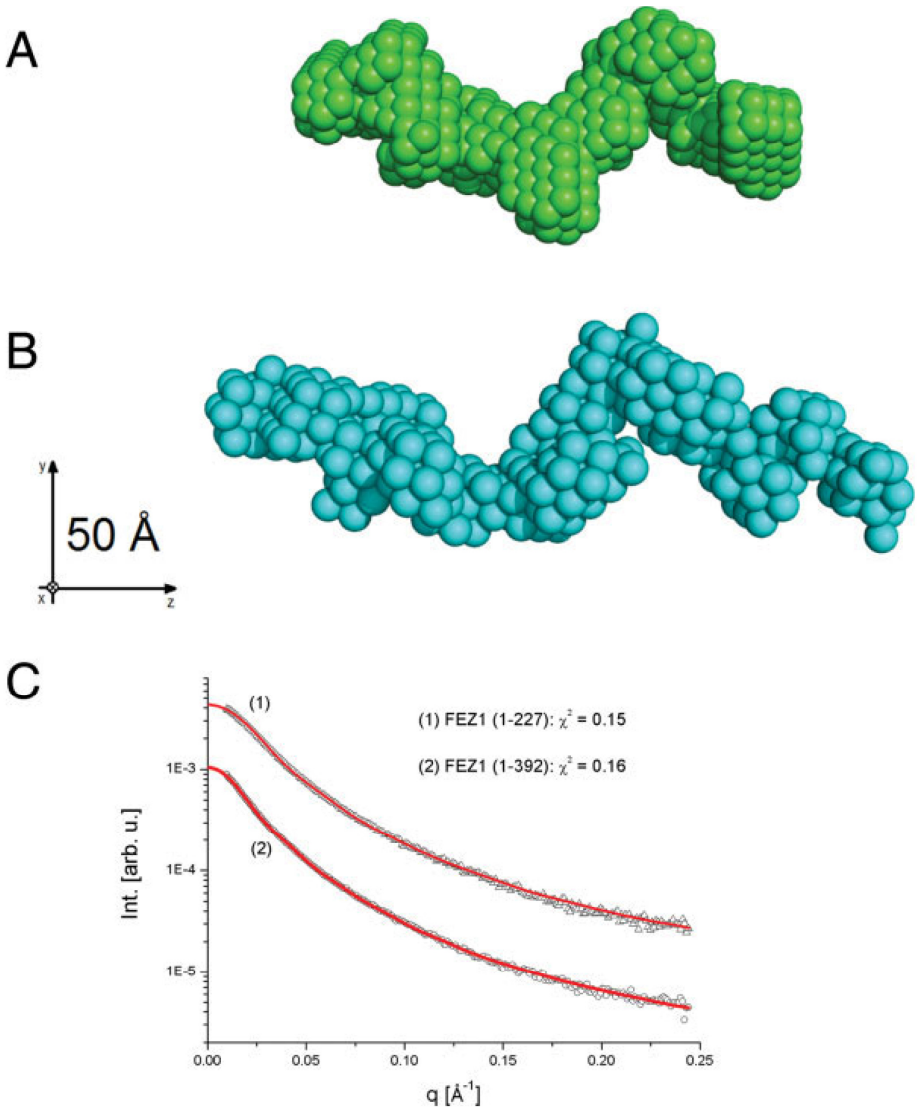

Figure 3

Low resolution *ab initio* models derived from the SAXS data. (**A**) Selected view of the 6xHis-FEZ1(1-227) dimer model (green). (**B**) Selected view of the 6xHis-FEZ1(1-392) dimer model (blue). The models were displayed by the program PyMOL.[67] (**C**) Curve fitting evaluated from the most typical model to the experimental data using DAMMIN.

(>aa 270). Two of them also scored high in phosphorylation probability in the NetPhos program [S326 and T331, Fig. 5(A)].

Based on these predictions we next employed both 6xHis-FEZ1(1-392) and 6xHis-FEZ1(1-227) in *in vitro* phosphorylation assays with recombinant PKC isoforms α, δ *e* ζ as well as with PKC-Pan [Fig. 5(D)]. 6xHis-FEZ1(1-227) as well as the control protein GST suffered some phosphorylation, but only by PKC-Pan suggesting that this phosphorylation may be rather unspecific. FEZ1(1-392) however was strongly phosphorylated by all tested PKC isoforms, especially by PKC Pan and PKC δ. The fact that the full length but not the N-terminal region of FEZ1 was phosphorylated under the same conditions, suggests strongly that the C-terminal region of FEZ1 could be the main target of phosphorylation by PKCs, as predicted theoretically [Fig. 5(A–C)]. The N-terminal of FEZ1(1-227) in contrast has only few predicted sites of phosphorylation by PKC and the observed phosphorylation by PKC Pan might be unspecific, as also indicated by the much weaker intensity of the band when compared to that of full length FEZ1.

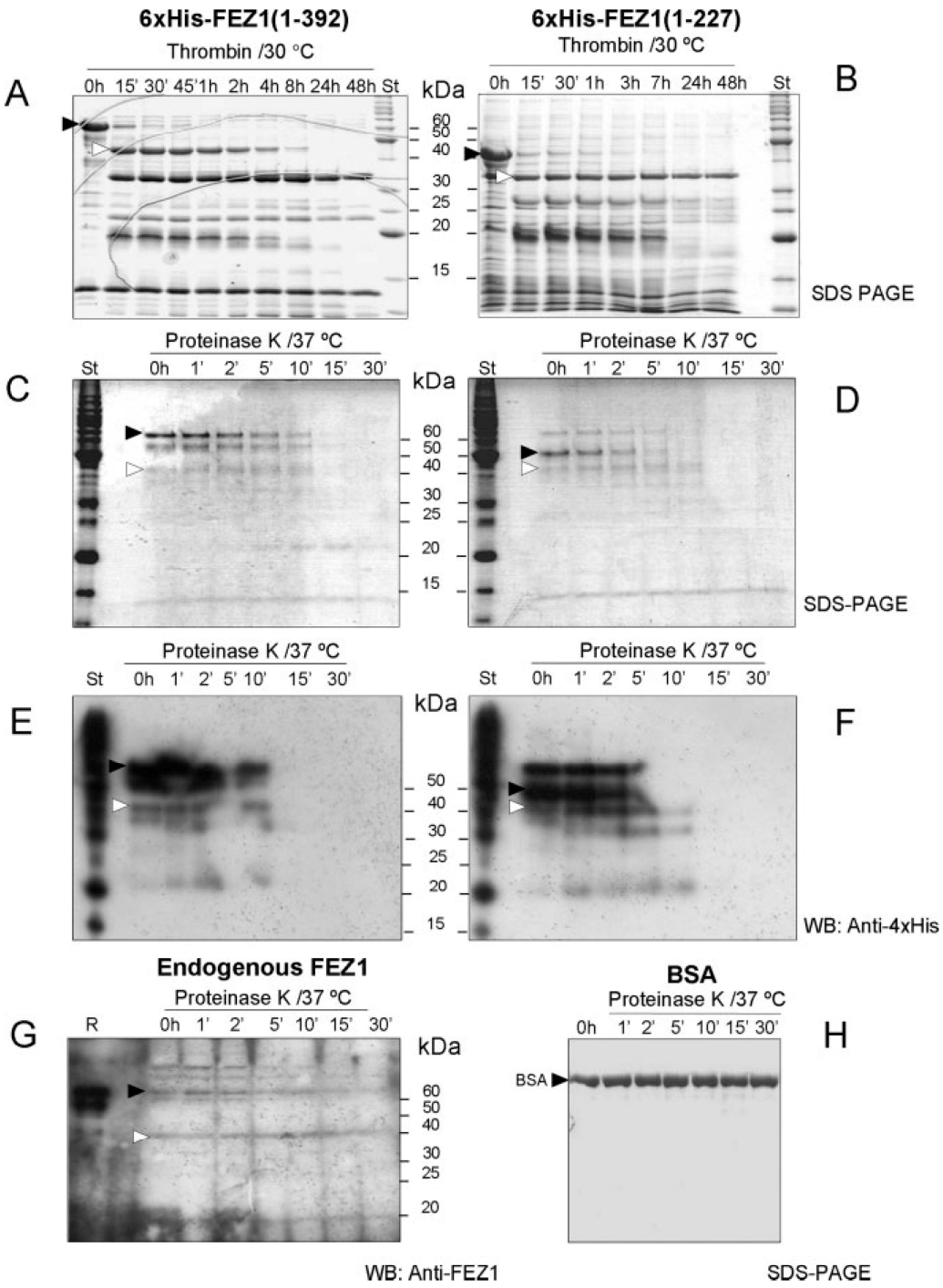

Figure 4

Limited proteolysis of 6xHis-FEZ1(1-392), 6xHis-FEZ1(1-227) and endogenous, cellular FEZ1 results in a common stable N-terminal fragment of ~40 kDa. (**A–D**) After incubation for the indicated times at the indicated temperatures of 6xHis-FEZ1(1-392) or 6xHis-FEZ1(1-227) with thrombin or proteinase K, samples were analyzed by SDS-PAGE (12.5% acryl amid). (**E–F**) anti-4xHis Western blot analysis of the proteolysis profile of the FEZ1 proteins obtained after digestion with proteinase K. (**G**) Proteolysis of endogenous FEZ1 from Hek 293 lysate, with proteinase K, followed by Western blot (anti FEZ1). (**H**) Control SDS-PAGE of proteinase K digested BSA. St: Protein molecular weight standard; R- recombinant 6xHis-FEZ1(1-392). The black arrows indicate undigested FEZ1 (A-G) or undigested BSA (H) and the white arrows the stable fragment from the N-terminus of FEZ1.

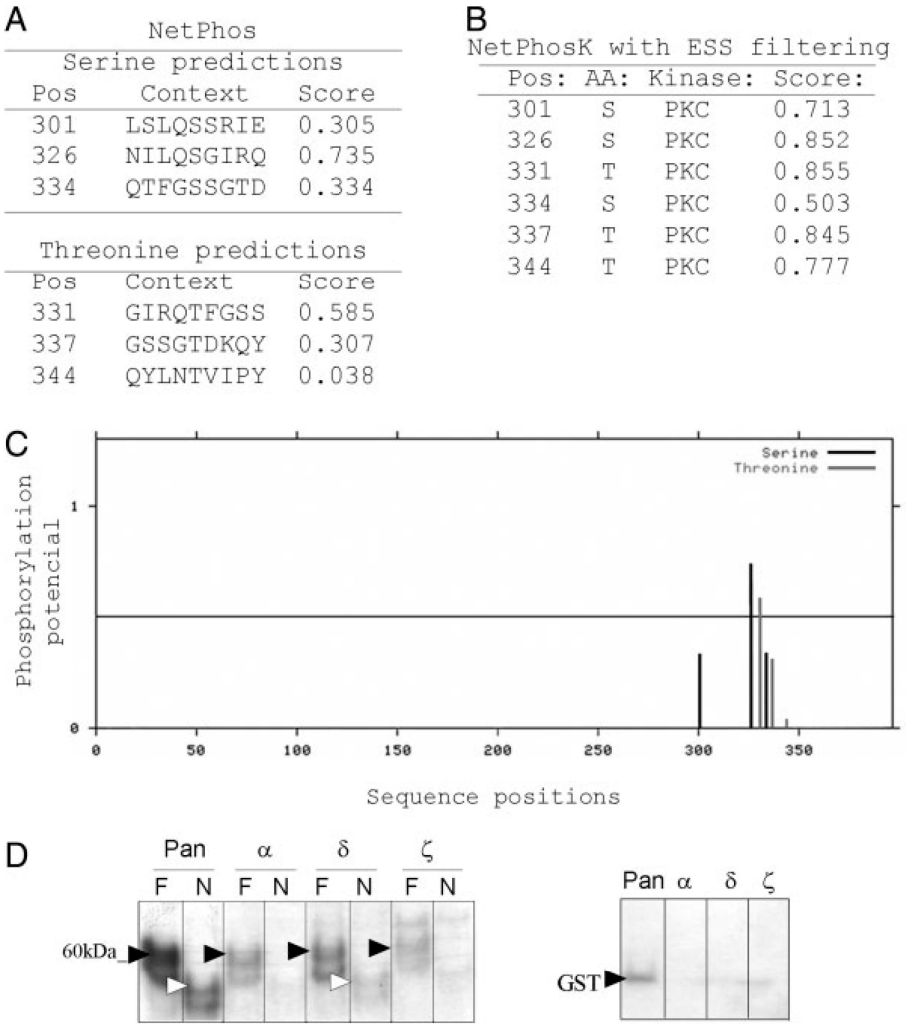

Figure 5

PKCα, δ and ζ phosphorylate 6xHis-FEZ1 mainly in its C-terminal region *in vitro*. (**A,B**) Commons predicted phosphorylation sites in human FEZ1 amino acid sequence as identified by NetPhos (A) and NetPhosK programs (B). (**C**) Graphic plot of the phoshorylation site prediction in FEZ1 as predicted by NetPhos. The peaks indicate the localization in the amino acid sequence (*x* axis) and the probability (*y* axis) of the phosphorylation. Only common PKC specific sites also predicted by NetPhosK are shown. (D) *In vitro* phosphorylation by different isoforms of PKC of 6xHis-FEZ1(1-392) (=F), 6xHis-FEZ1(1-227) (=N) and GST control protein. The indicated proteins have been submitted to *in vitro* phosphorylation by indicated PKC isoform, then analyzed by SDS-PAGE and autoradiography. The autoradiography is shown. The black arrows indicate phosphorylated 6xHis-FEZ1(1-392) (left panel) or GST control (right panel). White arrows indicate phosphorylated 6xHis-FEZ1(1-227).

These data in summary suggest that FEZ1 C-terminus is the main target of phosphorylation by PKCs. The fact that the C-terminal region also interacts with all the FEZ1 interacting proteins,[10] indicates that it may represent a critical region for phosphorylation dependent regulation of a subset of the interactions.

FEZ1 dimerization does not depend on its C-terminus or phosphorylation status

Next, we performed *in vitro* FEZ1/FEZ1 pull down assays to test if the phosphorylation status of FEZ1 influences its dimerization and to map protein regions involved in the dimerization process (see Fig. 6). In a first round of experiments we coupled full length or 6xHis-FEZ1(1-227) in both its apo- or phospho-forms (the latter previously phosphorylated by PKC *in vitro*) to Ni-NTA sepharose beads. A subsequent incubation was performed with either apo- or phospho GST-FEZ(1-392) or GST-FEZ(1-227) [Fig. 6(A,B)]. The results show clearly that the phosphorylation status of neither the beads-coupled FEZ1 nor that of GST-FEZ1 in the supernatant had any influence on the dimerization of FEZ1. Furthermore, we can also observe

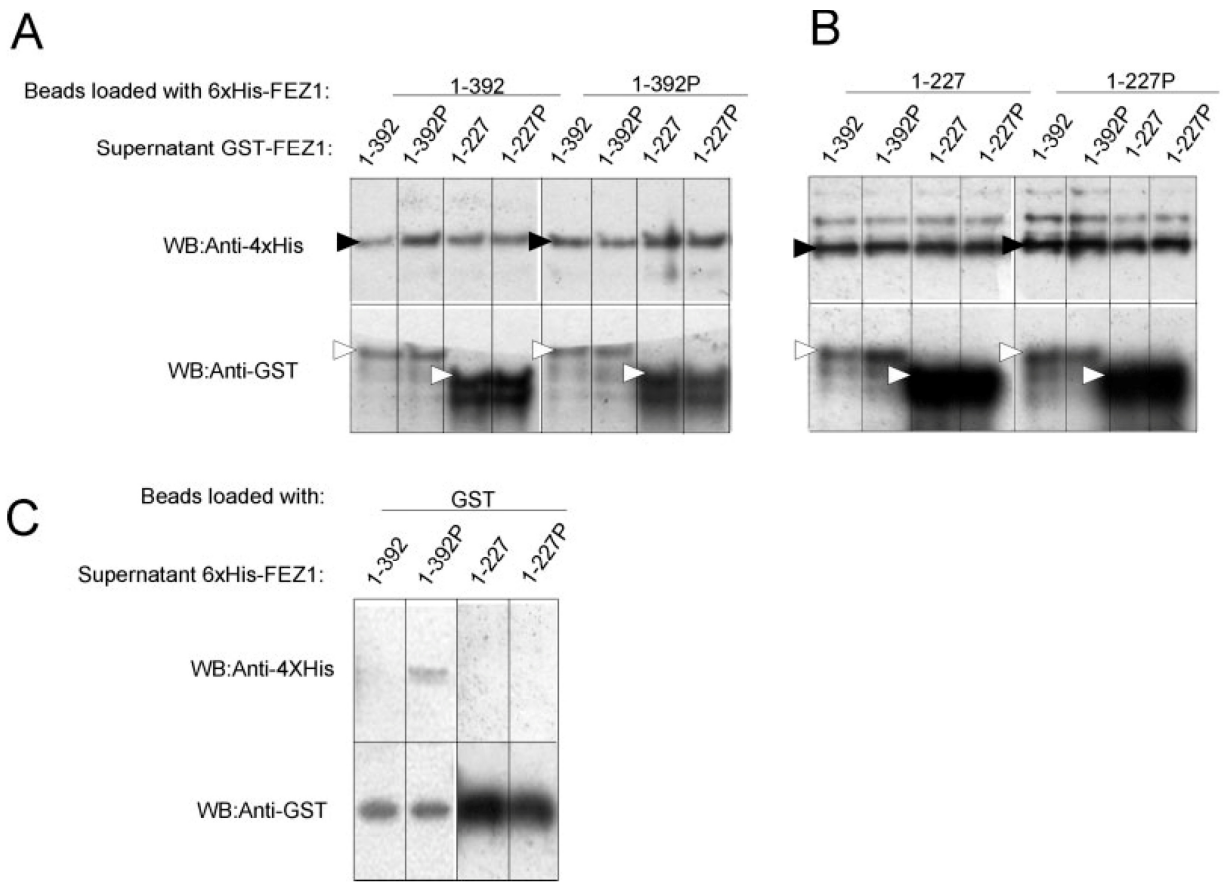

Figure 6

FEZ1 dimerization does not depend on its C-terminal region and is not influenced by its phosphorylation status. (**A,B**) *In vitro* pull-down assay between apo- or phospho-6xHis- or GST-FEZ1(1-392) (A) or FEZ1(1-227) constructs (B). 6xHis-FEZ1 fusion constructs were coupled to Ni-NTA sepharose beads, and the similar constructs fused to GST (as indicated in the figure) added to the supernatant for interaction (P, Phospho protein). After high stringency washes using NP-40 buffer, the aliquots were separated on two separate SDS-PAGE and transferred to a PVDF membranes for Western blot analysis. Blots were developed using either the monoclonal mouse anti-5xHis tag antibody or anti-GST monoclonal antibody 5.3.3. The black arrows indicate the positions of the 6xHis-proteins and the white arrows the GST fusion proteins. (C) GST was loaded onto glutathione sepharose beads. After washing beads were incubated with indicated 6xHis-FEZ1 apo- or phospho-proteins and washed stringently again. After separation on two separate SDS-PAGE the blots were developed as above.

that the dimerization occurs predominantly through the N-terminal region of FEZ1. In a second round of control experiments we coupled GST to glutathione-sepharose beads and subsequently incubated them with apo- or phospho-6xHis-FEZ1(1-227) or -FEZ1(1-392) [Fig. 6(C)]. No significant interaction was observed this time, except a weak but unspecific interaction between GST and phospho-6xHis-FEZ1(1-392). This demonstrates the specificity of the dimerization experiments described above. In summary, these data suggest, that FEZ1 dimerizes via its N-terminal domain and that in the dimer the outwards pointing C-terminal regions, which contain the coiled-coil regions, are free to interact with other proteins. Furthermore, the C-terminals of the FEZ1 dimer are accessible to phosphorylation by PKC, which may regulate some of the interactions.

FEZ1 phosphorylation does not promote conformational changes

The *in vitro* phosphorylation of neither 6xHis-FEZ1(1-227) nor 6xHis-FEZ1(1-392) promotes any significant changes in the secondary structure when monitored by circular dichroism spectroscopy [Fig. 7(A,B)]. Three Trp residues which are located in the N-terminal region of FEZ1 can be used as fluorescence probes to assay any changes in tertiary structure upon phosphorylation. However, no significant differences were observed in the fluorescence emission spectra of apo- and phospho-6xHis-FEZ1(1-227) or -FEZ1(1-392) [Fig. 7(C,D)]. Together these data indicate that the phosphorylation of FEZ1 does not promote any spectroscopically detectable changes in its conformation. This is in agreement with the observations that dimerization

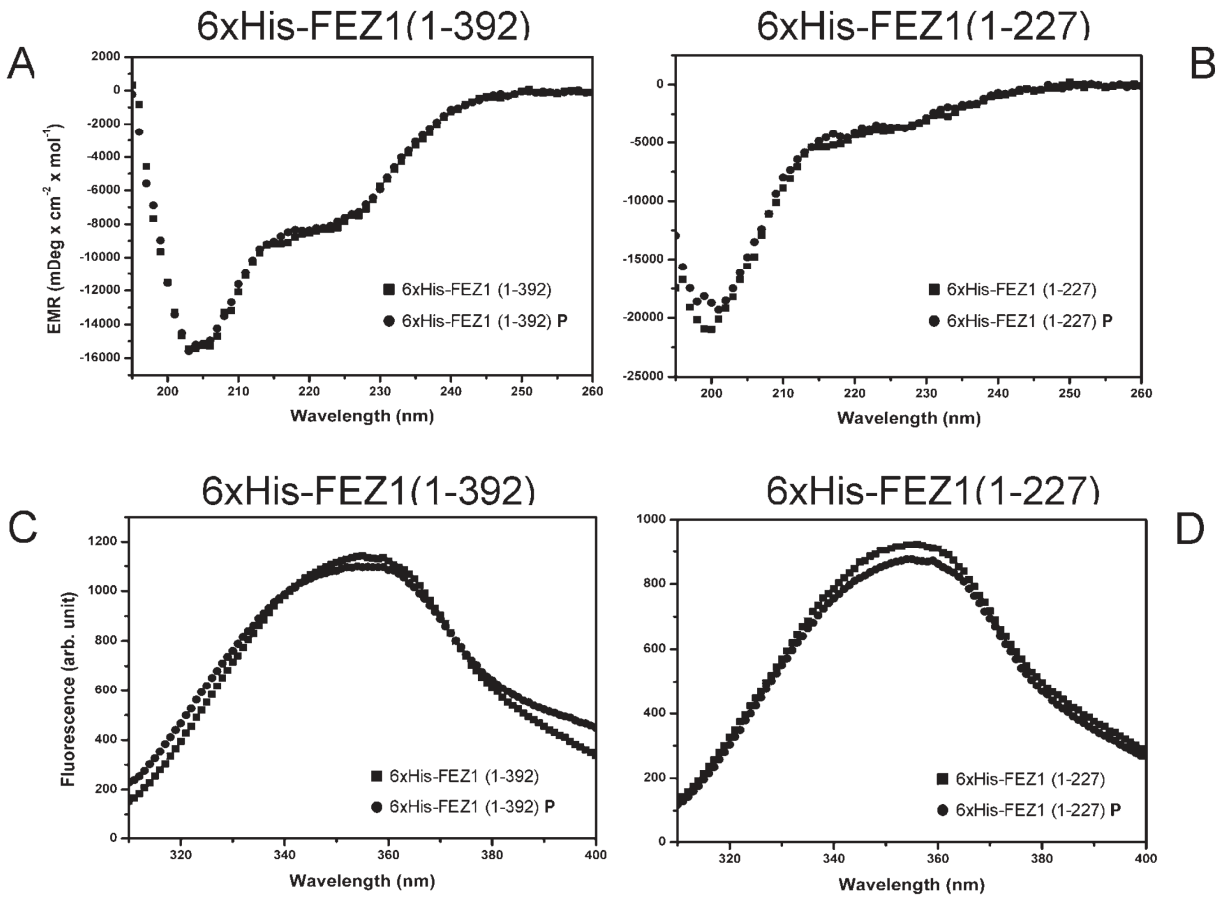

Figure 7

In vitro phosphorylation by PKC-ζ does not promote detectable conformational changes in FEZ1. (**A**) Circular dichroism experiment of 6xHis-FEZ1(1-392). Residual molar ellipticity of apo- and phospho (P) 6xHis-FEZ1(1-392) was measured from 195 to 260 nm in 20 m*M* Tris-HCl buffer, pH 7.5 with 10 m*M* $MgCl_2$ at 25°C, using a Jasco J-810 spectropolarimeter. (**B**) Circular dichroism experiment of apo- and phospho-6xHis-FEZ1(1-227). (**C**) Fluorescence spectroscopy experiment of apo- and phospho-6xHis-FEZ1(1-392). Samples were excited at 283 nm and fluorescence emission was recorded from 310 to 400 nm. (**D**) Fluorescence spectroscopy experiment of apo- and phospho-6xHis-FEZ1(1-227).

occurs at the N-terminus and phosphorylation predominantly at the C-terminus, which is not involved in the dimerization and structure maintenance but whose main function may be, as our data suggest, to interact with other proteins.

FEZ1 phosphorylation inhibits its interaction with CLASP2 *in vitro*

To test whether the phosphorylation status of FEZ1 can influence its interaction with other interacting proteins, we performed *in vitro* pull down assays between apo- and phospho-6xHis-FEZ1(1-392) and a subset of those proteins or protein fragments we had previously described to interact with FEZ1 (see Fig. 8).[10] Among the six GST fusion proteins tested, CLASP2(1046-1251) ceased to interact with FEZ1(1-392) when the latter had been phosphorylated by PKC *in vitro*. The observed lack of interaction with CLASP2 is specific, since none of the other five proteins showed a decreased interaction after phosphorylation of FEZ1 and GST even showed a weak but unspecific binding to phospho- but not apo-FEZ1. CLASP2 is a protein of important intracellular transport functions and localizes to the growing tip of microtubule.[60] A multiprotein transport complex associated to microtubule and consisting of FEZ1/JIP1/Kinesin has also been described.[8] Together, this suggests that FEZ1 may be involved in microtubular transport processes and that the interaction with CLASP2 could be regulated by phosphorylation.

DISCUSSION

FEZ1 is an orthologue of the *C. elegans* protein UNC-76 and both proteins have been shown to be of crucial

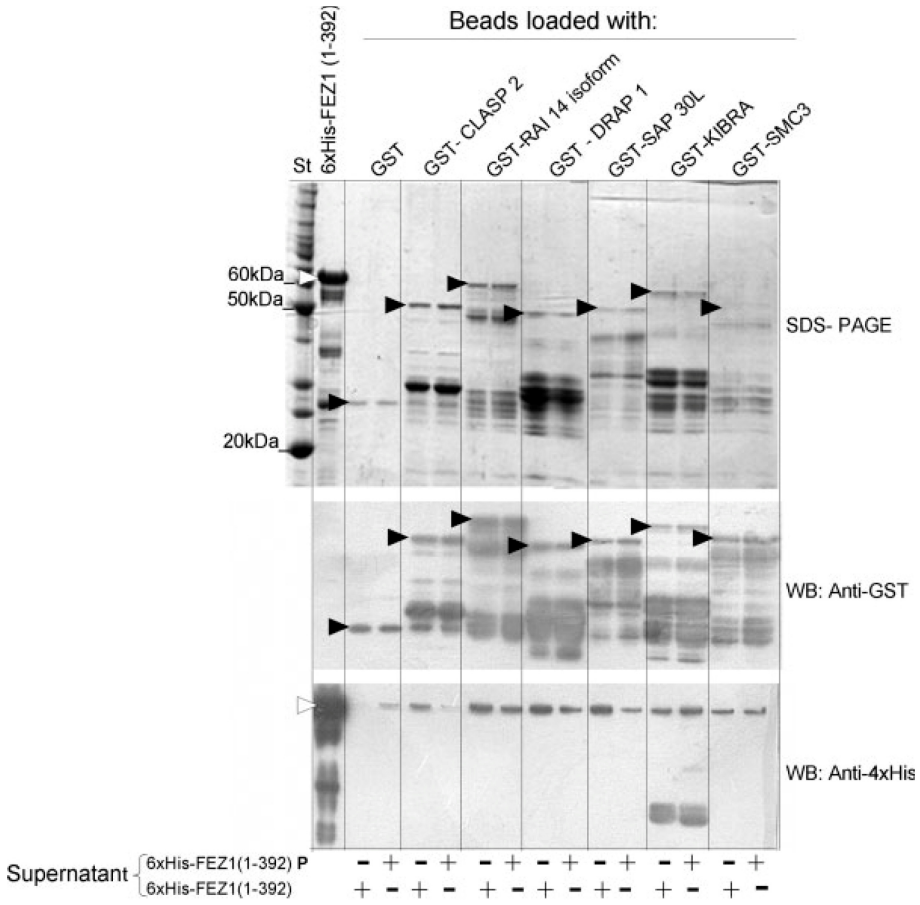

Figure 8

Phosphorylation of 6xHis-FEZ1(1-392) by PKC-ζ inhibits its interaction with the FEZ1 interaction domain of protein CLASP2 *in vitro*. *In vitro* pull-down assays between apo-(=FEZ1) or phospho-6xHis-FEZ1(1-392) (=FEZ1P) and selected proteins or protein fragments fused to GST that have been previously identified to interact with FEZ1.[10] GST, GST-CLASP2(1046-1251), GST-RAI14-isoform(720-983), GST-DRAP1(1-205), GST-SAP30L(1-183), GST-KIBRA(869-113), and GST-SMC3(881-1217) were loaded onto glutathione-sepharose beads. After washing the loaded beads were incubated with purified apo-6xHis-FEZ1(1-392) or phospho-6xHis-FEZ1(1-392), previously phosphorylated *in vitro* by PKC-ζ. After high stringency washes, samples were analyzed by Coomassie-stained SDS-PAGE and Western blotting. Blots were developed with monoclonal mouse anti-GST antibody 5.3.3 or anti-4xHis monoclonal antibody. Black arrows indicate the positions of the GST fusion proteins and the white arrows the position of FEZ1. ST, molecular weight standard proteins.

importance in neuronal differentiation and axonal outgrowth and elongation.[1,3,5] Recent experimental data pin point FEZ1 main activity in the course of axonal outgrowth to a microtubule associated cargo transport function,[7] since the inhibition of FEZ1 protein expression via iRNA-mediated interference leads to a retardation of the anterograde mitochondrial transport along the neurites of hippocampal neurons. Furthermore, the mitochondria in theses cells are elongated and the axon formation and neuronal polarization are inhibited, possibly in consequence of a lack of mitochondrial anterograde transport and an associated lack of metabolic energy supply in the growing axon tip. Further recent molecular evidence support this vision by associating FEZ1 physically and functionally to the heavy chain of the molecular motor protein Kinesin-1.[8] It was demonstrated that FEZ1 cooperates in conjunction with JIP-1 to activate the molecular motor activity of Kinesin-1.

Here we report a 3D low resolution structural model of the FEZ1 dimer, which we obtained by studying both the full length 6xHis-FEZ1 as well as a deletion construct representing amino acids 6xHis-FEZ1(1-227) of its N-terminus by SAXS measurements and *ab initio* modeling.

FEZ1 C-terminal region is an important protein–protein docking domain where all of the interacting proteins identified and tested up to now interact.[9,10] If we assume that the two C-termini of the full length FEZ1 dimer point outwards, away from the center of the dimer, which seem to involve its N-terminus [compare Fig. 3(A) and 3(B)], this may suggest that the interacting

hub proteins, which have the need to interact with multiple proteins.[12] Furthermore, multiple functions have been described for various natively unfolded proteins, similar to FEZ1, which has been implicated in transcriptional regulation, intracellular transport and neuronal cell development.[13,64,65]

The majority of these functions are regulated by protein phosphorylation, which in this case may not regulate the protein activity and binding to other proteins through conformational changes, since natively unfolded proteins tend to be rather structurally disordered. Regulation of interaction may occur rather by simple electrostatic or steric blockage of a region important in contacting a specific interacting protein. Indeed our studies of the *in vitro* phosphorylation of FEZ1 by PKC suggest that this could be the case also for FEZ1. We found that the overall secondary and tertiary structures of FEZ1 are basically not affected by its phosphorylation through PKC. The additional findings that the phophorylation is almost absent in the N-terminal region of FEZ1 suggested that the C-terminal is the main site for phosphorylation, *in vitro*. This is further supported by the fact that dimerization, which involved the N-terminal region of FEZ1, is not at all affected by phosphorylation.

The C-terminus represents on the other hand the main protein docking region of FEZ1, suggesting that phophorylation could be an important event for the regulation of interaction with other proteins. We indeed found that interaction with the microtubular tip protein CLASP2 *in vitro* is practically blocked after phosphorylation of FEZ1. The interaction of FEZ1 with CLASP2 may be of crucial importance to understand the mechanism underlying our recent observation that the over-expression of GFP-FEZ1 in Hek293 cells causes the microtubular dependent formation of multi-lobulated nuclei, a hall mark of aggressive leukemia cells.[66] Further studies must address the importance of FEZ1 phosphorylation *in vivo* in this process and the elucidation of the mechanism that causes the multi-lobulation of the nuclei will be important for our understanding of the steps that lead to development of these cancer cells. It is however tempting to speculate that FEZ1 bivalency and its characteristic as a hub protein, able to interact with many proteins, especially the microtubular components including CLASP2, KIF3A, and tubulin, may prove to be essential to explain the observed phenotype.

In summary, our data suggest that human FEZ1 has several features of natively unfolded proteins. Its dimer configuration in solution, may suggest that it could act as a bivalent transport adaptor protein. The two C-terminal regions of the dimer are pointing outwards and may serve as docking domains for cargos and/or to make contact with microtubules via CLASP2, KIF3A or other connecting proteins, yet to be identified. Future high resolution structural studies of protein complexes may reveal the details of the previously described interactions with cargo proteins or microtubule associated proteins.[9,10] Functional cellular studies should also be performed to determine FEZ1 exact role in transport processes and the exact mode by which it connects to microtubules.

ACKNOWLEDGMENTS

The authors thank Maria Eugenia R. Camargo, Zildene D. Correa and Adriana C. Alves for technical assistance. This work was performed at the: Laboratório Nacional de Luz Síncrotron, Campinas, SP, Brasil.

REFERENCES

1. Bloom L, Horvitz HR. The *Caenorhabditis elegans* gene *unc*-76 and its human homologs define a new gene family involved in axonal outgrowth and fasciculation. Proc Natl Acad Sci USA 1997; 94:3414–3419.
2. Fujita T, Ikuta J, Hamada J, Okajima T, Tatematsu K, Tanizawa K, Kuroda S. Identification of a tissue-non-specific homologue of axonal fasciculation and elongation protein zeta-1. Biochem Biophys Res Commun 2004;313:738–744.
3. Kuroda S, Nakagawa N, Tokunaga C, Tatematsu K, Tanizawa K. Mammalian homologue of the *Caenorhabditis elegans* UNC-76 protein involved in axonal outgrowth is a protein kinase C zeta-interacting protein. J Cell Biol 1999;114:403–411.
4. Honda A, Miyoshi K, Baba K, Taniguchi M, Koyama Y, Kuroda S, Katayama T, Tohyama M. Expression of fasciculation and elongation protein zeta-1 (FEZ1) in the developing rat brain. Brain Res Mol Brain Res 2004;122:89–92.
5. Okumura F, Hatakeyama S, Matsumoto M, Kamura T, Nakayama K. Functional regulation of FEZ1 by the U-box-type Ubiquitin ligase E4B contribuyes to neuritogenesis. J Biol Chem 2004; 279:53533–53543.
6. Suzuki T, Okada Y, Semba S, Orba Y, Yamanouchi S, Endo S, Tanaka S, Fujita T, Kuroda S, Nagashima K, Sawa H. Identification of FEZ1 as a protein that interacts with JC virus agnoprotein and microtubules. J Biol Chem 2005;280:24948–24956.
7. Ikuta J, Maturana A, Fujita T, Okajima T, Tatematsu Kenji, Tanizawa K, Kuroda S. Fasciculation and elongation protein zeta-1 (FEZ1) participates in the polarization of hippocampal neuron by controlling the mitochondrial motility. Biochem Biophys Res Commun 2007;353:127–132.
8. Blasius TL, Cai D, Jih GT, Toret CP, Verhey KJ. Two binding partners cooperate to activate the molecular motor Kinesin-1. J Cell Biol 2007;176:11–17.
9. Stelzl U, Worm U, Lalowski M, Haenig C, Brembeck FH, Goehler H, Stroedicke M, Zenkner M, Schoenherr A, Koeppen S, Timm J, Mintzlaff S, Abraham C, Bock N, Kietzmann S, Goedde A, Tokso ZE, Droege A, Krobitsch S, Korn B, Birchmeier W, Lehrach H, Wanker EE. A human protein-protein interaction network: a resource for annotating the proteome. Cell 2005;122:957–968.
10. Assmann EM, Alborghetti MR, Camargo MER, Kobarg J. FEZ1 dimerization and interaction with transcription regulatory proteins involves its coiled-coil region. J Biol Chem 2006;281:9869–9881.
11. Jeong H, Mason SP, Barabasi AL, Oltvai ZN. Lethality and centrality in protein networks Nature 2001;411:41–42.
12. Patil A, Nakamuraa H. Disordered domains and high surface charge confer hubs with the ability to interact with multiple proteins in interaction networks. FEBS Lett 2006;580:2041–2045.
13. Dunker AK, Cortese MS, Romero P, Iakoucheva LM, Uversky VN. Flexible nets. The roles of intrinsic disorder in protein interaction networks. FEBS J 2005;272:5129–5148.

14. Ekman D, Light S, Bjorklund AK, Elofsson A. What properties characterize the hub proteins of the protein-protein interactrion network of *Saccharomyces cerevisiae*? Genome Biol 2006,7:R45.
15. Haynes C, Oldfield CJ, Ji F, Klitgord N, Cusick ME, Radivojac P, Uversky VN, Vidal M, Iakoucheva LM. Intrinsic disorder is a common fetature of hub proteins from four eukaryotic interactomes. PLoS Comput Biol 2006,2:e100.
16. Dosztanyi Z, Chen J, Dunker AK, Simon I, Tompa P. Disorder and sequence repeats in hub proteins and their implications for network evolution. J Proteome Res 2006;5:2985–2995.
17. Singh GP, Dash D, Intrinsic disorder in yeast transcriptional regulatory network. Proteins 2007;68:602–605.
18. Tompa P. The interplay between structure and function in intrinsically unstructured proteins. FEBS Lett 2005;579:3346–3354.
19. Uversky VN, Fink AL. Conformational behavior of human alpha-synuclein is modulated by familial Parkinson's disease point mutations A30P and A53T. Neurotoxicology 2002;23:553–567.
20. Uversky VN, Gillespie JR, Millett IS, Khodyakova AV, Vasiliev AM, Chernovskaya TV, Vasilenko RN, Kozlovskaya GD, Dolgikh DA, Fink AL, Doniach S, Abramov VM. Natively unfolded human prothymosin alpha adopts partially folded collapsed conformation at acidic pH. Biochemistry 1999;38:15009–15016.
21. Tidow H, Melero R, Mylonas E, Freund SMV, Grossmann JG, Carazo JM, Svergun DI, Valle M, Fersht A. Quaternary structures of tumor surppressor p53 and a specific p53-DNA complex. Proc Natl Acad Sci USA 2007;104:12324–12329.
22. Romero P, Obradovic Z, Dunker AK. Sequence data analysis for long disordered regions prediction in the calcineurin family. Genome Inf Ser 1997;8:110–124.
23. Romero P, Obradovic Z, Li X, Garner EC, Brown CJ, Dunker AK. Sequence complexity of disordered protein. Proteins 2001;42:38–48.
24. Uversky VN, Gillespie JR, Fin AL. Why are natively unfolded proteins unstructured under the physiological conditions? Proteins: Struct Funct Genet 2000;42:415–427.
25. Oldfield CJ, Cheng Y, Cortese MS, Brown CJ, Uversky VN, Dunker AK. Comparing and combining predictors of mostly disordered proteins. Biochemistry 2005;44:1989–1200.
26. Prilusky J, Felder CE, Zeev-Ben-Mordehai T, Rydberg E, Man O, Beckmann JS, Silman I, Joel L, Sussman JL. FoldIndex: a simple tool to predict whether a given protein sequence is intrinsically unfolded. Bioinformatics 2005;21:3435–3438.
27. Linding R, Jensen LJ, Diella F, Bork P, Gibson TJ, Russell RB. Protein disorder prediction: implications for structural proteomics. Structure 2003;11:1453–1459.
28. MacCallum RM. Order/disorder prediction with self organizing maps. Online paper. Available at: http://www.forcasp.org/paper2127.html. CASP 6 meeting.
29. Cheng J, Sweredoski M, Baldi P. Accurate prediction of protein disordered regions by mining protein structure data. Data Mining Knowl Discov 2005;11:213–222.
30. Linding R, Russell RB, Neduva V, Gibson TJ. Glob plot: exploring protein sequences for globularity and disorder. Nucleic Acids Res 2003;31:3701–3708.
31. Dosztanyi Z, Csizmok V, Tompa P, Simon I. IU Pred: web server for the prediction of intrinsically unstructured regions of proteins based on estimated energy content. Bioinformatics 2005;21:3433–3434.
32. Coeytaux K, Poupon A. Prediction of unfolded segments in a protein sequence based on amino acid composition. Bioinformatics 2005;21:1891–1900.
33. Yang ZR, Thomson R, McNeil P, Esnouf RM. RONN: the bio-basis function neural network technique applied to the detection of natively disordered regions in proteins. Bioinformatics 2005;21:3369–3376.
34. Vullo A, Bortolami O, Pollastri G, Tosatto S. Spritz: a server for the prediction of intrinsically disordered regions in protein sequences using kernel machines Nucleic Acids Res 2006;34:W164–W168.
35. Garbuzynskiy SO, Lobanov MY, Galzitskaya OV. To be folded or to be unfolded? Protein Sci 2004;13:2871–2877.
36. Galzitskaya OV, Garbuzynskiy SO, Lobanov MY. Prediction of natively unfolded regions in protein chain. Mol Biol (Mosk) 2006;40:341–348.
37. Vucetic S, Brown CJ, Dunker AK, Obradovic Z. Flavors of protein disorder. Proteins 2003;52:573–584.
38. Obradovic Z, Peng K, Vucetic S, Radivojac P, Brown CJ, Dunker AK. Predicting intrinsic disorder from amino acid sequence. Proteins 2003;53:566–572.
39. Obradovic Z, Peng K, Vucetic S, Radivojac P, Dunker AK. Exploiting heterogeneous sequence properties improves prediction of protein disorder. Proteins 2005;7:176–182.
40. Lupas A, Van Dyke M, Stock J. Predicting coiled coils from protein sequences. Science 1991;252:1162–1164.
41. Wolf E, Kim PS, Berger B. MultiCoil: a program for predicting two and three-stranded coiled coils. Protein Sci 1997;6:1179–1189.
42. Cavalcanti LP, Torriani IL, Plivelic TS, Oliveira CLP, Kellermann G, Neuenschwander. Two new sealed sample cells for small angle X-ray scattering from macromolecules in solution and complex fluids using synchrotron radiation. R Rev Sci Inst 2004;75:4541–4546.
43. Orthaber D, Bergmann A, Glatter O. J Appl Crystallogr 2000;33:218–255.
44. Guinier A, Fournet G. Small angle scattering of X-rays, translated by Walker CB and Yudowitch KL. New York: Wiley; 1955, pp 5–78.
45. Feigin LA, Svergun DI. Structure analysis by small angle X-ray and neutron scattering. New York: Plenum Press; 1987, pp 59–104.
46. Glatter O, Kratky O. Small angle X-ray scattering. New York: Academic Press; 1982, pp 17–50.
47. Kirste RG, Oberthür RC. Small angle X-ray scattering. In: Glatter O, Kratky O, editors. London, New York: Academic Press; 1982, pp 387–431.
48. Debye PJ. Molecular-weight determination by light scattering. Phys Colloid Chem 1947;51:18–32.
49. Calmettes P, Durand D, Desmadril M, Minard P, Receveur V, Smith JC. How random is a highly denatured protein? Biophys Chem 1994;53:105–114.
50. Perez J, Vachette P, Russo D, Desmadril M, Durand D. Heat-induced unfolding of neocarzinostatin, a small all-beta protein investigated by small-angle X-ray scattering. J Mol Biol 2001;308:721–743.
51. Moncoq K, Broutin I, Craescu CT, Vachette P, Ducruix A, Durand D. SAXS study of the PIR domain from the Grb14 molecular adaptor: a natively unfolded protein with a transient structure primer? Biophys J 2004;87:4056–4064.
52. Svergun DI. Determination of the regularization parameter in indirect-transform methods using perceptual criteria. J Appl Cryst 1992;25:495–503.
53. Svergun DI. Restoring low resolution structure of biological macromolecules from solution scattering using simulated annealing. Biophys J 1999;76:2879–2886.
54. Volkov VV, Svergun DI. Uniqueness of ab initio shape determination in small-angle scattering. J Appl Cryst 2003;36:860–864.
55. Denning DP, Uversky V, Patel SS, Fink AL, Rexach M. The *Saccharomyces cerevisiae* nucleoporin Nup2p is a natively unfolded protein. J Biol Chem 2002;36:33447–33455.
56. Uversky VN. Natively unfolded proteins: a point where biology waits for physics. Protein Sci 2002;11:739–756.
57. Rizos AK, Tsikalas I, Morikis D, Galanakis P, Spyroulias GA, Krambovitis E. Characterization of the interaction between peptides derived from the gp120/V3 domain of HIV-1 and the amino terminal of the chemokine receptor CCR5 by NMR spectroscopy and light scattering. J Non-Cryst Solids 2006;352:4451–4458.
58. Gasteiger E, Hoogland C, Gattiker A, Duvaud S, Wilkins MR, Appel RD, Bairoch A. Protein identification and analysis tools on the ExPASy server. In: Walker JM, editor. The proteomics protocols handbook. Totowa, NJ: Humana Press; 2005, pp 571–607.

59. Fontana A, Polverino de Laureto P, Spolaore B, Frare E, Picotti P, Zambonin M. Probing protein structure by limited proteolysis. Acta Biochim Pol 2004;51:299–321.
60. Mimory-Kiyouse Y, Grigoriev I, Lansberger G, Sasaki H, Matsui C, Severin F, Galjart N, Grosveld F, Vorobjev I, Tsukita S, Akhmanova A. CLASP1 and CLASP2 bind to EB1 and regulate microtubule plus-end dynamics at the cell cortex. J Cell Biol 2005;168:141–153.
61. Naghavi MH, Hatziioannou T, Gao G, Goff SP. Overexpression of fasciculation and elongation protein ζ-1 (FEZ1) induces a post-entry block to retroviruses in cultured cells. Genes Dev 2005;19:1105–1115.
62. Fujita T, Maturana AD, Ikuta J, Hamada J, Walchli S, Suzuki T, Sawa H, Wooten MW, Okajima T, Tatematsu K, Tanizawa K, Kuroda S. Axonal guidance protein FEZ1 associates with tubulin and kinesin motor protein to transport mitochondria in neurites of NGF-stimulated PC12 cells. Biochem Biophys Res Commun 2007; 361:605–610.
63. Shimizu K, Shirataki H, Honda T, Minami S, Takai Y. Complex formation of SMAP/KAP3, a KIF3A/B ATPase motor-associated protein, with a human chromosome-associated polypeptide. J Biol Chem 1998;273:6591–6594.
64. Dafforn TR, Smith CJI. Natively unfolded domains in endocytosis: hooks, lines and linkers. EMBO reports 2004;5:1046–1052.
65. Ward JJ, Sodhi JS, McGuffin LJ, Buxton BF, Jones DT. Prediction and functional analysis of native disorder in proteins from the three kingdoms of life J Mol Biol 2004;337:635–645.
66. Lanza DCF, Trindade DM, Assmann EM, Kobarg J. Over-expression of GFP-FEZ1 causes generation of multi-lobulated nuclei mediated by microtubules in HEK293 cells. Exp Cell Res 2008, doi: 10.1016/j.yexcr, 2008.02.012
67. DeLano WL. The PyMOL molecular graphics system, DeLano Scientific, Palo Alto, CA, USA, 2002.

Artigo 2

Over-expression of GFP-FEZ1 causes generation of multi-lobulated nuclei mediated by microtubules in HEK293 cells

Lanza DC, Trindade DM, Assmann EM, Kobarg J.

Experimental Cell Research (2008)314(10):2028-2039

Received 19 October 2007;
Revised version received 20 February 2008
Accepted 26 February 200
Available online 4 March 2008

doi:10.1016/j.yexcr.2008.02.012
pISSN: 0014-4827
eISSN: 1090-2422
NLM ID: 0373226

Over-expression of GFP-FEZ1 causes generation of multi-lobulated nuclei mediated by microtubules in HEK293 cells

Daniel C.F. Lanza[a,b], *Daniel M. Trindade*[a,b], *Eliana M. Assmann*[a], *Jörg Kobarg*[a,b,*]

[a]*Laboratório Nacional de Luz Síncrotron, Campinas SP, Brazil*
[b]*Instituto de Biologia, Universidade Estadual de Campinas, Campinas, SP, Brazil*

ARTICLE INFORMATION

Article Chronology:
Received 19 October 2007
Revised version received
20 February 2008
Accepted 26 February 2008
Available online 4 March 2008

Keywords:
Microtubule transport
Flower-like nuclei
Multi-lobulated nuclei
Centrosome

ABSTRACT

FEZ1 (Fasciculation and elongation protein zeta 1) is an ortholog of the *Caenorhabditis elegans* protein UNC-76, involved in neuronal development and axon outgrowth, in that worm. Mammalian FEZ1 has already been reported to cooperate with PKC-zeta in the differentiation and polarization of PC12 neuronal cells. Furthermore, FEZ1 is associated with kinesin 1 and JIP1 to form a cargo-complex responsible for microtubule based transport of mitochondria along axons. FEZ1 can also be classified as a hub protein, since it was reported to interact with over 40 different proteins in yeast two-hybrid screens, including at least nine nuclear proteins. Here, we transiently over-expressed GFP-FEZ1full in human HEK293 and HeLa cells in order to study the sub-cellular localization of GFP-FEZ1. We observed that over 40% of transiently transfected cells at 3 days post-transfection develop multi-lobulated nuclei, which are also called flower-like nuclei. We further demonstrated that GFP-FEZ1 localizes either to the cytoplasm or the nuclear fraction, and that the appearance of the flower-like nuclei depends on intact microtubule function. Finally, we show that FEZ1 co-localizes with both, α- and especially with γ-tubulin, which localizes as a centrosome like structure at the center of the multiple lobules. In summary, our data suggest that FEZ1 has an important centrosomal function and supply new mechanistic insights to the formation of flower-like nuclei, which are a phenotypical hallmark of human leukemia cells.

Introduction

The protein FEZ1 (Fasciculation and Elongation protein Zeta-1) was initially identified as an ortholog of the *Caenorhabditis elegans* protein UNC-76, necessary for the formation and elongation of axon bundles in that worm [1]. FEZ1 is expressed during all phases of the central nervous system development in rats and is required for neurite extension, neuronal

development and also the differentiation of PC12 cells, where it actuates together with protein kinase C zeta -PKCζ [2]. Several reports have indicated FEZ1 to be essential for neuronal polarization and transport processes, especially of mitochondria [3]. On a mechanistic level the transport function of FEZ1 has been physically and functionally connected to the scaffolding protein JIP1 and the heavy chain of kinesin 1 [4]. Another report demonstrated that FEZ1 not only interacts with the polyoma viral agnoprotein, but also directly with microtubules [5]. The inhibition of the latter interaction diminishes neurite outgrowth in PC12 cells. Finally, fibroblast which super-express FEZ1 become resistant to retroviral infection, possibly due to an inhibition of the capsids transport to, or entry in the nucleus of the cell, where the life cycle of the virus is completed [6].

FEZ1 has been frequently identified as a prey protein in two-hybrid assays of several other proteins, including NEK1 [7], PKCζ [2] and the polyomavirus agno protein [5]. Since FEZ1 N-terminus has auto-activating activity in the yeast-two-hybrid assay, only recently its C-terminal was explored as a bait in two independent screens, that resulted in the identification of 36 new proteins that interact with FEZ1 [8,9]. The high number of interacting proteins allows the classification of FEZ1 as a hub protein. The identified interacting proteins can be grouped in functional groups ranging from neuronal development (KIBRA, RAB3-GAP), microtubule transport (CLASP2, SMC3, PTPRS), to nuclear functions, including transcriptional regulation (DRAP1, BAF60a, SAP30L, HTAT-SF1) and sister chromatid cohesion (SMC3). The large number of nuclear proteins identified suggests that FEZ1 may have some nuclear function. While some of the many identified FEZ1 interacting proteins may represent interacting partners that are required for its direct functions (PKC-zeta, JIP1, CLASP2) others may represent rather transported cargo proteins.

Here we studied the effect of the over-expression of GFP-tagged full-length FEZ1 (1–392) and a construct representing only its N-terminal region (GFP-FEZ1, 1–227) on HEK293 cells. We not only observed that GFP-FEZ1(1–392) localizes to the nuclear fraction but also the pronounced formation of flower-

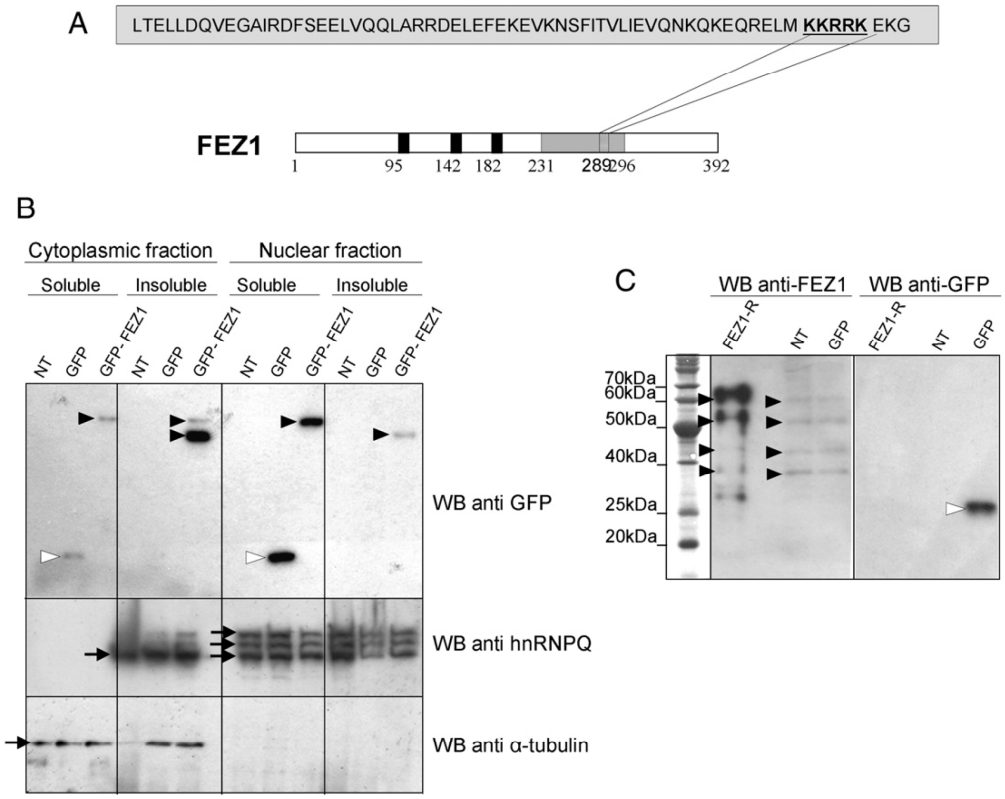

Fig. 1 – FEZ1 presents C-terminal nuclear localization signal (NLS) and is present in the nucleus when over-expressed in HEK293 cells. (A) The NLS predictor PSORT II software indicates a NLS in the region between the amino acids 289 and 293 of FEZ1. In its N-terminal region FEZ1 contains three motifs rich in glutamic acid residues (black boxes) and at its C-terminal region an extensive coiled-coil region (grey box) of up to 65 amino acids (residues 231–296). (B) Lysates of HEK293 cells expressing GFP and GFP-FEZ1 (1–392) were separated in cytoplasmic and nuclear, soluble and insoluble fractions, and analyzed by Western blotting where GFP (white arrowhead) and GFP-FEZ1 (1–392) (black arrowhead) were identified. As controls, untransfected HEK293 cells were used (NT). Anti-hnRNPQ and anti-α-tubulin western blots were performed for loading control of nuclear and cytoplasmic fractions, respectively (black arrows). (C) Demonstration of the specificities of the GFP antibody and the anti-FEZ1 antiserum used in this study. Lysates of HEK 293 cells non-transfected (NT) or transfected to express GFP (GFP) were analyzed by Western blot with anti-GFP (white arrowhead) or anti-FEZ1 (black arrowheads). Recombinant bacterially expressed and purified 6xHisFEZ1 was also used as a positive control (FEZ1-R).

like multi-lobulated nuclei upon its super-expression, in all transfected cells. Nocodazole treatment completely abolished the multi-lobulated nucleus formation, indicating the necessity of intact microtubule for the formation of the flower-like nuclei. Furthermore, both endogenous FEZ1, as well as GFP-FEZ1 (1–392) co-localize with α-tubulin but especially with γ-tubulin, which is located at the microtubule organization center localized in the center of the multiple lobules. Together, this suggests an important role for FEZ1 in the molecular mechanisms that underlie the development of flower-like nuclei, which occur with regularity in certain types of leukemia.

Materials and methods

Plasmid constructions

FEZ1 (1–392) or truncated FEZ1 (1–227) encoding nucleotide sequences were amplified by PCR and cloned into bacterial expression vector pET28a (Novagen/EMD Biosciences, San Diego, CA) as described [9]. Full-length FEZ1 (1–392) or truncated FEZ1 (1–227) were subcloned in pEGFPC2 vector (Clontech) for expression of GFP-tagged proteins in human cells.

Transfection

Adherent HEK293 or HeLa cells were cultivated on cover slips in 24-well or in 6-well plates containing MEM medium, 10% FCS and penicillin and streptomycin at a concentration of ~1.2×10^4 cells/plate (24-well) or ~5×10^4 cells/plate(6-well) at 37 °C and 5% CO_2 atmosphere. Transfections were performed by the calcium phosphate method and monitored by inverted fluorescence microscope.

Subcellular fractionation of HEK293 cells and commercial antibodies

Untransfected control cells or cells transfected with either empty pEGFP vector or pEGFP-FEZ1 (1–392) construct were utilized 40 h post-transfection. The first step of fractionation was the separation of the intact nuclei and cytoplasm total fractions. Cells were harvested and washed twice in ice-cold phosphate buffer (PBS), (137 mM NaCl, 0.3 mM KCl, 8.1 mM Na_2HPO_4, 6.7 mM KH_2PO_4, pH 7.2), resuspended in ice-cold low salt buffer (LSB) (10 mM Tris–HCl pH 7.4, 320 mM sucrose, 2 mM $MgCl_2.6H_2O$, 0.3 mM $CaCl_2.2H_2O$, 0.4% NP-40, 0.5 mM fresh DTT), homogenized, and incubated at 0 °C for 12 min with gentle agitation every 2 min. Nuclei were precipitated by centrifugation at 800 ×*g* for 2 min at 4 °C and the supernatant (cytoplasmic fraction) was collected. The nuclear fraction were suspended in PBS and sonicated on ice for 15 s. The cytoplasmic and nuclear fractions were submitted to 20,000 ×*g* centrifugation at 4 °C for 20 min and the supernatants were considered as the soluble fractions and the pellets as the insoluble fractions. The fractions were subjected to SDS-PAGE 10% and analyzed by Western blotting using an rabbit polyclonal anti-GFP (1:2000, Sigma), mouse monoclonal anti-hnRNPQ (1:5000, Abcam) or mouse monoclonal anti α-tubulin (1:2500, Santa Cruz Biotechnology) primary antibodies and secondary goat anti-rabbit (1:5000, Santa Cruz Biotechnology) or rabbit anti-mouse (1:5000, Sigma) HRP conjugated antibodies.

FEZ1 antiserum and immuno-fluorescence microscopy

HEK293 cells previously transfected with GFP-constructs or not, were fixed in a solution containing 2% (w/v) paraformaldehyde, 50 μM Taxol and 50 mM EGTA at room temperature for 20 min, and then permeabilized and blocked in a mixture of 0.3% (v/v) Triton X-100, and 3%(w/v) glycine solution in PBS at room temperature for 30 min. The cells were incubated at room temperature for 1 h with a specific polyclonal antiserum (1:50) that had been generated by four subsequent immunizations of rabbits with 1 mg 6xHis-FEZ1 (131–392) fusion protein. We also used a mouse anti α- or γ-tubulin (both 1:200, Santa Cruz Biotechnology, Sigma, respectively) in PBS containing 0.1% BSA (w/v). Subsequently, the cells were incubated at room temperature for 1 h with an FITC-conjugated chicken anti-rabbit IgG (1:200) and an TRITC-conjugated bovine anti-mouse (1:200) (Santa Cruz Biotechnology). Hoechst 33258 (1 μg/mL) dye was used to stain the nuclei. Cells were examined with Nikon fluorescence microscope. Confocal microscopy analyses were performed on a Carl Zeiss SLM 510 META microscope.

Immunoprecipitation

Cells were harvested (approximately 1×10^7 cells) and washed twice in PBS, resuspended in 500 μl of lysis buffer (PBS containing 1% vol (v/v) of Triton X-100) and sonicated on ice for 15 s. After centrifugation (10,000 ×*g* at 4 °C) for 10 min the supernatant was incubated with a rabbit anti-FEZ1 polyclonal

Fig. 2 – Super-expression of the GFP-FEZ1 (1–392) but not GFP-FEZ1 (1–227) in HEK293 cells causes the formation of multi-lobulated "flower-like" nuclei. (A) Schematic representation of human FEZ1 (1–392) and the N-terminal fragment FEZ1 (1–227) GFP-tagged proteins. See also legend of Fig. 1A. (B, C) When cells were transfected to express GFP-FEZ1 (1–392), a multi-lobulated nucleus phenotype was observed in a large proportion of the transfected cells and its numbers increases with the time after transfection (A. T.). Color is available in the online version only. (D, E) Bars in the graphics represent the number of cells expressing GFP-FEZ1 (1–392) (D) and GFP (E) with regular nuclei (1) or with nuclei showing multiple lobules (2–4, or >4), in a total of 100 transfected green fluorescent cells analyzed, 16, 40 and 64 h after transfection. Error bars are given for the average values of three independent experiments. (F) Detail of the multi-lobulated nucleus, observed in HEK 293 cells transfected with GFP-FEZ1 (1–392) showing the central junction of the lobules (white arrow). (G) Cell transfected with GFP-FEZ1(1–227) construct shows regular nucleus (40 h A.T.). Nuclei stained with Hoechst 33258. (H) Bars represent the number of GFP-FEZ1 (1–227) expressing cells with regular or multi-lobulated nuclei 40 h A.T. (I) HeLa cells transfected with GFP-FEZ1 (1–392) construct also have multi-lobulated nuclei 40 h A.T. 1: cell with two lobules, 2: cell with multiple nuclei, 3: GFP control transfection, 4: GFP-FEZ1 (1–227) transfected cells again do not show flower-like nuclei.

antibody in G-Sepharose 4 fast flow beads (GE Healthcare). As a negative control serum we used the rabbit polyclonal antibody anti-ZBRK1 that had been generated by four subsequent immunizations of rabbits with 1 mg of the fusion protein 6xHis-ZBRK1 that is functionally unrelated to FEZ1 and tubulin [7]. Next, beads were thoroughly washed with the lysis buffer

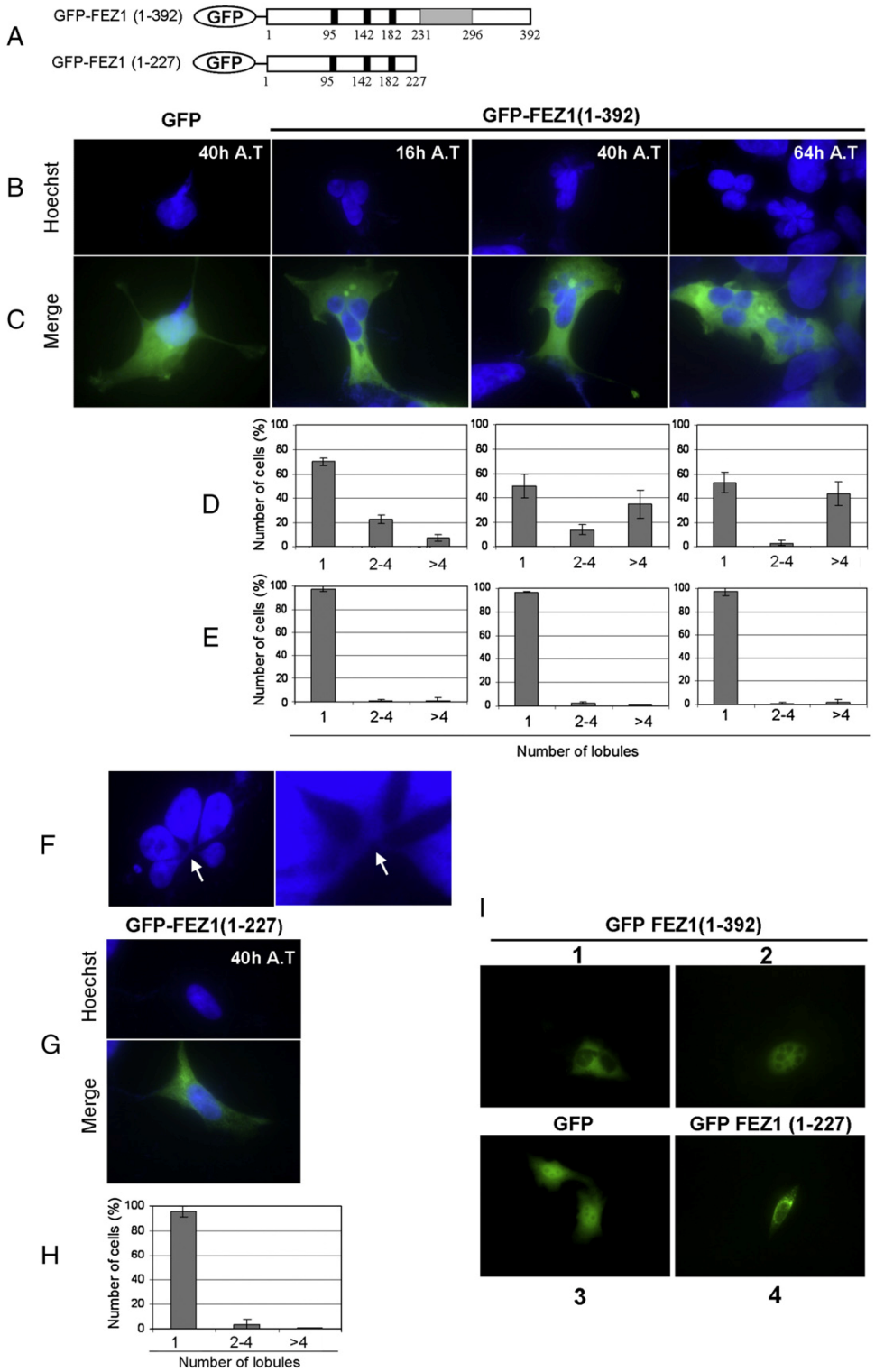

and then subjected to Western blotting with a monoclonal mouse anti-α-tubulin antibody (Santa Cruz Biotechnology) or γ-tubulin antibody (Sigma) primary and HRP-conjugated goat anti-mouse secondary antibodies.

Fluorescence in situ hybridization (FISH)

HEK293 cells were cultivated in a glass slides until reach ~70% confluency and than transfected with pEGFPC2-FEZ1 (1–392) construct. For the ploidy determination the non polymorphic 4q probe was used in HEK293 transiently transfected with GFP-FEZ1 (1–392) ~40 h after transfection, according to fabricant (Aquarius probes).

FACS analysis

Cells were harvested at 40 h post-transfection, washed with PBS+EDTA (5 mM) and fixed and permeabilized with 70% ethanol at −20 °C for 5 min. Cells were resuspended in PBS and treated with 500 μg/ml RNaseA and 50 μg/ml propidium iodide at 37 °C for 30 min to stain DNA, and subsequently subjected to flow cytometry using a FACS Scalibur (BD). The gates were defined by intensities of DNA and GFP staining from mixed population of transfected and non-transfected HEK293 cells. Non transfected cells (less than 50%), dead cells and debris were excluded by gating on fluorescence, forward scatter and pulse-width profiles. At least 24.000 cells were counted for each curve. Microscopic control experiments confirmed that 40–50% of the GFP-FEZ1 but almost none of the control GFP expressing cells presented the flower-like nuclei.

Results

FEZ1 amino acid sequence analysis

Human FEZ1 presents two overlapping nuclear localization signals, as predicted by the program PSORT II (http://psort.nibb.ac.jp/form2.html). The first signal is represented by amino acids 289 to 292, and the second signal by amino acids 290 to 293. Both signals are localized in the predicted *coiled-coil* region (aa 231–296) at FEZ1 C-terminus (Fig. 1A).

GFP-FEZ1 (1–392) is localized in both cytoplasm and nucleus

The results of these theoretical predictions as well as some preliminary observation that the expression of the C-terminus of FEZ1 (221–392) in *E. coli* resulted in the predominant localization of this fragment in the insoluble fraction of the cells lysate (data not show), prompted us to analyze the cellular fractionation of an over-expressed GFP-FEZ1 construct in human cells. We transiently transfected HEK293 cells with GFP-FEZ1 (1–392) construct and performed cellular fractionation of the cells lysate in cytoplasmic and nuclear, soluble and insoluble fractions (Fig. 1B). The results showed clearly that GFP-FEZ1 (1–392) is present in all of the four mentioned sub-fractions. The detection of GFP-FEZ1 with the anti-GFP antibody is specific since Fig. 1C shows that anti-GFP does not detect other proteins in the lysates.

Interestingly, a significant fraction of the cytoplasmic GFP-FEZ1 (1–392) can be found in the insoluble and of the nuclear GFP-FEZ1 (1–392) in the soluble sub-fraction. The results may suggest that a good fraction of GFP-FEZ1 (1–392) may be associated with the plasma membrane in both the cytoplasm as well as in the nucleus. It had been previously observed that FEZ1 can be found in association with cell membranes in COS-7 cells [2]. Since relatively little GFP-FEZ1 (1–392) can be found in the soluble fraction of the cytoplasm, we may conclude that FEZ1 does not occur in free form in the cytoplasm but is rather associated with membranes or membrane containing organelles, possibly including mitochondria, which have been described previously to be associated with a multiple protein complex involved in microtubular transport processes, and which contains the proteins FEZ1, KIF and JIP [4,10].

As a control for cytoplasmic and nuclear preparations we used the proteins hnRNPQ and α-tubulin as nuclear and cytoplasmic marker proteins, respectively. hnRNPQ is predominantly nuclear, and represents three typical bands in the nuclear fractions, that represent the different isoforms hnRNPQ1-3 [11]. Although we also found a significant fraction of hnRNPQ in the cytoplasm, this seems not to represent a contamination of this fraction with nuclear proteins, since there is a predominance of the lowest molecular weight isoform in the cytoplasmic fraction, whereas the nuclear fraction is composed of approximately equal amounts of all three isoforms. In any case we can rule out that the nuclear fraction has been contaminated with cytoplasmic proteins, since no α-tubulin could be detected in the nuclear fractions. This demonstrates that the GFP-FEZ1 detected in the nuclear fraction is found in either the nuclear lumen or associated with the nuclear membranes. We conclude therefore, that FEZ1 although predominantly cytoplasmic, can associate with the nucleus and may have nuclear functions. This is in good agreement with previous findings that FEZ1 can interact with several nuclear proteins [8,9]. Possibly our observation was facilitated because of the cell model HEK293 we chose. HEK293 have a large nucleus and have not previously been tested for GFP-FEZ1 sub-cellular localization. This together with the super-expression and the high rate of transfection usually obtained with these cells may have allowed the nuclear visualization of GFP-FEZ1 in the Western blot.

Over-expression of GFP-FEZ1 in HEK293 cells leads to multi-lobulated nuclei

We then further analyzed the functional changes in HEK293 cells after super-expression of two different GFP-FEZ1 constructs: GFP-FEZ1 (1–392) and GFP-FEZ1 (1–227), which only contains the poly Glu motifs, but not the coiled-coil region (Fig. 2A).

We analyzed the transiently transfected cells from 16 to 64 h after transfection by fluorescence microscopy (Fig. 2). The super-expression of GFP-FEZ1 (1–392) but never of GFP (Figs. 2B,C) or GFP-FEZ1 (1–227) (Fig. 2G) caused the appearance of multi-lobulated nuclei only in the transfected cells. A detailed analysis of the flower-like nucleus phenotype shows what appears to be a common central focal point to which the cytoplasmic bridges between the different lobules converge (Fig. 2F).

The appearance of the multi-lobulated, "flower-like" nuclei was accompanied at different time points ranging from 16, to 40 and 64 h post-transfection, and the numbers of lobules were counted per 100 transfected cells (Figs. 2D,E). The average values of three independent experiments are shown in the graphics for GFP-FEZ1 (1–392 (D) and GFP transfected cells (E). For GFP-FEZ1 (1–227) transfected cells (Fig. 2G) the graphic of 40 h after transfection is shown in Fig. 2H. At 16 h post-transfection 23% of the GFP-FEZ1 (1–392) transfected cells presented already 2–4 lobules and 7% had more than 4 nuclear lobules, indicating that the multi-lobulated nuclei already had appeared previous of the first time point analyzed.

The number of lobules increases progressively with time culminating in 44% of the transfected cells presenting more than 4 lobules after 64 h transfection. Interestingly, the number of transfected cells with a regular nucleus at 16 h post-transfection represents 70% but remains relatively constant at approximately 50% for the remaining time of the experiment (40 h, 64 h), whereas the number of cells with 2–4 lobules decreases from 23% (16 h), via 14% (40 h) to 3% (64 h) as time progresses. It is further noteworthy that the great majority of multi-nucleated cells had a more intense green fluorescence emission than the transfected cells, which did not present the phenotype. Altogether, this may indicate that higher expression levels of GFP-FEZ1 (1–392) construct may be associated with a more pronounced multi-lobulated nucleus phenotype (not shown).

Furthermore, the phenotype is not restricted to the HEK293 cell line (Fig. 2I). We observed the same phenotype also in HeLa cells transiently transfected with GFP-FEZ1 (1–392) (Fig. 2I, 1 and 2), but neither with GFP (Fig. 2I, 3) or GFP-FEZ1 (1–227) (Fig. 2I, 4). With HeLa however, the overall transfection rate was low in comparison with that of Hek 293 (ca. 20%) The lack of the phenotype upon over-expression of the N-terminal region of FEZ1 in fusion with GFP, may indicate that the C-terminal region of FEZ1 is necessary for the formation of flower-like nuclei. In a previous study we had shown the importance of the C-terminus of FEZ1 for its interaction with the majority of the interacting proteins identified to date [9].

The formation of multi-lobulated nuclei depends on intact microtubules

FEZ1 has been previously reported to be physically and functionally associated with microtubules [4,5]. Furthermore, the cytoplasmic bridges that intersect the lobules and converge to a central focus may also suggest a possible involvement of microtubule associated processes (Fig. 2F). Therefore, we tested if the microtubular de-polymerizing drug nocodazole could inhibit the GFP-FEZ1 (1–392) mediated formation of the multi-lobulated nuclei (Fig. 3A). The addition of nocodazole (10 μg/ml) 22 h after transfection with the GFP-FEZ1 (1–392) expressing vector construct, not only abolished the formation of the multi-lobulated nuclei but evidently also reverted the fraction of >40%

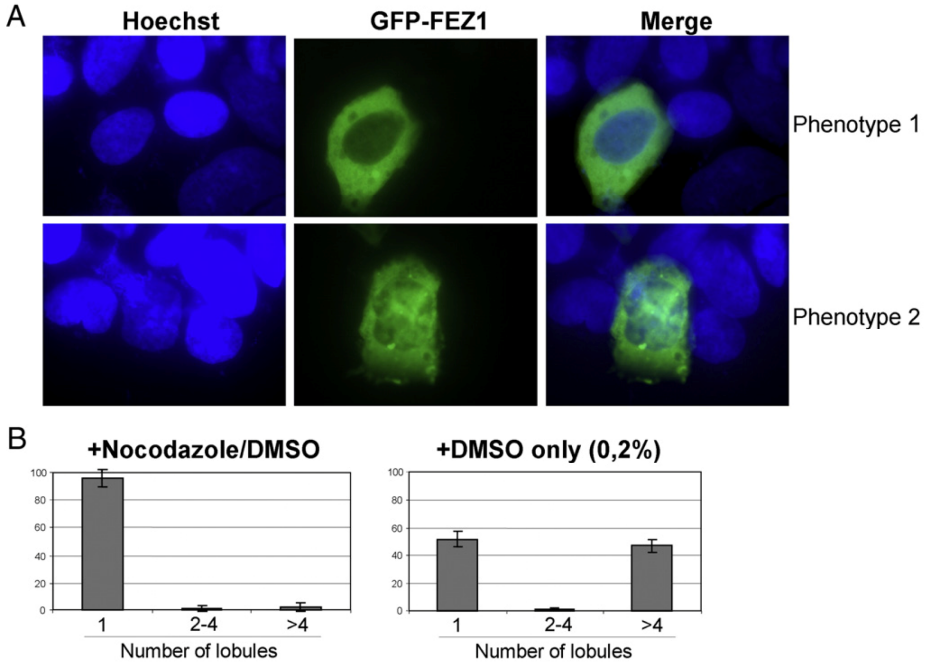

Fig. 3 – Effect of nocodazole treatment on the formation of the flower-like phenotype. (A) HEK293 cells transfected with GFP-FEZ1 (1–392) construct were after 24 h incubated for 18 h with DMSO only (control) or 10 μg/ml nocodazole in DMSO. Two phenotypes were observed after treatment. See text for details. (B) The bars represent the number of cells with normal or lobulated nuclei after treatment with DMSO alone or with DMSO/nocodazole for 18 h (22 h after transfection). The same numbers were also observed after only 6 h of treatment, 22 h post-transfection (not shown). Color is available in the online version only.

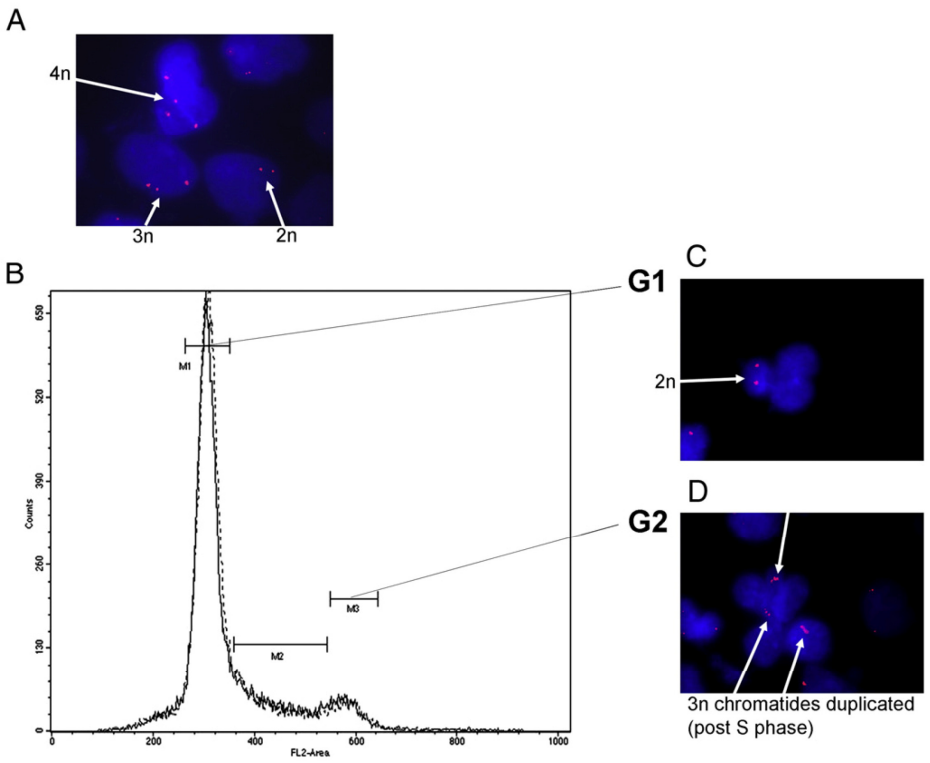

Fig. 4 – Formation of multi-lobulated nuclei does not cause cell cycle arrest of GFP-FEZ1 expressing HEK 293 cells. (A) HEK293 are hypo-triploid human cells and the chromosome 4 (q arm) marker is typically visible as two (diploid for 4q marker), three (triploid for 4q marker) or four (tetraploid for 4q marker) fluorescent red dots in the nucleus of the untransfected cell population. Color is available in the online version only. (B) DNA content histogram of GFP expressing (dashed line) and GFP-FEZ1 (1–392) expressing cells (solid line) 40 h after transfection. (C) A tri-lobulated nucleus (possibly diploid, maybe in G1 phase) of a GFP-FEZ1 (1–392) expressing Hek 293 cell. Two of the lobules do not represent the 4q marker. This practically excludes the possibility of the lobules presenting complete multiple nuclei. (D) At least tetra-lobulated nucleus of a GFP-FEZ1(1–392) over-expressing Hek293 cell (probably triploid and after S phase). The 3 split, double-labeled dots seem to indicate that the division of the chromatids had probably already occurred (G2 phase).

of the transfected cells that should contain 2 or more lobules at this time point, since not a single multi-lobular cell could be observed up to 40 h after transfection (Fig. 3B). The same was also observed after only 6 h of nocodazole treatment, 22 h post-transfection (not shown). DMSO only treated control cells behaved like the regular GFP-FEZ1 expressing cells and resulted in strong flower-like nuclei formation 40 h post-transfection. Together, these data suggests that GFP-FEZ1 (1–392) depends on

Fig. 5 – Microtubule rearrangement caused by over-expression of GFP-FEZ1 (1–392). (A) Endogenous FEZ1 in HEK293 cells co-localizes along microtubules. FEZ1 was immuno-stained with a secondary anti-rabbit FITC-conjugated antibody (green) and α-tubulin with a secondary anti-mouse Rhodamine conjugated antibody (red). (B) GFP expression in HEK293 cells does not promote alterations in the microtubule arrangement or the co-localization of FEZ1 and α-tubulin. (C–D) Over-expression of GFP-FEZ1 (1–392) construct causes rearrangement of microtubules (C) and the formation of microtubular loops (D) that seem to incise the nuclear envelope and thereby cause a multi-lobulated nucleus. (E) After ~16 h of transfection and over-expression of GFP-FEZ1 (1–392) the nucleus is incised by a microtubular assisted process (white arrows indicate interlobular cytoplasmic bridges containing microtubule bundles). Nuclei in all photos were counter-stained with Hoechst 33258 (blue).
(F) Co-immunoprecipitation of endogenous FEZ1 and α-tubulin. The lysates of HEK293 cells were immuno-precipitated with an anti FEZ1 antibody and analyzed by Western blot with an anti α-tubulin antibody. The anti-ZBRK rabbit serum was used as an unrelated control serum. (G) GFP-FEZ1 and α-tubulin co-localize during flower-like nucleus formation. Successive confocal microscopy slices (1 to 4) show the nuclear lobules wrapped by both GFP-FEZ1 (1–392) and α-tubulin. GFP-FEZ1 (1–392) predominates in the region between the lobules. (H) Detailed from slice 1. The black arrow on top of the panel indicates the position of transversal section seen in (I). (I) Transversal section of the cell shows two (blue) lobules "sandwiched" by GFP-FEZ1 (1–392) (left, green) and α-tubulin (right, red). The yellow regions in B and C clearly show superimposition of GFP-FEZ1 (1–392) and α-tubulin patterns, suggesting locally defined interaction.

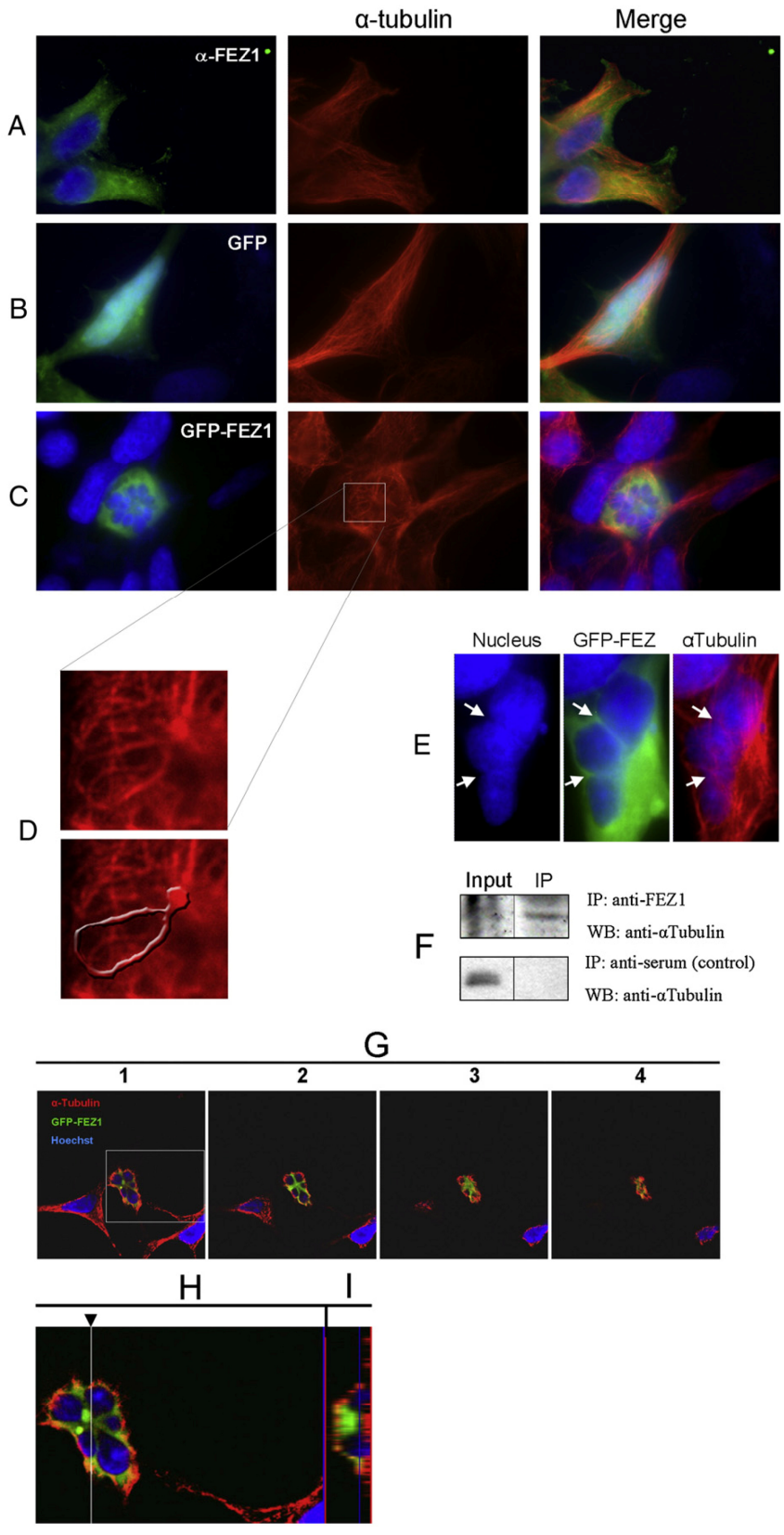
α-tubulin
Merge
A
α-FEZ1
B
GFP
C
GFP-FEZ1
D
Nucleus
GFP-FEZ
αTubulin
E
Input
IP
F
IP: anti-FEZ1
WB: anti-αTubulin
IP: anti-serum (control)
WB: anti-αTubulin
G
1
2
3
4
α-Tubulin
GFP-FEZ1
Hoechst
H
I

intact microtubules in order to promote the generation of the multi-lobular nucleus phenotype.

Interestingly, we observed two distinct of the GFP-FEZ1 expressing cells after the Nocodazole treatment (Fig. 3A). Phenotype 1 has a regularly shaped nucleus with little GFP-FEZ1 and the more frequently found Phenotype 2 has a non-lobulated greenly stained nucleus, suggesting presence of GFP-FEZ1. This may indicate that despite the nocodazole induced reversion of the flower-like nuclei, GFP-FEZ1 remains in close association with the nucleus membrane. Intriguingly, the number of the cells of phenotype 2 equals approximately the total number of cells with flower-like nuclei observed in the DMSO treatment (not shown). This seems to suggest that phenotype 2 may be a "reverted form" of the cells that previously showed flower-like nuclei.

FISH gives further evidence for the hypothesis of single multi-lobulated nuclei instead of multiple nuclei

In order to address whether the observed phenomena represents true multi-lobulated nuclei and not multiple nuclei, each with an own complete set of chromosomes, we performed FISH experiments with a probe that detects the chromosome 4 of the human genome. HEK293 ploidy varies between the diploid triploid and tetraploid stages, being mostly populated in the hypo-triploid stage (Fig. 4A). The rate of cells with higher ploidies is ~4%. The three regular nuclei in non-transfected control cells at the center of panel A represent 2, 3 or 4 red labelings, allowing to speculate that these three cells are diploid (2), hypo-triploid (3) tetraploid (4). The analysis of the tri- (Fig. 4C) and tetra-lobulated (Fig. 4D) nuclei showed that only some of the lobules contained the red labeled dot representing FISH chromosome 4, while others did not. This excludes the possibility that not each lobule represents an independent complete nucleus with a complete set of chromosomes, but rather suggests that a subdivision/lobulation of the nucleus is occurring.

The formation of multi-lobulated nuclei does not cause arrest of the cells in a specific phase of the cell cycle

We further tested by FACS analysis I if multi-lobulated nuclei causes alteration in the proportion of cells in different phases of the cell cycle (Fig. 4B). A superposition of two histograms of Hek293 cells transfected to express either GFP or GFP-FEZ1 (1–392) shows that there is no difference of the proportion of cells in the different phases of the cell cycle. The FISH analysis also suggests that the presence of cells with multi-lobulated nuclei occurs in cells with two single spotted labelings (indication of G1 phase, 2n) (Fig. 4C) and three double spotted labelings (3n) that indicate post-S phase chromatid duplication (Fig. 4D).

Cytoskeleton rearrangement and formation of microtubular bundles between nuclear lobules

In non-transfected cells, endogenous FEZ1 shows co-localization with tubulin, confirming the results of previous co-precipitation studies of FEZ1 with α- and β-tubulin [4,5] (Fig. 5A). We further confirmed this interaction by immunoprecipitation of tubulin and immunodetection of FEZ1 (Fig. 5F). In control cells (Fig. 5B) GFP is distributed in the cytoplasm in a diffuse way and tubulin is found as in the non-transfected cells in regular bundles throughout the cell. Upon super-expression of GFP-FEZ1 (1–392) we observed that it now co-localizes with tubulin predominantly in the perinuclear region and in the cytoplasmic bridges that separate the lobules already formed (Figs. 5C–E). The tubulin localized in the cytoplasmic bridges between the lobules seems to form "loops" (Fig. 5D) that may originate and terminate at the central focal point which can be found between the lobules.

Successive slices observed in confocal microscopy show that GFP-FEZ1 (1–392) is present in the regions between lobules and in the center of the flower-like structure (Fig. 5G). A detail of slice 1 was analyzed in the transversal direction and showed that there is a clear, punctual co-localization of GFP-FEZ1 (1–392) and α-tubulin (Figs. 5 H, I). GFP-FEZ1 (1–392) seems to almost form a "bridge" between the outer layers of α -tubulin found below and above the constricted lobules of the nucleus. The over-expression of GFP-FEZ1 (1–392) may promote an artificial association between different microtubular bundles, which provokes somehow the observed constriction of the nucleus that results in the observed lobules.

FEZ1 co-localizes with the γ-tubulin labeled microtubule organization center localized at the center of multiple incisions

Co-localization studies of both GFP-FEZ1 (1–392) as well as endogenous FEZ1 with γ-tubulin showed the clear superimposition of the two proteins at the microtubule organizing center (MTOC) (Fig. 6A) and at the center of the structure that seem to hold the five lobules (Fig. 6D). This structure shows a strong co-localization of γ-tubulin and GFP-FEZ1 (1–392) (Fig. 6C, merge) and may represent the centrosome/MTOC. Confocal microscope analysis of a single plain confirmed the co-localization of GFP-FEZ1 with γ-tubulin at both the central region and in the periphery of the lobules where the incisions occur (arrows in Fig. 6F).

The observed "anchorage" of the lobules around the MTOC (Fig. 6D) remembers the way gas-filled balloons are secured at a central fixing-point (see also Fig. 2F). We may further speculate that, like in analogy of the balloons, the individual lobules may interact with the center through attractive forces, likely mediated by the microtubules. Although speculative at this point, this hypothesis may be tested by further experiments. In line with this argumentation is however the obserõvation that nocodazole, an inhibitor of microtubular functions, completely abrogates the lobule formation. In GFP expressing control cells (Fig. 6B) γ-tubulin can be found more dispersed in a perinuclear region.

Discussion

Upon over-expression of GFP-FEZ1 (1–392) in HEK293 we observed that 64 h post-transfection over 40% of the transfected cells develop so-called flower-like nuclei, consisting of 2 to many nuclear lobules, which arrangement remembers that of the petals of a flower.

The choice of rapidly dividing and easily transfectable HEK293 cells as a model system might have been crucial to

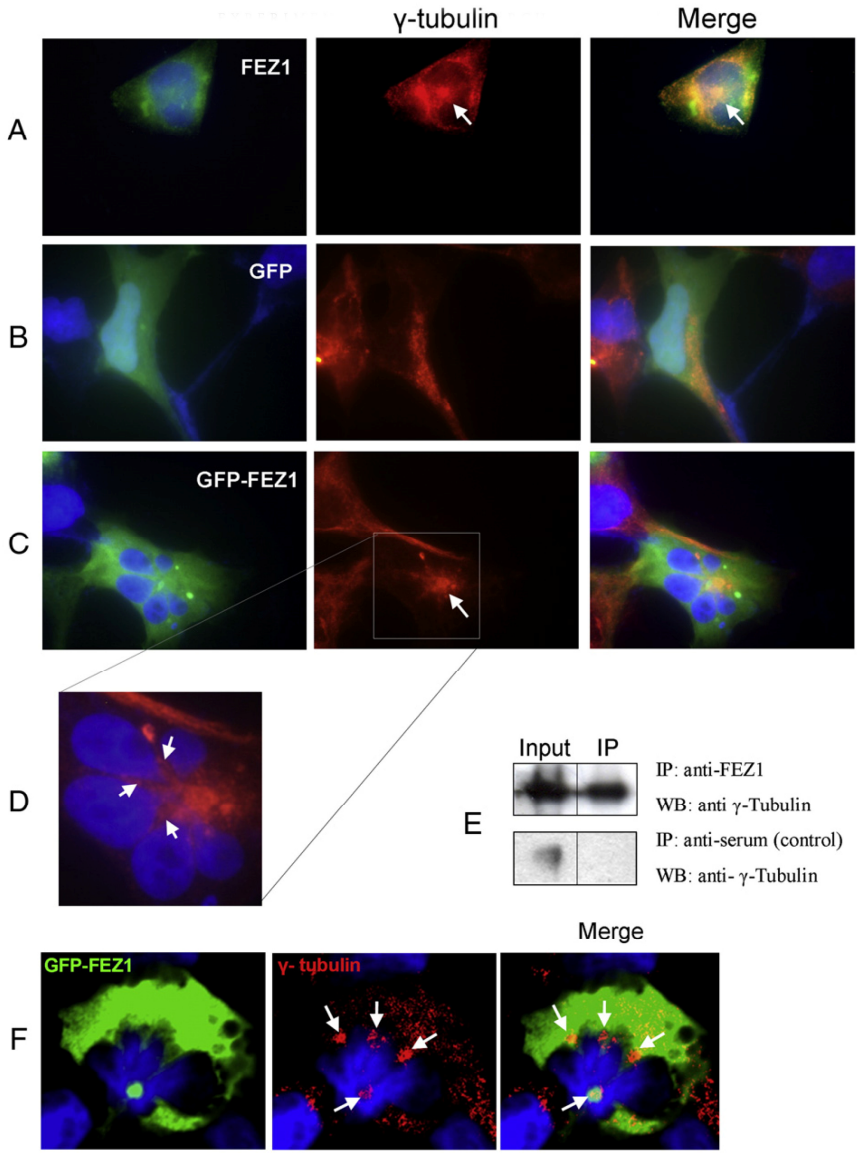

Fig. 6 – γ-tubulin and FEZ1 co-localize at the centrosome and in the periphery of the multi-lobulated nuclei. (A) Endogenous FEZ1 co-localizes with γ-tubulin in a microtubular organization center (MTOC). FEZ1 was immuno-stained with a secondary anti-rabbit FITC-conjugated antibody and γ-tubulin with a secondary anti-mouse Rhodamine conjugated antibody. (B) HEK293 cells expressing GFP, present γ-tubulin dispersed in the cytoplasm and in a perinuclear fashion. (C) GFP-FEZ1 (1–392) co-localizes with γ-tubulin in a MTOC region indicated by the white arrow. (D) Close-up of the region in (C) shows presence of γ-tubulin in the center of the multi-lobulated nucleus and the white arrows indicate that it is also present in the incision spaces between the emerging lobules. Nuclei in all photos were stained with Hoechst 33258 (blue). (E) Co-immuno-precipitation of endogenous FEZ1 and γ-tubulin. The lysates of HEK293 cells were immuno-precipitated with a polyclonal anti-FEZ1 antibody or with anti-ZBRK1 control polyclonal antibody. Immuno-precipitates and total lysates (input) were analyzed by Western blot with an anti γ-tubulin antibody. (F) Single confocal microscopy plain shows GFP-FEZ1 and γ-tubulin co-localization in defined spots in the same plain around the region surrounding the nuclear lobules (white arrows).

allow this intriguing observation, since no flower-like nuclei were observed previously in differentiated neuronal cells transfected with GFP-FEZ1. HEK293 cells originated from rare neuronal cells from fetal kidney and therefore represent some neuronal characteristics, although they are morphologically different [12].

The flower-like phenotype had been previously reported to be caused by over-expression of nuclear versions of the protein tyrosine kinase Chk [13]. As in our case the phenotype formation was dependent on intact microtubules, since it was also abolished by nocodazole treatment. The kinase activity of Chk was not a requirement for flower-like nuclei formation in

COS1 cells. Whereas Chk over-expression provoked a flower-like phenotype which led to an arrest of the cell cycle, our super-expression of GFF-FEZ1 (1–392) did promote flower-like nuclei in approximately 50% of the transfected cells after 40 h, but no alteration of the transfected cells cycle profile in comparison with GFP transfected control cells. This interesting difference seems to indicate that in our case the cell cycle continues and this may mean that in our case the formation of the flower-like nuclei does not impede cell division itself.

The flower-like nuclei phenotype had been reported also in human multi-drug resistant acute lymphocytic leukemia cell lines that are resistant to Vincristine [14]. These authors proposed that the multi-lobulation may be caused by the atypical organization of cytoskeleton elements, possibly associated with the multiple drug resistance of these cells. The flower-like nuclei are indeed widely observed in leukemia and this feature is considered a morphological hallmark for malign T lymphocytes, which can be observed in more than 50% of the patients with Adult T Cell Leukemia/lymphoma (ATLL) [14–16]. Nuclear contraction and the generation of the multi-lobulated nuclei are related to the forming of tubulin and actin "loops" and involve abnormal microtubule functions.

It is therefore noteworthy that FEZ1 has been reported as a microtubular associated protein that is possibly directly involved in transport functions [3,5]. Its over-expression in HEK293 cells may therefore be interpreted as a dominant-negative effect, which results in altered microtubular functions. Possibly the large fusion of GFP to the N-terminus of FEZ1 promotes a lack or gain of function for FEZ1, which function or interaction with other microtubule associated factors may no longer be regulated or reversible.

Therefore, the observed formation of the loops deserves some attention since the loop formation precedes directly the multi-lobulation of the nuclei and these two events seem to be functionally or even causatively associated. However, there occurs also some loop formation without the observation of lobule formation (Fig. 5D). Possibly, in that cases the "shrinking" loop did not "catch" the nucleus, so no lobulation is observed for that loop.

Since under normal conditions the majority of microtubules are anchored with the "minus" ends to the centrosome, we may hypothesize that the loop formation could involve the additional anchorage of the "plus" ends. Since we find a massive co-localization of GFP-FEZ1 (1–392), α- and γ-tubulin at the central structure, which likely represents the centrosome, we might speculate that FEZ1 is somehow involved in the supposed loop-closing, which may ultimately culminate in the lobulation process.

FEZ1 has been reported to interact with several proteins in several independent studies but especially in two large scale yeast two-hybrid analysis [8,9]. With the new functional association of FEZ1 to the centrosome and to the multi-lobular phenotype in mind we re-analyzed the list of FEZ1 interacting proteins, to find other proteins that may be involved in these functions, too.

Interactions with kinesin 1 [4] and CLASP2 [9] link FEZ1 to the microtubule and especially to the microtubular tip, where CLASP2 is associated. If we furthermore consider that FEZ1 dimerizes we may speculate that the described "loop" formation may involve "incorrect" interactions of FEZ1 populations localized at the microtubular tip (FEZ1/CLASP2) with FEZ1 or interacting proteins localized at the centrosome or along the microtubule. The loop formation would in this case be promoted by the super-expression of GFP-FEZ1 and could be mediated by excessive occupation of physiological binding sites.

FEZ1 has been further described to interact with SMC3, a protein found to localize to the centromeres of sister-chromatids [9]. Is it possible that the observed formation of the multi-lobulated nucleus in GFP-FEZ1 (1–392) over-expressing cells is somehow associated with the processes of chromatids separation and chromosome transport involving protein-protein interactions between FEZ1 and SMC3.

We initially identified FEZ1 as an interacting partner of NEK1's regulatory domain [7]. Other members of the large family of mammalian Neks (NIMA related kinases), such as Nek2, have been previously described to be associated with centrosome function [17]. Most interestingly, the super-expression of mutated versions of Nek1 caused a significant percentage of these cells to represent what the authors described as multi-nucleated cells [18]. Further studies are required to evaluate if in the case of Nek1 over-expression there is the formation of true multiple nuclei or rather multi-lobulated nuclei, as those described by us here in case of the over-expression of GFP-FEZ1. Nonetheless, the physical interaction of the proteins Nek1 and FEZ1 [7] and the novel discovery of possibly similar modifications [18, this report] in the nuclear morphology strongly suggest a biological relation that should be addressed in future research.

Together these findings suggest that a multi-protein machinery is responsible for the coordinated assembly of the microtubular tip and that the coordinated assembly and disassembly of these structures is highly regulated and involves kinases and possibly phosphorylation dependent regulation of its components. Disturbances or super-expression of any of the involved components (FEZ1, Nek1, Chk) can result in dramatic phenotypes, such as the flower-like nuclei. Our new data suggest that FEZ1 may be another new and important component of this system and its correct function may be essential for the harmonic division of the nucleus. FEZ1 may prove to be an essential connecting element between centromeres, microtubules and centrosomes, since it has been described to interact with protein components found in all three of these macromolecular structures. The future detailed study of the exact processes underlying the phenomenon of flower-like nuclei formation through super-expression of FEZ1 is not only of interest to understand the function of FEZ1 itself. The flower-like nuclei are a hall mark of leukemia cells and may indicate a general genetic instability of the cancer cells. Therefore, further studies of the molecular mechanisms that govern the formation of these abnormal multi-lobulated nuclei are of utmost importance for our better understanding of cancer cells.

Acknowledgments

This work was financially supported by the Fundação de Amparo à Pesquisa do Estado São Paulo (FAPESP), through the projects SmolbNet, CEPID, 05/00235-1 (personal grant to J.K.), as well as by a post-doc fellowship to E.M.A., and PhD fellowships to D.C.F.L., D.M.T., Further financial support was from the

Conselho Nacional de Pesquisa e Desenvolvimento (CNPq) and the LNLS. We thank Maria Eugenia R. Camargo and Zildene D. Correa for their technical assistance. We further thank Dr. José Andrés Yunes and Lilian J. G. Zambaldi (Centro Boldrini, Campinas) for their help with FACS and FISH experimentation and interpretation.

REFERENCES

[1] L. Bloom, H.R. Horvitz, The *Caenorhabditis elegans* gene unc-76 and its human homologs define a new gene family involved in axonal outgrowth and fasciculation, Proc. Natl. Acad. Sci. 94 (1997) 3414–3419.

[2] S. Kuroda, N. Nakagawa, C. Tokunaga, K. Tatematsu, K. Tanizawa, Mammalian homologue of the *Caenorhabditis elegans* UNC-76 protein involved in axonal outgrowth is a protein kinase C zeta-interacting protein, J. Cell Biol. 114 (1999) 403–411.

[3] J. Ikuta, A. Maturana, T. Fujita, T. Okajima, Kenji, Tatematsu, K. Tanizawa, S. Kuroda, Fasciculation and elongation protein zeta-1 (FEZ1) participates in the polarization of hippocampal neuron by controlling the mitochondrial motility, Biochem. Biophys. Res. Commun. 353 (2007) 127–132.

[4] T.L. Blasius, D. Cai, G.T. Jih, C.P. Toret, K.J. Verhey, Two binding partners cooperate to activate the molecular motor Kinesin-1, J. Cell Biol. 176 (2007) 11–17.

[5] T. Suzuki, Y. Okada, S. Semba, Y. Orba, S. Yamanouchi, S. Endo, S. Tanaka, T. Fujita, S. Kuroda, K. Nagashima, H. Sawa, Identification of FEZ1 as a protein that interacts with JC Virus Agnoprotein and microtubules, J. Biol. Chem. 280 (2005) 24948–24956.

[6] M.H. Naghavi, T. Hatziioannou, G. Gao, S.P. Goff, Overexpression of fasciculation and elongation protein zeta-1 (FEZ1) induces a post-entry block to retroviruses in cultured cells, Genes Dev 19 (2005) 1105–1115.

[7] M.J. Surpili, T.M. Delben, J. Kobarg, Identification of proteins that interact with the central coiled coil region of the human protein kinase NEK1 involved in the cell cycle regulation, Biochemistry 42 (2003) 15369–15376.

[8] U. Stelzl, U. Worm, M. Lalowski, C. Haenig, F.H. Brembeck, H. Goehler, M. Stroedicke, M. Zenkner, A. Schoenherr, A. Koeppen, J. Timm, S. Mintzlaff, C. Abraham, N. Bock, S. Kietzmann, A. Goedde, E. Toksöz, A. Droege, S. Krobitsch, B. Korn, W. Birchmeier, H. Lehrach, E.E. Wanker, A human protein-protein interaction network: a resource for annotating the proteome, Cell 122 (2005) 957–968.

[9] E.M. Assmann, M.R. Alborghetti, M.E.R. Camargo, J. Kobarg, FEZ1 dimerization and interaction with transcription regulatory proteins involves its coiled-coil region, J. Biol. Chem. 15 (2006) 9869–9881.

[10] T. Fujita, A.D. Maturana, J. Ikuta, J. Hamada, S. Walchli, T. Suzuki, H. Sawa, M.W. Wooten, T. Okajima, K. Tatematsu, K. Tanizawa, S. Kuroda, Axonal guidance protein FEZ1 associates with tubulin and kinesin motor protein to transport mitochondria in neurites of NGF-stimulated PC12 cells, Biochem. Biophys. Res. Commun. 361 (2007) 605–610.

[11] D.O. Passos, A.J.C. Quaresma, J. Kobarg, The methylation of the C-terminal region of hnRNPQ (NSAP1) is important for its nuclear localization, Biochem. Biophys. Res. Commun. 346 (2006) 517–525.

[12] G. Shaw, S. Morse, M. Ararat, F.L. Graham, Preferential transformation of human neuronal cells by human adenoviruses and the origin of HEK293 cells, FASEB J. 16 (2002) 869–871.

[13] Y. Nakayama, N. Yamaguchi, Multi-lobulation of the nucleus in prolonged S phase by nuclear expression of Chk tyrosine kinase, Exp. Cell Res. 304 (2005) 570–581.

[14] R. Fukuda, A. Hayashi, A. Utsunomiya, Y. Nukada, R. Fukui, K. Itoh, K. Tezuka, K. Ohashi, K. Mizuno, M. Sakamoto, M. Hamanoue, T. Tsuji, Alteration of phosphatidil 3-kinase cascade in the multilobulated nuclear formation of adult T cell leukemia/lymphoma (ATLL), Proc. Natl. Acad. Sci 102 (2005) 15213–15218.

[15] J. Huang, P. Sweet, L.M. Slater, A.C. Sartorelli, M.F. Leung, Microtubule-dependent multilobular organization of the nucleus in sensitive and multidurg-resistant L_0 leukemia cells, Cancer Lett 106 (1996) 29–41.

[16] Y. Sato, N. Hachiya, H. Kuno, T. Asoh, K. Oizumi, Cerebrospinal fluid atypical lymphocytes in Japanese encephalitis, J. Neurol. Sci. 160 (1998) 92–95.

[17] A.J. Faragher, A.M. Fry, Nek2A kinase stimulates centrosome disjunction and is required for formation of bipolar mitotic spindles, Mol. Biol. Cell. 14 (2003) 2876–2889.

[18] E. Feige, O. Shalom, S. Tsuriel, N. Yissachar, B. Motro, Nek1 shares structural and functional similarities with NIMA kinase (2006), Biochim. Biophys. Acta 1763 (2006) 272–281.

Artigo 3

FEZ1 interacts with CLASP2 and NEK1 in coiled-coil regions and their cellular co-localization suggests centrosomal functions and regulation by PKC

Daniel C. F. Lanza, Gabriela V. Meirelles, Marcos R. Alborghetti, Camila H. Abrile, Guido Lenz and Jörg Kobarg

Manuscrito Submetido para revista Molecular and Cellular Biochemistry

pISSN: 0300-8177
eISSN: 1573-4919
NLM ID: 0364456

Abstract

FEZ1 was initially described as a neuronal protein that influences axonal development and cell polarization. CLASP2 and NEK1 proteins are present in a centrosomal complex and participate in cell cycle and cell division mechanisms, but their functions were always described individually. Here we report that NEK1 and CLASP2 co-localize with FEZ1 in a perinuclear region in mammalian cells, and observed that coiled-coil interactions occur between FEZ1/CLASP2 and FEZ1/NEK1 in vitro. These three proteins co-localize and interact with endogenous γ-tubulin. Furthermore, we found that CLASP2 is phosphorylated, interacts with active PKC isoforms, and that FEZ1/CLASP2 co localization is inhibited by PMA treatment. Our results provide evidence that these three proteins cooperate in centrossomal functions and open new directions for future studies.

Keywords

Flower like nuclei, NIMA, CLIP, cytoskeleton, tubulin.

Introduction

The protein FEZ1 (Fasciculation and elongation protein zeta 1) was initially described as an orthologue of the UNC-76 protein, which performs important functions in the neuronal development of *C. elegans* [1]. Later, it was observed that FEZ1 interacts with cytoskeleton elements, mainly α-tubulin [2], and participates in microtubular transport mechanisms. FEZ1 associates physically to JIP1 and Kinesin-1, is indispensable for the formation of the cargo complex and participates in mitochondrial transport [3,4]. Its interaction with PKCζ is crucial for neuronal differentiation in PC12 cells [5]. Recently, it was observed that FEZ1 knockout mice presented hyperactivity, under novel social or stressful conditions as well as enhanced responsiveness to psychostimulants. These and other works confirming the importance of FEZ1 for the central nervous system development and actuation in schizophrenia causative mechanisms [6]. Our group identified the interactions of FEZ1 with NEK1 (Nima related kinase1) and CLASP2 (Clip associated protein 2) in two independent yeast two hybrid assays, using the NEK1 regulatory domain or FEZ1 C-terminal region as baits, respectively [7,8].

NEKs (NIMA-related kinases) represent a family of serine/threonine kinases implicated mainly in the control of the cell cycle at the G2/M checkpoint [9]. In mice the mutations *kat* and *kat2J* of the NEK1 gene cause the polycystic kidney disease (PKD) [10,11]. Murine NEK1 localizes to the centrosomes in the interphase, and remains associated with the mitotic spindle during mitosis [12]. NEK1 interacts with proteins involved in the PKD, double-strand DNA break repair at the G2/M transition phase of the cell cycle, and neuronal cell development in vertebrates [7]. Some studies related that mNEK1 protein localizes to the cilial basal body and participates in the cell cycle associated ciliogenesis [13,14].

The protein CLASP2 was initially described to be associated to CLIPs, linker proteins located mainly at the end of growing microtubules, where they function primarily as "anti catastrophe" factors [15]. Recently, it was observed that glycogen synthase kinase 3beta directly phosphorylates CLASPs at multiple sites in the domain required for MT plus end tracking [16]. CLASP2 has functions in mitotic spindle organization and kinetochore alignment during the cell division and participates in the formation of noncentrossomal microtubule organization centers [15-18].

We observed that FEZ1 dimerizes and shows an elongated shape, allowing its Cterminal coiled-coil regions to interact with other proteins [19]. We have also shown that FEZ1 interacts with tubulin and that its over-expression causes modifications in the microtubular spindle organization that leads to the formation of "flower like" nuclei, frequently observed in leukemic lymphocytes [20].

Here, we show the co-localization of FEZ1 with NEK1 and CLASP2(1192-1407) in mammalian cells and showed that these interactions occur through the coiled coil sites of these proteins. Furthermore, we observe that PKC phosphorylates CLASP2, and the addition of PMA was shown to inhibit its co-localization with FEZ1. Our data suggest a possible mutual function of these proteins in a centrossomal candidate region.

Materials and methods

Plasmid Constructions

FEZ1(1-392) or and truncated FEZ1(1-227) encoding nucleotide sequences were amplified by PCR and cloned into bacterial expression vector pET28a (Novagen/EMD Biosciences, San Diego, CA) as described [8]. FEZ1(229-269) was sub-cloned from 6xHis-FEZ1(1-392) into

pET28a. Full-length FEZ1(1-392) and the fragments FEZ1(1- 227) and FEZ1(221-392) were sub-cloned into pEGFPC2 vector (Clontech). Truncated CLASP2(1046-1407) and sequences was sub-cloned into pGEX-4T2 (GE Healthcare, Waukesha, WI) as described [8]. CLASP2(1192-1407) was sub-cloned from the CLASP2(1406-1407) construct to pDsRed-Monomer-C1 (Clontech). Human full-length NEK1 cloned into pCMV5-FLAG vector was sub-cloned into pDsRed-Monomer-C1. Truncated GST-NEK1(441-621) and GST-NEK1(497-555) constructions were subcloned from the pDsRed-Monomer-C1 construction into pGEX-4T2 and a modified version of pET28a containing a GST tag. All sequences were confirmed by DNA sequencing.

In vitro binding assays

GST-CLASP2(1046-1407), GST-NEK1(441-621) and GST-NEK1(497-555) or GST only (control) from bacterial lysate were allowed to bind to 50µl of glutathione sepharose beads in PBS for 1h at 4°C. Then, the experiment was performed as described by Assmann and co-workers [8].

Transient transfection

All transfections shown in this paper are transient, and were performed using the calcium phosphate precipitation method. Adherent HEK293 or COS-7 cells were cultivated in 24-well plates as described in [20]. For FLAG-NEK1 production, cells were cultivated in bottles and transfection was performed when the cells reached confluency of 60%

FEZ1 and NEK1 microscopy

HEK293 or COS-7 cells previously transfected or not with GFP constructs were fixed as described [20]. The cells were blocked with 1%BSA in PBS for 1h. For endogenous FEZ1 or NEK1 detection, the cells were incubated at room temperature for 1h with 1%BSA in PBS containing a specific polyclonal rabbit antiserum for FEZ1 [20] and NEK1 . We also used a monoclonal anti-γ-tubulin antibody (1:5000, Sigma) in PBS containing 1%BSA (w/v). Subsequently, the cells were incubated at room temperature for 1h with an FITC or TRITC-conjugated secondary antibodies (Santa Cruz Biotechnology). Hoechst 33258 (1µg/mL) was used to stain nuclei. Cells were examined in a Nikon fluorescence microscope.

In vivo binding assays

HEK293 cells were harvested (approximately 1x10$_7$ cells) and washed twice in PBS, re suspended in 250µl of cold PBS and sonicated on ice for 15 seconds. After centrifugation (10.000 x g at 4ºC) for 10 min the supernatant was incubated with Glutatione Sepharose beads containing GST-CLASP2(1046-1407) added for 2 hours for identification of γ-tubulin, and for 24h for identification of activated PKC interactions. Next, beads were washed with PBS and the supernatant was subjected to SDS-PAGE and Western blotting (WB) with a monoclonal mouse anti- γ-tubulin, monoclonal anti-GST antibody 5.3.3 (hybridoma supernatant 1:5) antibody, anti phospho PKCζ (Thr410/403) or anti-phospho PKCα (Thr638/641) rabbit polyclonal antibodies (Cell Signaling) and subsequent specific HRP secondary antibodies. For immunoprecipitation of FLAG-NEK, anti-flag monoclonal antibody was added to GSepharose 4 fast flow beads (GE Healthcare) and then the beads were added to lysate of transfected HEK293 cells. Next, beads were washed with PBS and then subjected to WB.

PMA treatment and *in vitro* phosphorylation

~1x10$_4$ cells growing in a 24 well plates were incubated for 4 hours with 200 ng/ml of PMA, ~40 hours after the transfection. Then the cells were fixed and submitted to immunocytochemistry as described above. For *in vitro* phosphorylation ~3 µg of purified GST-CLASP2(1046-1407) were incubated in 25 µl of the reaction mixture (20 mM Tris, 10 mM $MgCl_2$, 50 nm PMA; 20 mM ATP, pH 7.5) with 50 ng of PKCζ-Pan (a mixture of predominantly classical PKC isoforms α, βI and βII, purified from the rat brain) or recombinant PKCζ. For PKCζ were added 3.7 kBq of [γ-^{32}P]ATP (~220 TBq/ mmol). The mixture was incubated at 30ºC for 30 min. Samples were analyzed by SDS-PAGE 10% and subsequent WB and autoradiography.

Results and Discussion

The C-terminal coiled-coil region of FEZ1 is necessary for its interaction with CLASP2(1046-1407) and NEK1(441-621).

FEZ1, CLASP2 and NEK1 show coiled-coil regions, as predicted by the "Coils" software, using a score window 28 (http://www.ch.embnet.org/software/COILS_form. html) (Figures 1A,

B and C). We previously confirmed the presence of major alpha helix content in the C terminal region of FEZ1 (aminoacids 221 to 392) using low resolution structural analysis [19].

A pull down assay using full length FEZ1 protein [6xHis-FEZ1(1-392)], or a truncated FEZ1 without the C- terminal region [6xHis-FEZ1(1-227)], showed that the interactions with both, GST-CLASP2(1046-1407) or GST-NEK1(441-621), but not GST, occur predominantly in dependence of the C-terminal region of FEZ1 (Figure 1D). Interestingly, GST-NEK1(497-555), the second coiled-coil region of Nek1, interacts not only with full length 6xHis-FEZ1(1-392) but also with the N-terminal construct 6xHis- FEZ1(1-227). This finding may suggest that GST-NEK1(497-555) interacts with other regions at the N terminus of FEZ1. We speculate that this NEK1 region (from aminoacid 497 to 555) interacts naturally with other coiled-coil inside the NEK1 structure, and in this case, the fragment alone can interact with the N-terminal region of FEZ1. Our hypothesis is in agreement with the observation that the N-terminal region of FEZ1 does not interact with GST-NEK1(441-621).

Using the region from FEZ1 amino acids 229 to 269, we observe that this region alone is able to interact with GST-CLASP2(1046-1407), GST-NEK1(441-621) and GST-NEK1(497 555) (Figure 1D). These results indicate that the coiled-coil domains alone can provide interaction between these proteins. To confirm the stability of the interaction of 6xHis FEZ1(229-269) with NEK1 (GST-NEK1441-621 or 497-555) these proteins were coexpressed in bacteria. The copurification, reveals that the coiled-coil regions interact in a stable form, which is preserved after passage of the *E. coli* lysate through the GST-Trap column under stringent purification conditions (Supplementary Figure S1). The helical-wheel analysis (Supplementary Figure S2) shows the possibility of stable interactions of FEZ1 coiledcoil with CLASP2 and NEK1 coils, in agreement with the known versatility of the coiled-coil motifs for engaging in different protein-protein interactions [21].

The co-localization and interaction of dsRED-CLASP2, NEK1 and FEZ1, with endogenous γ-tubulin suggests a concerted centrossomal function

Endogenous FEZ1 interacts and co-localizes with γ-tubulin in HEK293 cells [20,22]. Here we observed that dsRED-CLASP2 and endogenous NEK1 colocalize with endogenous γ tubulin in HEK293 cells (Figures 2A and B respectively). Recombinant GST CLASP2(1046-1407)

interacts specifically with endogenous γ-tubulin in HEK293 lysates (Figure 2C). NEK1 is a large and somewhat unstable protein, maybe prone to rapid proteolysis. Its detection from cell lysates in western blots is difficult, and frequently we did not even observe it after "over"expression. Immunoprecipitation of "over"expressed FLAG-NEK1 from HEK293 coprecipitated endogenous γ-tubulin (Figure 2D). The reported interactions suggest a centrossomal concerted role not only as previously reported individualy for NEK1 and CLASP2 [14, 16, 17] but also for FEZ1.

FEZ1 co-localizes with dsRED-CLASP2(1192-1407) and with endogenous NEK1 in a perinuclear region

GST-CLASP2(1046-1407) interacts with full length 6xHis-FEZ1(1-392), but not with 6xHis FEZ1(1-227) in a pull down assay (Figure 1C). These region of full CLASP2 contains its major predicted coiled-coil region (Figure 1B). Three distinct phenotypes could be observed 48h after transfection of HEK293 cells with the construction dsRED CLASP2(1192-1407) (called dsRED-CLASP2 from here) (Figure 3A). In the phenotypes called 1 and 2, which together make up ~27,9% of the total transfected cells, a clear punctate red localization was observed, whereas the phenotype 3 shows only a diffuse red staining throughout the cell (~72,1% of total transfected cells) (Figure 3A white arrows). The co-staining with γ-tubulin (Figure 2A) allowed us to propose that the punctate appearance of dsRED-CLASP2 in the phenotypes 1 and 2 represents most likely the centrosomal region.

The dsRED-CLASP2 fragment co-localizes with endogenous FEZ1. This co-localization was observed in ~15,45% of the total of transfected cells, 48hs after transfection. Probably, the localization of this small CLASP2 fragment is determinated by the punctate localization of endogenous FEZ1. In other transfected cells that not shown FEZ1 in a punctate form, the perfect co-localization with dsRED-CLASP2 was not observed. We observed that in more than 60% of cells that show endogenous FEZ1 in a punctate perinuclear form, as observed in figure 3B, this punctate region merges with endogenous γ-tubulin localization.

Analysis of transfected COS-7 cells and HEK293 cells (not show) showed co-localization of GFP-FEZ1(1-392) and GFP-FEZ1(221-392) with both dsRED-NEK1 (not show) or endogenous NEK1 in a perinuclear region (Figure 3C, D). A full-length GFP-FEZ1(1-392) but especially the C-terminal construct FEZ1(221-392) showed a clearly localized pattern. The

construct GFP-FEZ1(221-392) contains basically the two major coiled-coil regions of FEZ1. Together with the previous data (Figure 2A, B) and data from the literature [12,14,20] we suggest that the centrossomal region is inside of the yellow stained merge region in figure 3D and that the coiled-coils are important for the FEZ1/NEK1 interaction at this site.

The observation of these results was facilitated by the use of fragments in conjunct with endogenous proteins. All these proteins have several different functions and consequently different localizations in the cell. As an example, CLASP2 protein have been described in different cell sites such as ends of microtubules, trans-Golgi network and in kinetochore [15-17]. The observation of a small CLASP2 fragment that interacts and co-localizes specifically with FEZ1 in a punctate form is a goal that provides an individual approach for only one of the possible localization sites for this protein. The same observation can be applied in NEK1 pull down analysis showed here, that permits to observe the individual capacity of different coils of NEK1, to interact only with coils in the C-terminal of FEZ1 (Figure 1 A).

CLASP2(1046-1407) is phosphorylated *in vitro*, interacts with endogenous active PKC isoforms and PMA addition disrupts its co-localization with endogenous FEZ1 in HEK293 cells.

Most interestingly, 4 hours after addition of PMA, a PKC activator, the phenotypes 1 and 2 that was observed after the transfection of HEK293 cells with dsRED-CLASP2 practically disappeared, decreasing from 27,9% to only ~3,06% of the total number of transfected cells (Figure 3A-graphic) . This seems to indicates that the localization of CLASP2(1192-1407) to the centrosome candidate region may depend on PKC activity.

The co-localization of dsRED-CLASP2 in a punctate perinuclear region coincides with the localization of endogenous FEZ1 in HEK293 cells, and this phenotype is also abolished after PMA treatment (Figure 4A). The proportion of cells with FEZ1 and dsRED-CLASP co-localization decreases from 15,45% to only 2,77% of the total number of transfected cells, after PMA treatment (Figure 4A graphic). Likely the co-localization of both proteins in a perinuclear region is influenced by their phosphorylation status that in turn may cause the abolishment of the interaction with other centrossomal proteins. Our previous results showed that after PKC phosphorylation, FEZ1 does no longer interact with CLASP2(1046-1407) *in vitro* [19]. These previous data added to our results reported in Figures 3 and 4, suggest that FEZ1 and

CLASP2(1192-1407) are located in a centrossomal candidate region and this localization is disrupted by increase in PKC activity.

Furthermore, by using specific anti-phospho PKCs we observed that GSTCLASP2(1046-1407) interacts with active endogenous PKC isoforms α/β and ζ from HEK293 cell lysates (Fig. 4B). The PMA addition to the cell cultures activates the classical and novel PKC isoforms. Although the PKCα/β band was not observed in the input after PMA activation, we observed it after the interaction with GSTCLASP2(1046-1407). Possibly, PKCα/β remained in the insoluble membrane fraction, but in contact with GST CLASP2(1046-1407) we were able to identified it. The PKCζ was identified both, before and after the PMA addition, thereby confirming the known fact that atypical PKCs are not activated by PMA. There are evidences that phosphorylation is important in the regulation of protein interactions with FEZ1. PKCζ phosphorylation causes translocation of FEZ1 from de cell membrane to cytoplasm [5], and we observed that PKC phosphorylates FEZ1, and thereby inhibits its interaction with CLASP2(1192-1407)[19].

To investigate the phosphorylation of GST-CLASP2(1046-1407), we performed the phosphorylation reaction using PKCpan, that contains isoforms activated by PMA, and PKCζ, that was shown to phosphorylate FEZ1 [5]. Using anti-Phospho-Ser and anti Phospho-Thr primary antibodies, we were able to detect a specific band in the Western Blot, that indicates that GST-CLASP2(1046-1407), but not GST, was phosphorylated *in vitro* by PKCpan (Figure 4C). When we used the isoform PKCζ, which is not activated by PMA, we also observed a specific phosphorylation of GST-CLASP2(1046-1407) but not of control protein GST-RAI (Figure 4E). These results validate the hypothesis that FEZ1 and CLASP2 interact and maybe even that its putative concerted functions are regulated by phosphorylation through different members of the PKC family, possibly also by NEK1 itself.

Concluding, the same cellular localization of FEZ1, NEK1, CLASP2 and γ- tubulin, indicates that the function of these proteins may overlap in temporal and spatial fashion on the centrosome. The centrosome is a very dynamic cellular structure, involved in various processes, principally in cell cycle and cell polarization. The coiled-coil mediated phosphorylation dependent interactions among FEZ1, NEK1 and CLASP2 reported here, demonstrate the versatility and dynamic of the interactions occurring at the centrossome.

Discussion

The actuations of CLASP2 and NEK1 have not previously been reported to be connected. Here, we show that NEK1, CLASP2 and FEZ1 co-localize with endogenous γ-tubulin in mammalian cells and that NEK1 and CLASP2 colocalizes with FEZ1 in a centrossomal/perinuclear region.

Furthermore, our pull down experiments showed that NEK1 and CLASP2 interactions with FEZ1, can occur only in a specific coiled-coil region of FEZ1. The versatility of the coiled-coil interactions may allow specificity without the loss of dynamical rearrangements. In a recent work, we showed that FEZ1 has an elongated shape, and forms dimers in solution [19]. The dimerization occurs in the N-terminal region of FEZ1 and the C-terminal coiled-coil region is free and exposed to allow protein-protein interactions. The C-terminal region of FEZ1 (from amino acid 221 to 392), that presents the major coiled-coil region, interacts with more than 40 different proteins, and presents several predicted phosphorylation sites, including PKC sites [19]. The results shown here allow us to speculate that the FEZ1 dimer may simultaneous interact with both NEK1 and CLASP2, through its C-terminal coiled-coil regions. Another interesting finding is the change in dsRED-CLASP2(1192-12407) cellular co-localization promoted by PMA treatment. Subsequent co-precipitation and *in vitro* phosphorylation assays showed that CLASP2(1046-1407) is phosphorylated by different PKC isoforms. CLASP2 phosphorylation may therefore inhibit its localization to a centrosome candidate region, which may be mediated by binding to FEZ1. In support of this hypothesis, a previous report showed that FEZ1 sub-cellular localization is altered by inhibition of PKCs in PC12 cells [5] and here we also observed that after PMA treatment the FEZ1/CLASP2 co-localization is abolished.

In a review Bisgrove and Yost pointed out that there may be a functional link between the pathophysiology of the poly cystic kidney disease (PKD), the mechanosensorial functions of the polycysteins (Pkd1 and 2) in the context of the primary cilia and the intraflagellar transport [23]. This view is supported by the discovery of the concerted action of several proteins involved in these processes that when their genes are affected by mutations cause the PKD, including: Nek1, Nek8 (centrosome and cilia functions), Kif3a (transport), Pkd1 and 2 (mechanosensors). Here we add with FEZ1 (transport adaptor) and CLASP2 (microtubular tip function) two new players to this scenario. Our findings may emphasize the view that the PKD may not only manifest itself in consequence of direct gene disruption of its key signaling components such as Pkd1 and 2, but

also in an indirect fashion, through a incorrect cilliary localization of its components. In this context we now begin to understand the importance of Kif3, which when missing also causes PKD [24] and of also of FEZ1, which is intimately associated to microtubular transport processes and furthermore interacts physically with Nek1 [7] and Kif3 [3]. Future experiment will be directed add identifying the exact contribution and roles of all individual components in this intricate protein network, which disregulation leads through multiple pathways to the PKD.

Our data suggest that the functions of FEZ1, NEK1 and CLASP2 should be analysed together, in a context of cytosqueleton and centrossomal activities. FEZ1 dimer mediates interactions principally via the C-terminal coiled coil regions and our data suggest that FEZ1 could be a connection point between the NEK1 and CLASP2 activities. A concerted interaction of these proteins may open new avenues to the study of the highly dynamic centrossomal and microtubular functions.

Acknowledgements

Financially supported by: Fundação de Amparo à Pesquisa do Estado São Paulo, Conselho Nacional de Pesquisa e Desenvolvimento and LNLS. We thank Maria Eugenia Camargo and Jéssica Bernachi for technical assistance.

References

[1] L. Bloom, H.R. Horvitz, The Caenorhabditis elegans gene unc-76 and its human homologs define a new gene family involved in axonal outgrowth and fasciculation, Proc. Natl. Acad. Sci. 94 (1997) 3414-3419.

[2] T. Suzuki, Y. Okada, S. Semba, Y. Orba, S. Yamanouchi, S. Endo, S. Tanaka, T. Fujita, S. Kuroda, K. Nagashima, H. Sawa, Identification of FEZ1 as a protein that interacts with JC Virus Agnoprotein and microtubules, J. Biol. Chem. 280 (2005) 24948–24-56.

[3] T. L.Blasius, D. Cai, G.T. Jih, C.P. Toret, K.J. Verhey, Two binding partners cooperate to activate the molecular motor Kinesin-1, J. Cell. Biol. 176 (2007) 11–17.

[4] J. Ikuta, A. Maturana, T. Fujita, T. Okajima, T. Kenji, K. Tanizawa, S. Kuroda, Fasciculation and elongation protein zeta-1 (FEZ1) participates in the polarization of hippocampal neuron by controlling the mitochondrial motility, Biochem. Biophys. Res. Commun. 353 (2007), 127-132.

[5] S. Kuroda, N. Nakagawa, C. Tokunaga, K. Tatematsu, K. Tanizawa, Mammalian homologue of the Caenorhabditis elegans UNC-76 protein involved in axonal outgrowth is a protein kinase C zeta-interacting protein, J. Cell. Biol. 114 (1999) 403-411.

[6] N. Sakae, N. Yamasaki, K. Kitaichi, T. Fukuda, M. Yamada, H. Yoshikawa, T. Hiranita, Y. Tatsumi, J. I. Kira , T. Yamamoto, T. Miyakawa, K.I. Nakayama, Mice lacking the schizophrenia-associated protein FEZ1 manifest hyperactivity and enhanced responsiveness to psychostimulants, Hum Mol Genet 17 (2008) 3191-3203.

[7] M.J. Surpili M, T.M. Delben, J. Kobarg, Identification of proteins that interact with the central coiled-coil region of the human protein kinase NEK1 involved in the cell cycle regulation, Biochemistry 42 (2003) 15369-15376.

[8] E.M. Assmann, M.R. Alborghetti, M.E.R. Camargo, J. Kobarg, FEZ1 dimerization and interaction with transcription regulatory proteins involves its coiled-coil region, J Biol Chem 281 (2006) 9869-9881.

[9] L. O'Regan, J. Blot, A.M. Fry, Mitotic regulation by NIMA-related kinases, Cell. Div. 29 (2007) 2-25.

[10] C. Vogler, S. Homan, A. Pung, C. Thorpe, J. Barker, E.H. Birkenmeier, P. Upadhya, Clinical and pathologic findings in two new allelic murine models of polycystic kidney disease, J. Am. Soc. Nephrol. 12 (1999), 2534-2539.

[11] P. Upadhya, E.H. Birkenmeier, C.S. Birkenmeier, J.E. Barker, Mutations in a NIMA related kinase gene, Nek1, cause pleiotropic effects including a progressive polycystic kidney disease in mice, Proc. Natl. Acad. Sci. USA. 97 (2000) 217-221.

[12] M.R. Mahjoub, M.L. Trapp, L.M. Quarmby, NIMA-Related Kinases Defective in Murine Models of Polycystic Kidney Diseases Localize to Primary Cilia andCentrosomes, J. Am. Soc. Nephrol. 16 (2005) 3485-3489.

[13] O. Shalom, N. Shalva, Y. Altschuler, B.Motro. The mammalian Nek1 kinase is involved in primary cilium formation, FEBS Lett. 582 (2008) 1465-1470.

[14] M.C. White, L.M. Quarmby, The NIMA-family kinase, Nek1 affects the stability of centrosomes and ciliogenesis, BMC Cell Biol. 4 (2008) 9-29.

[15] Y. Mimori-Kiyosue, I. Grigoriev, G. Lansbergen, H. Sasaki, C. Matsui, F. Severin, N. Galjart, F. Grosveld, I. Vorobjev, S. Tsukita, A. Akhmanova, CLASP1 and CLASP2 bind to EB1 and regulate microtubule plus-end dynamics at the cell cortex, J. Cell Biol. 168 (2005) 141-153.

[16] P. Kumar, K.S. Lyle, S. Gierke, A. Matov, G. Danuser, T. Wittmann, GSK3beta phosphorylation modulates CLASP-microtubule association and lamella microtubule attachment. J. Cell Biol. 184 (2009) 895-908.

[17] A.L. Pereira, A.J. Pereira, A.R. Maia, K. Drabek, C.L. Sayas, P.J. Hergert, M. Lince Faria, I. Matos, C. Duque, T. Stepanova, C.L. Rieder, W.C. Earnshaw, N. Galjart, H. Maiato, Mammalian CLASP1 and CLASP2 cooperate to ensure mitotic fidelity by regulating spindle and kinetochore function, Mol. Biol. Cell 17 (2006) 4526-4542.

[18] A. Efimov, A. Kharitonov, N. Efimova, J. Loncarek, P.M. Miller, N. Andreyeva , P. Gleeson, N. Galjart, A.R. Maia, I.X. McLeod, J.R. Yates, H. Maiato, A. Khodjakov, A. Akhmanova, I. Kaverina, Asymmetric CLASP-dependent nucleation of noncentrosomal microtubules at the trans-Golgi network, Dev. Cell 12 (2007) 917-930.

[19] D.C. Lanza, J.C. Silva, E.M. Assmann, A.J. Quaresma, G.C. Bressan, I.L. Torriani, J. Kobarg, Human FEZ1 has characteristics of a natively unfolded protein and dimerizes in solution, Proteins 74 (2009)104-121.

[20] D.C. Lanza, D.M. Trindade , E.M. Assmann, J. Kobarg, Over-expression of GFPFEZ1 causes generation of multi-lobulated nuclei mediated by microtubules in HEK293 cells, Exp. Cell. Res. 314 (2008) 2028-2039.

[21] A. Lupas, M. Van Dyke, J. Stock, Predicting coiled-coils from protein sequences, Science 252 (1991) 1162-1164.

[22] S. Lee, C.L. Walker, B. Karten, S.L. Kuny A. A. Tennese, M. A. O'Neill, R. Wevrick, Essential role for the Prader–Willi syndrome protein necdin in axonal outgrowth, Hum. Mol. Genet. 14 (2005) 627-637.

[23] Bisgrove BW, Yost HJ (2006) The roles of cilia in developmental disorders and disease. Development 133: 4131-4143

[24] Lin F, Hiesberger T, Cordes K, Sinclair AM, Goldstein LSB, Somlo S, Igarashi P (2003) Kidney-specific inactivation of the KIF3A subunit of kinesin-II inhibits renal ciliogenesis and produces polycystic kidney disease. Proc Nat Acad Sci 100: 5286-5291

Legends of figures

Figure 1: FEZ1, CLASP2 and NEK1 have predicted coiled-coil sites and GSTCLASP2(1046-1407) and GST-NEK1(441-621) interactions with FEZ1 are strongly increased in presence of FEZ1 C-terminal coiled-coil region. (A,B,C) Constructs of FEZ1, CLASP2 and NEK1 used in the experiments. The graphs above the construct indicate the coiled-coil prediction by COILS [22] for the complete primary sequences of all proteins. The black regions indicate the predicted coiled-coil regions. (D) Pull-down assay showed that the interaction between 6xHis-FEZ1 and GSTCLASP2(1046-1407) occurs in the presence of the 6xHis-FEZ1 C-terminal region. A supernatant containing 6xHis-FEZ1(1-392) and 6xHis-FEZ1(1-227) was added to glutatione sepharose beads containing GST-CLASP2(1046-1407), GST-NEK1 (441- 621) and GST NEK1 (497-555) or GST. (E) Pull-down using 6xHis-FEZ1(229-269) in the supernatant

confirms the interaction of the FEZ1 coiled-coil alone with the coiledcoils of the indicated proteins. The molecular weight and presence of GST and 6xHistagged proteins were confirmed by coomassie-stained SDS-PAGE and WB. Black arrowheads indicate the positions of the GST fusion proteins in WB anti-GST and of 6xHis-fusions in WB anti 5xHis. The other bands in the same trail below the indicated band are degradation products of each target protein that remain with GST tag. St = molecular weight standard proteins.

Figure 2: dsRED-CLASP2, endogenous NEK1 and endogenous FEZ1, colocalize and interact with γ-tubulin. (A,B) The dsRED-CLASP2(1192-1407) and endogenous NEK1 colocalize with endogenous γ-tubulin in HEK293 cells (white arrowheads). The DNA was counter-stained with Hoechst. (C) GST-CLASP2 (1192-1407) recombinant protein (black arrowhead) interacts specifically with endogenous γ-tubulin (white arrowhead) from HEK293 cells lysate. The specificity of this interaction was controlled by unloaded and GST loaded beads. (D) Recombinant Flag-NEK1 immuno-precipitates (IP) endogenous γ tubulin from transfected HEK293 cells. The specificity of this interaction was confirmed by immunoprecipitation from the lysate of untransfected cells using anti-flag monoclonal antibody.

Figure 3: FEZ1 co-localizes with dsRED-CLASP2 and with endogenous NEK1 in a punctate perinuclear region of HEK293 and COS7 cells respectively. (A) The over-expression of dsRED-CLASP2(1192-1407) generates three different phenotypes, named 1, 2 and 3, in transfected HEK293 cells. The frequency of these phenotypes in three replicates in percentage of the transfected cells is shown in the graphics accompanying the panels. The addition of PMA affects this percentage as shown in the graphic. The error bars represent the standard deviation of the mean. (B) Endogenous FEZ1 co-localizes with dsRED-CLASP2(1192-1407) in a punctate perinuclear region in COS7cells. (C-D) Different GFP-FEZ1 constructs colocalize with dsRED-NEK1 in a perinuclear fashion in COS-7cells. (D) A more intense merge region is observed when NEK1 is labeled in cells that also over-express GFP-FEZ1(221-392), which contains the major coiled-coil regions of FEZ1.

Figure 4: The CLASP2 fragment is phosphorylated *in vitro*, interacts with endogenous active PKC isoforms and PMA addition disrupts its co-localization with endogenous FEZ1 in HEK293 cells. (A) The co-localization of endogenous FEZ1 and dsRED-CLASP2 is disrupted

after PMA addition. The frequency of co-localization was quantified, and is represented by the bars in the graphic. (B) Active PKCs from HEK293 lysates interacts with recombinant GST-CLASP2(1046-1407) after incubation with HEK293 lysate. (C) GST-CLASP2(1046-1407) is phosphorylated *in vitro* by PKC-Pan. Before (-P) and after the phosphorylation reaction (+P), samples were analyzed by Coomassie-stained SDS-PAGE and WB using anti-phospho-Ser/Thr primary antibodies. The proteins did not show unspecific phosphorylation when isolated inform the bacteria (-P = non phosphorylated control, that is: a reaction without PKC only). The band observed in +P indicates specific Ser/Thr phosphorylation on GST-CLASP2(1046-1407). GST was used as a negative control. (D) PKCζ phosphorylate GSTCLASP2(1046-1407) *in vitro*. The indicated proteins have been submitted to *in vitro* phosphorylation by PKCζ and were then analyzed by SDS-PAGE and autoradiography. The white arrowheads indicate phosphorylated GST-CLASP2(1046-1407) and black arrowheads indicate the negative control fusion protein GST-RAI isoform 14 (720-983). 6xHis-FEZ1(1-392) was used as a positive control. The asterisks (*) indicate the PKCζ autophosphorylation. St= molecular weight standard proteins.

Supplementary figure 1: The co-expression of GST-NEK1(441-621) or GST-NEK1(497-555) with 6xHis-FEZ1(229-269) results in the elution of a stably interacting complex. 6xHis FEZ1 (229-269) and GST only (control), GST-NEK1(441-621) or GST-NEK1(497-555) were produced simultaneously after co-transformation of *E. coli* BL21 (DE3). The co-purifications were performed using a GST-Trap column in an AKTA^{TM} FPLC^{TM} (GE Healthcare). After mechanical lysis with a French Press, soluble and insoluble fractions were separated by centrifugation and the cleared supernatant was then loaded onto a GST-Trap column pre-equilibrated with lysis buffer (137 mM NaCl, 2.7 mM KCl, 10 mM Na_2HPO4, 1.8 mM KH_2PO4, pH 7.4, and 1 mM phenylmethylsulfonyl fluoride), followed by extensive wash of the column with the same buffer. Bound proteins were eluted in a gradient of 0–100% of elution buffer (50 mM Tris-HCl and 20 mM reduced Gluthatione, pH 8,0). GST only does not co-purify with co-expressed 6xHis-FEZ1(229-269). The co-expressions and co-purifications are shown by Coomassie stained SDS-PAGE. White arrow heads indicate GST or GST-NEK fusion proteins as indicated on top of the figure. Black arrow heads indicate the copurified 6xHis-FEZ1(229-269). St= standard of molecular weight.

Supplementary figure 2: Helical wheel representations of the FEZ1 interactions with NEK1 and CLASP2 coiled coils. (A, B) Helical wheel representations of hetero dimeric coiled-coils based on the FEZ1 (amino acids 229-269) with NEK1 (amino acids 500-555) or FEZ1 with CLASP2 (amino acids 1269-1303) predicted heptad repeats. The view is from the N terminus down to the C terminus.

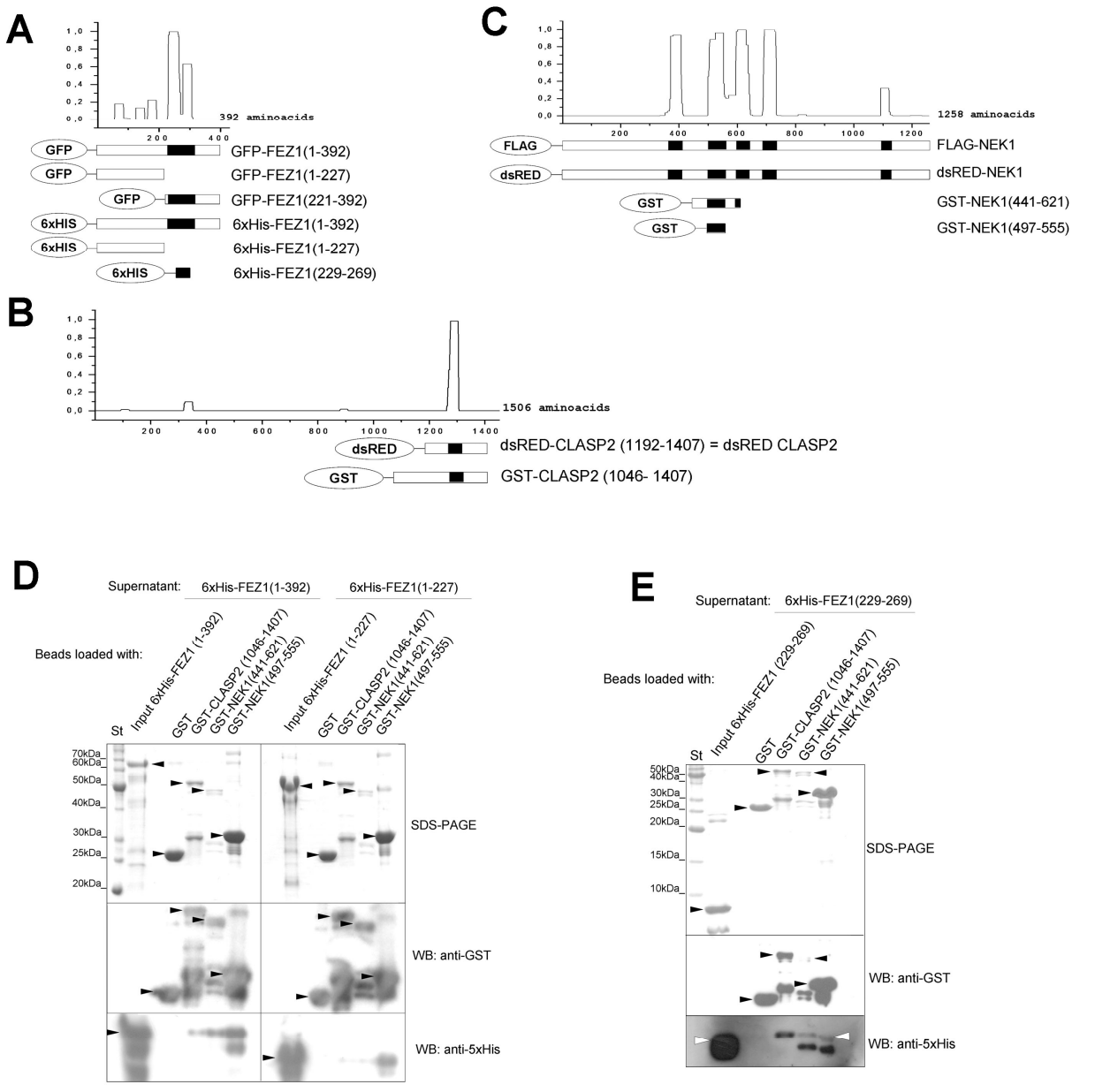
A
392 aminoacids
GFP
GFP-FEZ1(1-392)
GFP
GFP-FEZ1(1-227)
GFP
GFP-FEZ1(221-392)
6xHIS
6xHis-FEZ1(1-392)
6xHIS
6xHis-FEZ1(1-227)
6xHIS
6xHis-FEZ1(229-269)
C
1258 aminoacids
FLAG
FLAG-NEK1
dsRED
dsRED-NEK1
GST
GST-NEK1(441-621)
GST
GST-NEK1(497-555)
B
1506 aminoacids
dsRED
dsRED-CLASP2 (1192-1407) = dsRED CLASP2
GST
GST-CLASP2 (1046- 1407)
D
Supernatant:
6xHis-FEZ1(1-392)
6xHis-FEZ1(1-227)
Beads loaded with:
St
Input 6xHis-FEZ1 (1-392)
GST
GST-CLASP2 (1046-1407)
GST-NEK1(441-621)
GST-NEK1(497-555)
Input 6xHis-FEZ1 (1-227)
GST
GST-CLASP2 (1046-1407)
GST-NEK1(441-621)
GST-NEK1(497-555)
70kDa
60kDa
50kDa
40kDa
30kDa
25kDa
20kDa
SDS-PAGE
WB: anti-GST
WB: anti-5xHis
E
Supernatant:
6xHis-FEZ1(229-269)
Beads loaded with:
St
Input 6xHis-FEZ1 (229-269)
GST
GST-CLASP2 (1046-1407)
GST-NEK1(441-621)
GST-NEK1(497-555)
50kDa
40kDa
30kDa
25kDa
20kDa
15kDa
10kDa
SDS-PAGE
WB: anti-GST
WB: anti-5xHis

FIGURE 1

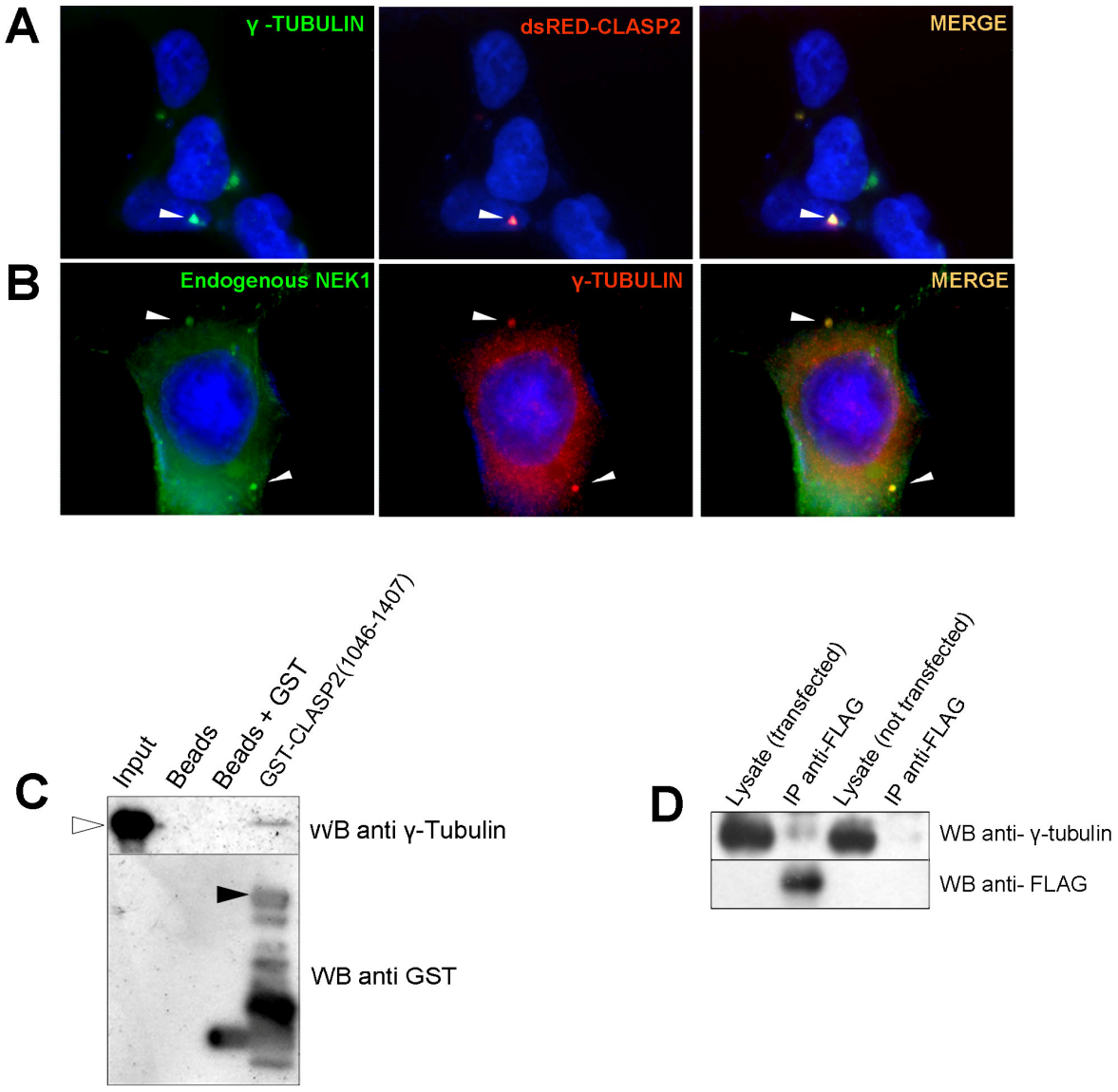
A
γ -TUBULIN
dsRED-CLASP2
MERGE
B
Endogenous NEK1
γ-TUBULIN
MERGE
C
Input
Beads
Beads + GST
GST-CLASP2(1046-1407)
WB anti γ-Tubulin
WB anti GST
D
Lysate (transfected)
IP anti-FLAG
Lysate (not transfected)
IP anti-FLAG
WB anti- γ-tubulin
WB anti- FLAG

FIGURE 2

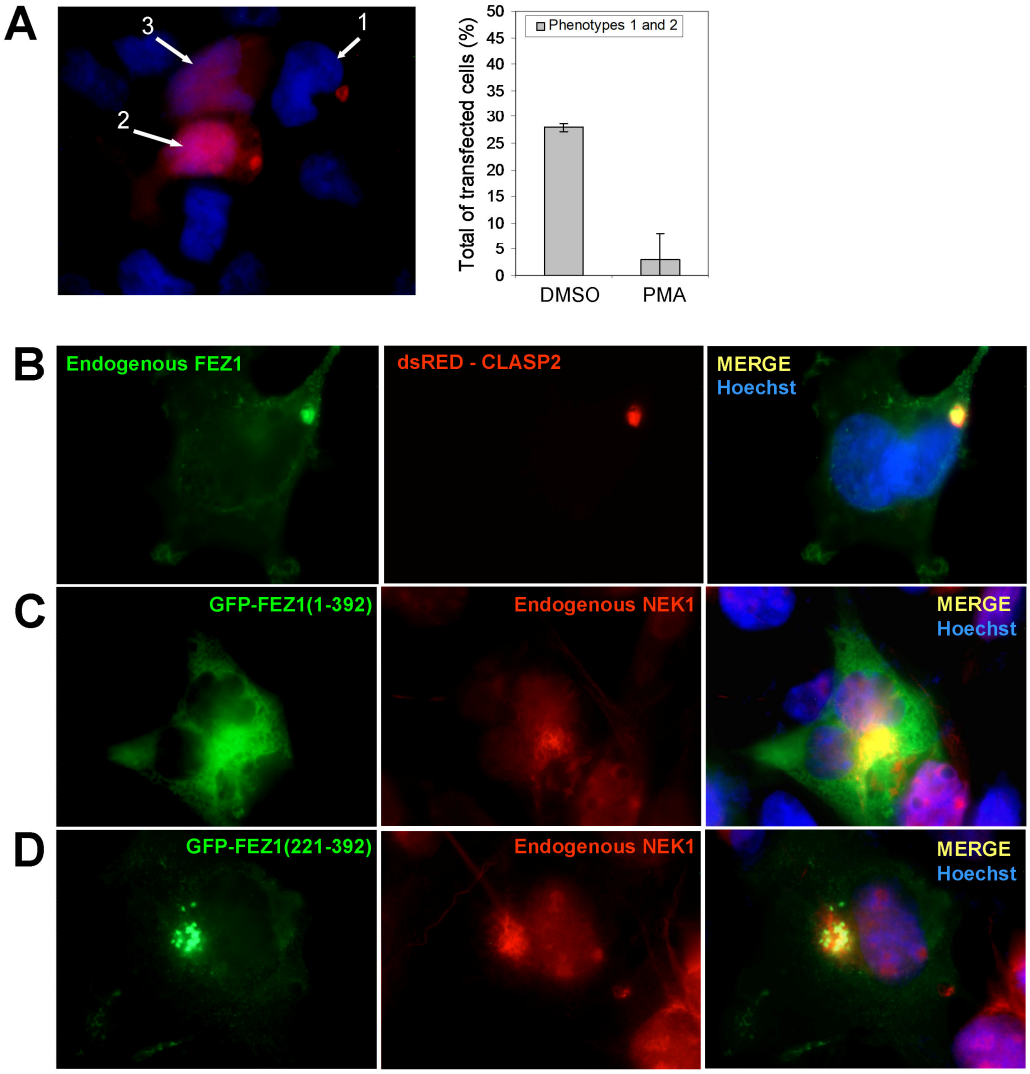
A
3
1
2
Phenotypes 1 and 2
Total of transfected cells (%)
50
45
40
35
30
25
20
15
10
5
0
DMSO
PMA
B
Endogenous FEZ1
dsRED - CLASP2
MERGE
Hoechst
C
GFP-FEZ1(1-392)
Endogenous NEK1
MERGE
Hoechst
D
GFP-FEZ1(221-392)
Endogenous NEK1
MERGE
Hoechst

FIGURE 3

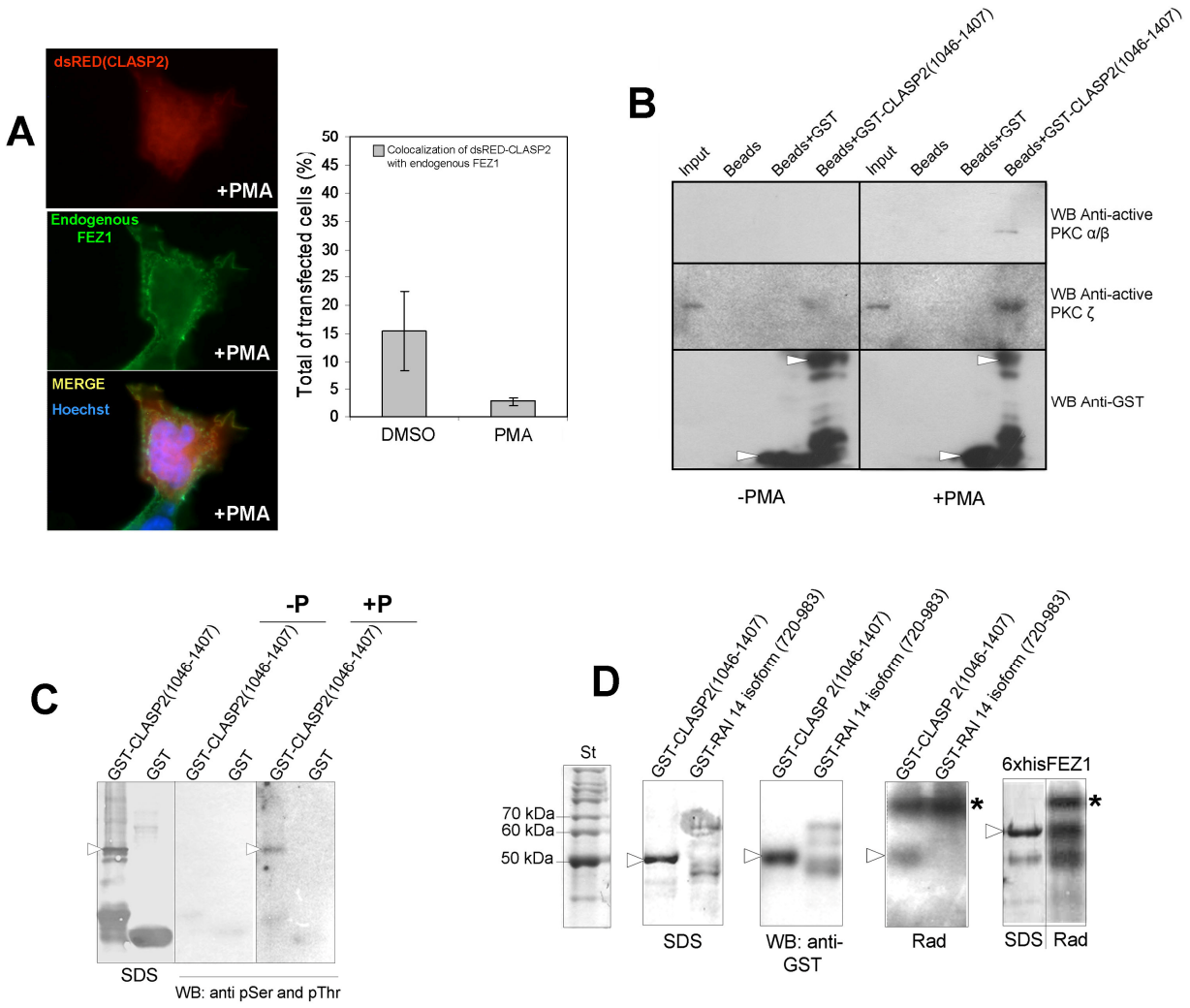
A
dsRED(CLASP2)
+PMA
Endogenous FEZ1
+PMA
MERGE
Hoechst
+PMA
Colocalization of dsRED-CLASP2 with endogenous FEZ1
Total of transfected cells (%)
50
45
40
35
30
25
20
15
10
5
0
DMSO
PMA
B
Input
Beads
Beads+GST
Beads+GST-CLASP2(1046-1407)
Input
Beads
Beads+GST
Beads+GST-CLASP2(1046-1407)
WB Anti-active PKC α/β
WB Anti-active PKC ζ
WB Anti-GST
-PMA
+PMA
C
-P
+P
GST-CLASP2(1046-1407)
GST
GST-CLASP2(1046-1407)
GST
GST-CLASP2(1046-1407)
GST
SDS
WB: anti pSer and pThr
D
St
70 kDa
60 kDa
50 kDa
GST-CLASP2(1046-1407)
GST-RAI 14 isoform (720-983)
GST-CLASP 2(1046-1407)
GST-RAI 14 isoform (720-983)
GST-CLASP 2(1046-1407)
GST-RAI 14 isoform (720-983)
6xhisFEZ1
SDS
WB: anti-GST
Rad
SDS
Rad

FIGURE 4

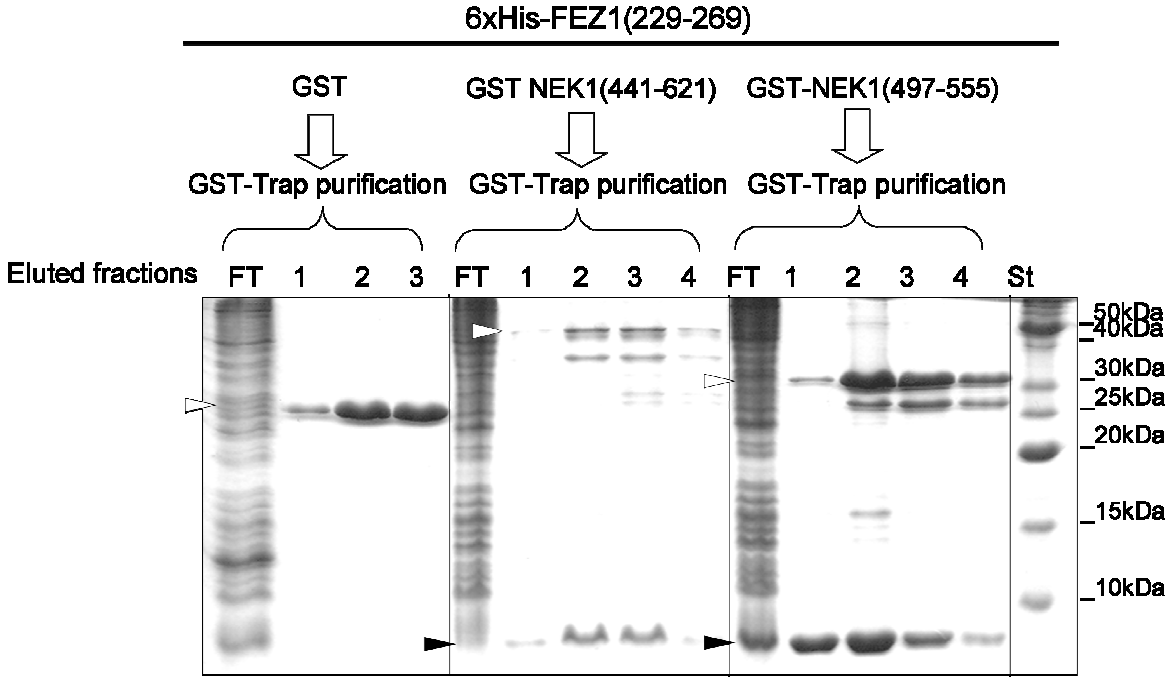

Supplementary figure 1

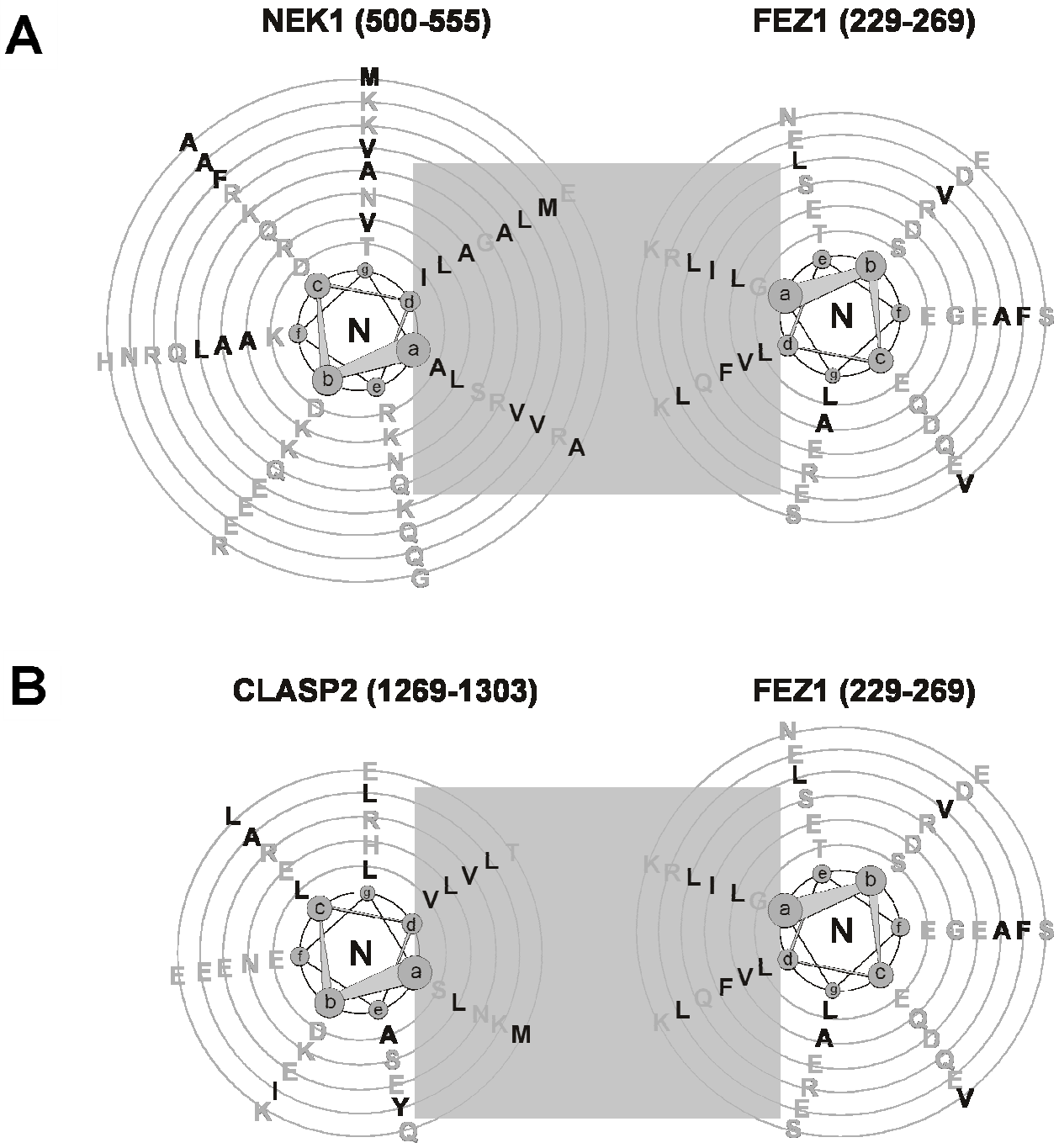

Supplementary figure 2

Artigo 4

The generation of flower like nuclei mediated by FEZ1 over-expression is affected by PKC and PI3K

Daniel C. F. Lanza [ab], Priscilla P. Zenatti[ac], José A. Yunes[bc] and Jörg Kobarg[ab]

[a]Laboratório Nacional de Luz Síncrotron, Campinas SP, Brasil [b]Instituto de Biologia, Universidade Estadual de Campinas, Campinas, SP, Brasil. [c]Hospital Infantil Boldrini, Campinas, SP, Brasil.

Address correspondence to: Jörg Kobarg, Laboratório Nacional de Luz Síncrotron, Centro de Biologia Molecular Estrutural, Rua Giuseppe Máximo Scolfaro 10.000, C.P.6192, 13084-971 Campinas - SP, Brasil, Tel.: (+55)19-3512-1125, Fax: (+55)19-3512- 1006, E-mail: jkobarg@lnls.br

Manuscrito em fase inicial de preparação

Abstract

FEZ1, first described as an orthologue of the neuronal protein UNC76 from *C elegans,* works with microtubules and motor proteins in transport mechanisms, and has been proposed to be involved during schizophrenia development. The over expression of FEZ1 causes the development of multi-lobulated nuclei, also called flower like nuclei, a typical hallmark of leukemic cells from Adult T Cell Leukemia/lymphoma patients. The formation of this phenotype is associated to a disruption in the microtubule spindle organization and is favored by PI3K activation, downstream AILIM-ICOS signaling. Other subsequent components and steps of this pathway are unknown. We observed that the number of flower like cells mediated by FEZ1 over-expression is influenced by PKC and PI3K activities, and that this phenotype is also even observed in lymphocytes infiltrated in the Central Nervous System, in some cases of childhood leukemia.

Introduction

FEZ1 was first described as an orthologue or UNC76 protein form *C elegans* involved in the development of the nervous system [1]. The first studies associated FEZ1 to neuronal differentiation, and abrogation of its actuation with DISC1 is considered as one of the causes of schizophrenia development [2,3]. FEZ1 is a substrate and functions in concert with PKCζ during neuronal differentiation. PKC phosphorylation causes FEZ1 migration from plasma membrane to cell cytoplasm in COS-7 cells [3]. Subsequent studies showed FEZ1 participation in Kinesin activation, mitochondrial transport and cellular polarization [4,5]. FEZ1 knockout mice show hyperactivity and other symptoms similar to symptoms observed in schizophrenia [6]. Recently, we observed that FEZ1 can form dimers in solution and belongs to the class of intrinsically unfolded proteins [7] in agreement with this versatility to interact with other proteins [19].

We observed that upon GFP-FEZ1 over-expression in HEK293 cells, over 40% of the transfected cells develop multi-lobulated nuclei, so-called flower-like nuclei, consisting of 2 to many nuclear lobules, which arrangement remembers that of the petals of a flower [8].

The flower-like phenotype had been previously reported also to be caused by over-expression of nuclear versions of the protein tyrosine kinase Chk [9]. The kinase activity of Chk was not a requirement for flower-like nuclei formation in COS1 cells. Whereas Chk over expression provoked a flower like phenotype which led to an arrest of the cell cycle, in the case of FEZ1 the arrest was not observed indicating that the cycle can continue despite the phenotype [8,9].

Other studies associate the flower like nuclei to cell multidrug resistance and cancer. In multidrug resistant human acute lymphocytic leukemia cell lines L_{100} and L_{1000}, the formation of flower like nuclei is linked to the drug resistance mechanism of this cells [10]. These flower like nuclei are indeed widely observed in leukemia and this feature is considered a morphological hallmark for malign T lymphocytes, which can be observed in more than 50% of the patients with Adult T Cell Leukemia/lymphoma (ATLL) [12, 13]. Malignant T cells in acute-type ATLL patients show flower-like nuclei that have been shown to be a specific morphological feature of malignant T cells [14]. ATLL-type multi-lobulated nuclei are produced through a distinct rearrangement of microtubules via PI3-kinase cascade that has been activated by both AILIM-ICOS (*Activation Inducible Lymphocyte Immuno mediatory Molecule Inducible Costimulator*) and cell surface molecules. The formation of ATLL-type multilobulated nuclei requires the alteration of PI3 kinase-Akt cascade activation via the downregulation of PTEN and or SHIP-1 [12].

Interleukin-7 (IL7) is a hematopoietic cytokine with critical functions in both B- and T-lymphocyte development and activates the PI3K pathway upstream, by signaling through the IL7 receptor [15]. Interestingly, some studies show IL7 participation in neuronal differentiation in hippocampus cells and maintenance other functions in central nervous system [16-18]. The mRNAs encoding IL7 and IL7 receptor (IL7R) are expressed *in vivo* during the developing brain, and treatment of cultures of embryonic brain with exogenous IL7 increases neuronal survival and results in greater numbers of cells manifesting neurite outgrowth [18]. The direct neurotrophic properties of IL7 combined with the expression of ligand and receptor in developing brain suggest that IL7 may be a neuronal growth factor of physiological significance during central nervous system (CNS) ontogeny [18].

In most studies [10,12] including our previous work [8] the flower like formation are dependent of intact microtubules. The multilobulation may be caused by the atypical organization

of cytoskeleton elements, that causes nuclei constriction with the flower like formation [8,12]. The multidrug resistance of L100 and L100 lymphocytic leukemic cell lines were related to the flower like phenotype that is a consequence of a different microtubule organization [10]. Nuclear contraction and generation of multi-lobulated nuclei are caused by tubulin and actin "loops" and involve abnormal microtubule functions [8,12].

Here we show that the flower like formation mediated by FEZ1 over-expression can be modulated by PKC and PI3K activities, in the second case, as observed in leukemic patients. In addition we showed the co-localization of FEZ1 with Il7R, and propose that FEZ1 is a new important component to be analyzed for the elucidation of IL7R function in neurons and in leukemic cells infiltrated in the central nervous system.

Materials and Methods

Plasmid constructions

Nucleotide sequences of FEZ1 (1–392), truncated FEZ1(1–227) and FEZ1(221-392) were amplified by PCR and cloned into bacterial expression vector pET28a (Novagen/EMD Biosciences, San Diego, CA) as described [19]. Full-length or truncated FEZ1 were subcloned in pEGFPC2 vector (Clontech) for expression of GFP tagged proteins in human cells. The IL7R nucleotide sequence was amplified by PCR and cloned in the pE6-V5 vector, for expression in mammalian cells.

Transfection

Adherent HEK293 or COS-7 cells were cultivated in 24-well plates containing DME medium, 10% FCS and penicillin and streptomycin at a concentration of ~1.2×104 cells/plate (24-well) or at 37 °C and 5% CO2 atmosphere. Transfections were performed by the calcium phosphate method and monitored by inverted fluorescence microscope.

Drug treatments

PMA (200ng/mL) and Staurosporine (50ng/mL) treatments were performed 43h after the transfection, and cells were fixed 5h after the treatment. The PI3K inhibitor (20μM) was added 48h after the transfection and the cells were fixed 12h after the treatment. Flower like nuclei of

transfected cells, from three independent experiments, were counted in a Nikon fluorescence microscope.

Immunocytochemistry

HEK293 or COS7cells used for immunocitochemstry analysis, were fixed in a solution containing 2% (w/v) paraformaldehyde, 50 μM Taxol and 50m MEGTA at room temperature for 20 min, and then permeabilized and blocked in a mixture of 0.3% (v/v) Triton X-100, and 3%(w/v) glycine solution in PBS at room temperature for 30 min. For detection of α-tubulin and IL7R the cells were incubated at room temperature for 1h with a monoclonal mouse anti α-tubulin (1:200) or polyclonal rabbit anti-V5 epitope (1:1000) (Santa Cruz Biotechnology, Sigma, respectively) in PBS containing 0.1% BSA (w/v). Subsequently, the cells were incubated at room temperature for 1 h with an Rhodamine-conjugated bovine anti-mouse or anti rabbit (1:200) (Santa Cruz Biotechnology). Hoechst 33258 (1 μg/mL) dye was used to stain the nuclei. Cells were examined with Nikon fluorescence microscope.

Patient samples

Cells were obtained from liquor or bone marrow of seven leukemic patients that received in Hospital Infantil Boldrini, located in the Campinas, São Paulo, Brazil, in the last ten years. The cell smear were fixed in glass slides and stained with Giemsa. All slides used to our analysis were the same slides used previously in the patient diagnostics and belongs to the database of the hospital. The nuclei of cells were analyzed and counted by common optical microscopy using a Nikon microscope.

Reverse transcription and real time PCR

Total RNA was isolated using TRIzol (Invitrogen) from bone marrow and liquor cells pellet. Integrity of the isolated RNA was assessed by separation on a 1% ethidium bromide-stained agarose gel. Contaminating DNA was removed using DNase I (Ambion Inc., Austin, TX) at a concentration of 1 unit/μg RNA in the presence of 20 mM Tris-HCl, pH 8.4, containing 2 mM $MgCl_2$ and 50 mM KCl for 15 min at 25 °C. Five μg of total RNA were used for cDNA synthesis in a total volume of 20 μL, using the first strand cDNA syntesis kit (GE Healtcare).

Real time PCR was performed in order to quantify FEZ1 mRNA transcription in leukemic cells. For PCR amplifications, 5 μL of the reverse transcription reaction were used as a template. The reaction product was amplified by real time PCR on the 7000 Sequence Detection kit (Applied Biosystems) according to the manufacturer's instructions. FEZ1 mRNA abundance was quantified as a relative value compared with an internal reference, β-actin, whose abundance was believed not to change between the varying experimental conditions. The primers used for real time PCR are as follows: forward'5-CGAGGCTCTGAATGGCAACT -3' and reverse primer '5-GAATCATTTTCACTCTTCTCATTGAACT-3' for FEZ1 and forward '5-TGGATCAGCAAGCAGGAGTATG-3' and reverse '5-GCATTTGCGGTGGACGAT-3' for β-actin. Quantitative values for FEZ1 and β-actin mRNA transcription were obtained from the threshold cycle number where the increase in the signal associated with an exponential growth of PCR products begins to be detected. Melting curves were generated at the end of every run to ensure product uniformity. The data were analyzed according to the manufacturer's instructions. FEZ1 mRNA of bone marrow and liquor cells was quantified as follows. The relative target gene expression level was normalized on the basis of β-actin expression as an endogenous RNA control. The Δ*Ct* values of the samples were determined by subtracting the average *Ct* value of FEZ1 mRNA from the average *Ct* value of the internal control β-actin.

Results and discussion

Different fragments of FEZ1 show different localizations in COS7 cells that suggest reticular/vesicular transport and microtubule associated processes.

Previously we observed that the FEZ1 over-expression causes de formation of the flower like nuclei in HEK293 and Hella cells, and that the formation of this phenotype is caused by alteration in the organization of microtubule spindle. When over-expressed in COS7 cells, FEZ1 full-length also shows a diffuse expression pattern in the cytoplasm, and causes the flower like phenotype in some cells (Figure 1A). However, different FEZ1 fragments, that consist of FEZ1 N-terminal (GFP-FEZ1 1-227) and C-terminal (GFP-FEZ1 221-392) regions, showed distinct nondiffuse cellular localizations, that can be associated to endoplasmic reticulum and Golgi complex/centrossome respectively (figure 1 A), two cellular structures/regions devoted to transport and vesicular delivery. In the GFP transfected control cells (Figure 1B) we observed a

diffuse cytoplasmatic and nuclear GFP expression, as expected. In Figure 1C it is clear that GFP-FEZ1(1-227) co-localizes with regions containing α-tubulin witch line the endoplasmic reticulum.

FEZ1 co-localizes with IL7R in a perinuclear region and in a endoplasmic reticulum candidate region.

The activation of PI3K pathway can be caused by several different stimuli in the cell periphery through the activation of membrane receptors such as IL receptors or G-proteins. We observed that FEZ1 co-localizes with IL7R. HEK293 cells do not express IL7R in a detectable form, such observed in lymphocyte no adherent cell lines. Furthermore, lymphocytes do not enable the perfect immuno-localization for endoplasmic reticulum and cytoskeleton analysis. Our analysis were possible because we used a co-transfection of a construct containing IL7R fused to a V5 epitope and GFP-FEZ1 constructs, in COS7 and HEK293 adherent cells (Figure 2).

We observed the typical vesicle formation and accumulation of IL7-R in the perinuclear Golgi apparatus and in the cytoplasm of control cells (Figure 2A). Surprisingly, IL7R showed a perfect merge with GFP-FEZ1(1-227) but not with GFP-FEZ1(221-392) after co-transfection in COS-7 cells. We can observe that GFP-FEZ1(1-227) exhibits a perfect merge with IL7R in the cytoplasmic reticulum web.

These results allow us to speculate that FEZ1 may act in the transport of IL7R from the Golgi complex to the cell membrane.

The PI3K activity affects the formation of flower like nuclei in HEK293 cells.

Previous work showed that the activation of PI3K pathway causes the formation of flower like cells in cancer patients [12]. Other work showed that the formation of flower like is linked to resistance to chemotherapeutic agents [10]. Here we show that the inhibition of the PI3K activity causes alterations in the typical flower like phenotype mediated by FEZ1 over-expression. As observed in Figure 3, after treatment with PI3K inhibitor for 12h, flower like nuclei show a significant regression to the normal nuclei, similar to observed with the addition of nocodazole [8] (Figure 3A e 3B). After the treatment, the number of cells containing perfect flower like nuclei reduced from 37% and 48%, to 11% of the total transfected cells (Figure 3 graphic). Probably FEZ1 action in the microtubule spindle is affected, causing the alterations in the

phenotype. These results suggest that the PI3K activation is involved in the formation of flower cells mediated by FEZ1 over-expression.

The PKC pathway affects the number of flower like cells, and the cellular localization of the GFP-FEZ1(221-392).

FEZ1 is phosphorylated by different PKC isoforms, and the major sites for phosphorylation are present in its C-terminal region. The phosphorylation of FEZ1 for PKCζ causes its translocation form the cell membrane to the cytoplasm [2]. Here we observed that the addition of PMA (PKC activator) or Staurosporine (St - PKC inhibitor), cause respectively an increase and decrease of the number of cells that presented the flower like nuclei mediated by GFP-FEZ1 over-expression (Figure 4). PMA or St was added 42 h after the transfection and 5-6 h after PMA and St addition the effects were detected (Figure 4 A). After PMA treatment the number of flower like cells increase form 33%, observed in control, to 48% of the total of transfected cells. The treatment with St for a same time causes the opposite, with a small reduction of the flower like cells from 33% to 23% of the total transfected cells (Figure 4 graphic).

Our results permit to speculate that the activation of PMA may cause FEZ1 availability to interact with microtubuli, and consequently an increase in the incidence of flower like nuclei.

In agreement with our previous results that showed that the major phosphorylation PKC sites are in the C-terminal region of FEZ1 [7] we observed that PMA and St treatments affects the cellular localization of GFP-FEZ1(221-392) (Figure, 4 B) but does not influences the cellular localization of GFP-FEZ1(1-227) (not show). PMA and St are added 42 hours after transfection causes alterations in the proportion of different localization patterns observed after GFP-FEZ1(221-392) expression in COS7 cells. This fragment shows three typical localizations/phenotypes which we called here (1) “perinuclear cluster”, that indicate a single cluster in a perinuclear fashion without other points in the cytoplasm observed in 67% of transfected cells, (2) “dotted” that represents a dotted localization in all cell extension and a expressive perinuclear location observed in 14% of transfected cells, and (3) “diffuse”, that represent the protein in a diffuse form around the cell, possibly associated to cell membrane, observed in 18% of the transfected cells. After PMA treatment for 5 hours, the proportion of the dotted phenotype is increased from 14% to 48% of the total of transfected cells, and the

perinuclear cluster and diffuse phenotypes reduce from 67% to 42% and 18% to 11% respectively. We observed also that after St treatment the opposite occurs, with increase in the proportion of phenotype diffuse from 18% to 30% of the total transfected cells number. However a significant reduction of dotted phenotype was not observed.

Flower like cells are observed in cancer cells infiltrated in the Central Nervous System of children with leukemia, and FEZ1 expression increase in infiltrated cells.

The infiltration of leukemic cells from bone marrow to CNS is a relatively rare event, and occurring only in a small fraction of the number of patients with Acute Limphoblastic Leukemia ALL). We investigate the presence of flower like cells in the database samples of seven ALL patients of the Hospital Infantil Boldrini located in Campinas, SP, Brazil.

Three typical phenotypes were identified: cells with normal nuclei, jagged nuclei, and flower like nuclei (figure 5A). These two final phenotypes do not occur in normal lymphocytes. Normal and jagged nuclei were observed in the bone marrow and liquor from patients but curiously we observed cells with flower like nuclei only in the liquor and never in the bone marrow in all seven patients analyzed. The major number of flower like cells detected in one of the seven patients were 38,46% of the total cells counted in the liquor. The patient with the small number showed 0,75% of the total number of cells counted in the liquor. The Figure 5 B shows that in mean, 65,53% of cells infiltrated in CNS showed normal nuclei, 17,51% showed jagged nuclei and 16,96% showed flower like nuclei. In the bone marrow we can observed only cells with normal nuclei (97,32%) and a small number of cells with jagged nuclei (2,68%).

To investigate if FEZ1 is present or altered in the cells of the leukemic patients, we obtained a sample from bone marrow and liquor of one patient. The RT-PCR analysis revealed that FEZ1 mRNA was increased 8 times in liquor cells when compared with the bone marrow cells. Its important to note that in this patient not all cells in the liquor contains flower like nuclei, so, the FEZ1 expression in the flower cells may be under estimated.

Other immunocytochemical analysis using the same sample and a commercial antibody revealed a typical pointed endogenous FEZ1 localization in a perinuclear region in leukemic lymphocytes from patient liquor.

Conclusions

The IL7 activates the PI3K cascade in lymphocytes, and previous works showed that PI3K activation is necessary to formation of flower like nuclei patients of ATLL [12]. Here we show that the flower like mediated by FEZ1 is affected by inhibition of PI3K and PKC activities. These mechanistic similarities suggest that FEZ1 could be involved in the flower like formation in leukemic patients.

Furthermore, different fragments of FEZ1 show distinct cellular localizations related to cell regions devoted to vesicular transport and FEZ colocalizes with IL7R in a perinuclear region. Probably FEZ1 actuates in the transport of IL7R to the cell membrane.

The flower like lymphocytes were observed only in liquor from ALL patients. The liquor, has characteristics of a nervous system microenvironment, and may contain several activators that favoring FEZ1 expression. In agreement, we observed FEZ1 overexpression in cells of liquor of one patient. Our results provide the initial evidences that FEZ1 over-expression maybe causes the flower like phenotype in cancer cells, and that this phenotype is influenced by PI3K and PKC pathways.

References

[1] L. Bloom, H.R. Horvitz, The Caenorhabditis elegans gene unc-76 and its human homologs define a new gene family involved in axonal outgrowth and fasciculation, Proc. Natl. Acad. Sci. 94 (1997) 3414–3419.

[2] S. Kuroda, N. Nakagawa, C. Tokunaga, K. Tatematsu, K. Tanizawa, Mammalian homologue of the Caenorhabditis elegans UNC-76 protein involved in axonal outgrowth is a protein kinase C zeta-interacting protein, J. Cell Biol. 114 (1999) 403–411.

[3] S. Matsuzaki, M. Tohyama. Molecular mechanism of schizophrenia with reference to disrupted-in-schizophrenia 1 (DISC1). Neurochem Int. (2007) 51:165-72.

[4] T.L. Blasius, D. Cai, G.T. Jih, C.P. Toret, K.J. Verhey, Two binding partners cooperate to activate the molecular motor Kinesin-1, J. Cell Biol. 176 (2007) 11–17.

[5] J. Ikuta, A. Maturana, T. Fujita, T. Okajima, Kenji, Tatematsu, K. Tanizawa, S. Kuroda, Fasciculation and elongation protein zeta-1 (FEZ1) participates in the polarization of hippocampal neuron by controlling the mitochondrial motility, Biochem. Biophys. Res. Commun. 353 (2007) 127–132.

[6] N. Sakae, N. Yamasaki, K. Kitaichi, T. Fukuda, M.Yamada, H. Yoshikawa, T. Hiranita, Y. Tatsumi, J. Kira, T. Yamamoto, T. Miyakawa, K. I. Nakayama. Mice lacking the schizophrenia-associated protein FEZ1 manifest hyperactivity and enhanced responsiveness to psychostimulants. Hum Mol Genet 17 (2008) 3191-203.

[7] D. C. Lanza , J. C. Silva, E. M. Assmann, A. J. Quaresma, G.C. Bressan, I. L. Torriani, J. Kobarg. Human FEZ1 has characteristics of a natively unfolded protein and dimerizes in solution. Proteins. 74 (2009) 104-21.

[8] D. C. Lanza, D.M. Trindade, E. M. Assmann, J. Kobarg. Over-expression of GFP-FEZ1 causes generation of multi-lobulated nuclei mediated by microtubules in HEK293 cells. Exp Cell Res. 314 (2008) 2028-39.

[9] Y. Nakayama, N. Yamaguchi, Multi-lobulation of the nucleus in prolonged S phase by nuclear expression of Chk tyrosine kinase, Exp. Cell Res. 304 (2005) 570–581.

[10] J. Huang, P. Sweet, L.M. Slater, A.C. Sartorelli, M.F. Leung, Microtubule dependent multilobular organization of the nucleus in sensitive and multidurg-resistant L0 leukemia cells, Cancer Lett 106 (1996) 29–41.

[12] R. Fukuda, A. Hayashi, A. Utsunomiya, Y. Nukada, R. Fukui, K. Itoh, K. Tezuka, K. Ohashi, K. Mizuno, M. Sakamoto, M. Hamanoue, T. Tsuji, Alteration of phosphatidil 3-kinase cascade in the multilobulated nuclear formation of adult T cell leukemia/lymphoma (ATLL), Proc. Natl. Acad. Sci. 102 (2005) 15213–15218.

[13] Y. Sato, N. Hachiya, H. Kuno, T. Asoh, K. Oizumi, Cerebrospinal fluid atypical lymphocytes in Japanese encephalitis, J. Neurol. Sci. 160 (1998) 92–95.

[14] M. Kikuchi, E. S. Jaffe, Ralfkiaer, E. in *Pathology and Genetics of Tumors of Haemopoietic and Lymphoid Tissues*, (2001) eds. Jaffe, E. S., Harris, N. L.,Stein, H. & Vardiman, J. W. (IARC Press, Lyon), p00–203.

[15] M. J. Palmer, V. S. Mahajan, L. C. Trajman, D. J. Irvine, D. A. Lauffenburger, J. Chen. Interleukin-7 receptor signaling network: an integrated systems perspective. Cell. Mol. Immunol. 5 (2008) 79-89.

[16] D. M. Araujo, C. W. Cotman. Trophic effects of interleukin-4, -7 and -8 on hippocampal neuronal cultures: potential involvement of glial-derived factors. Brain Res. 600 (1993) 49-55.

[17] M. F. Mehler, R. Rozental, M. Dougherty, D. C. Spray, J. A. Kessler. Cytokine regulation of neuronal differentiation of hippocampal progenitor cells. Nature. 362 (1993) 62-5.

[18] M. D. Michaelson, M. F. Mehler, H. Xu, R.E. Gross, J. A. Kessler. Interleukin-7 is trophic for embryonic neurons and is expressed in developing brain. Dev Biol. 179 (1996) 251-63.

[19] E.M. Assmann, M.R. Alborghetti, M.E.R. Camargo, J. Kobarg, FEZ1 dimerization and interaction with transcription regulatory proteins involves its coiled-coil region, J. Biol. Chem. 15 (2006) 9869–9881.

Legends of figures

Figure 1: FEZ1 different regions show different subcellular localizations that indicates roles in association of microtubule with vesicular transport mechanisms. (A) FEZ1 full-length showed diffuse expression pattern in COS7 cells. FEZ1(1-227) and FEZ1(221-392) fragments showed different nondiffuse subcellular localizations, as expected to endoplasmic reticulum and Golgi Complex respectively. (B) GFP alone control shows a diffuse localization and validate the specific localization of GFP-FEZ1 constructs. (C) GFP-FEZ1(1-227) localization accompanying and colocalizes with microtubule spindle in some regions, as expected for endoplasmic reticulum markers. In details the region inside the rectangle shows the GFP-FEZ1(1-227) network accompanying the microtubules marked in red.

Figure 2: GFP-FEZ1(1-227) but not GFP-FEZ1(221-392) co-localizes with IL7R in cellular regions candidates to endoplasmic reticulum. (A) Cells co-transfected with GFP and IL7R reveals that the typical IL7R cell localization is not affected by GFP expression, and that these proteins not show a specific co-localization pattern. (B) GFP-FEZ1(227) shows a perfect merge with IL7R in a perinuclear region and in the endoplasmic reticulum cytoplasmic network. In detail the cytoplasmic reticulum network. (C) GFP-FEZ1(221-392) not show co-localization with IL7R in a perinuclear region. In detail a putative Golgi region containing GFP-FEZ1(221-392) (green) and IL7R in some vesicles (red).

Figure 3: The inhibition of PI3K activity disrupts the typical flower like nuclei mediated by over-expression of GFP-FEZ1(1-392). After the treatment with PI3K inhibitor, the percentage of cells with the typical flower like nuclei observed in A decreased. The regression of the phenotype can be observed in B. The graphic bars were obtained from a mean of tree independent

experiments and represent the number of cells with normal nuclei and with a typical flower like nuclei after each treatment.

Figure 4: The activation or inhibition of PKC by PMA and Staurosporine respectively, affects the percentage of GFP-FEZ1(1-392) transfected cells that exhibits flower like nuclei, possibly by actuation in the FEZ1 C-terminal region. (A) The treatments with PMA and Staurosporine causesincrease or decrease in the number of HEK293 cells with flower like nuclei respectively. (B) The same treatments cause alterations in the subcellular localization of GFP-FEZ1(221-392). The proportion of tree phenotypes observed 48h after transfection is affected according to each treatment. The graphic bars represent the number of normal cells and flower like cells after each treatment and were obtained from a mean of tree independent experiments.

Figure 5: The flower like phenotype is observed in leukemic lymphocytes only when occur infiltration in the Central Nervous system of child patients. (A) Different nuclei morphology observed in childhood leukemia lymphocytes. (B) The flower like nuclei were observed only in lymphocytes infiltrated in the CNS. The bars in the graphic were obtained from a mean after counting the cells of seven patients, and represent the number of normal cells, jagged cells, and flower like cells found in bone marrow or liquor. (C) FEZ1 protein was identified in cells of this same patient using the immunofluorescence technique. (D) Relative quantification assay showed increase of FEZ1 mRNA in cells of CNS, when compared to FEZ1 mRNA in bone marrow cells of the unique patient analyzed.

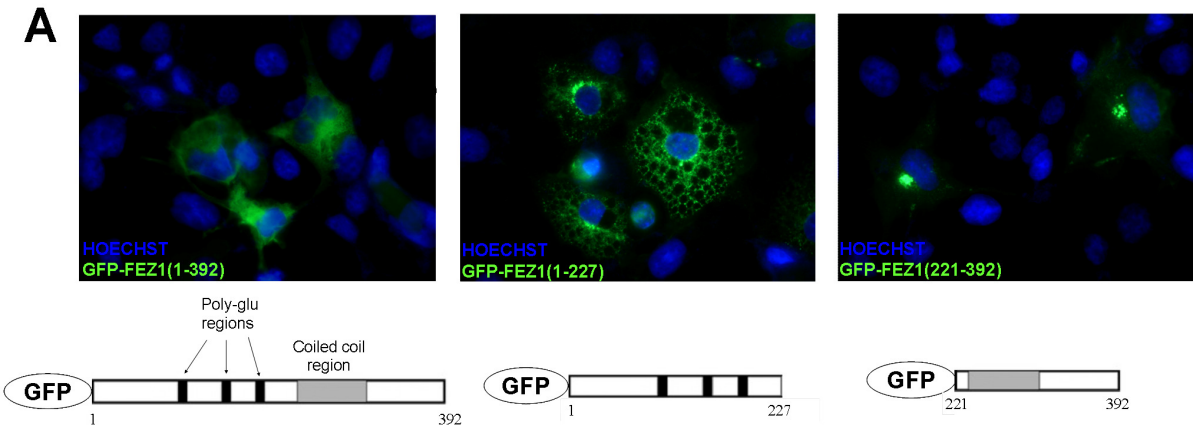
A
HOECHST
GFP-FEZ1(1-392)
HOECHST
GFP-FEZ1(1-227)
HOECHST
GFP-FEZ1(221-392)
Poly-glu regions
Coiled coil region
GFP
1
392
GFP
1
227
GFP
221
392

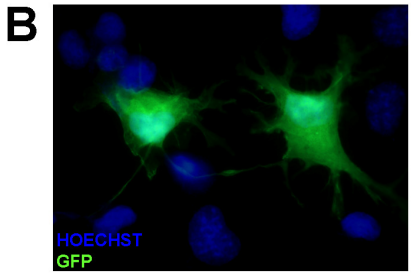
B
HOECHST
GFP

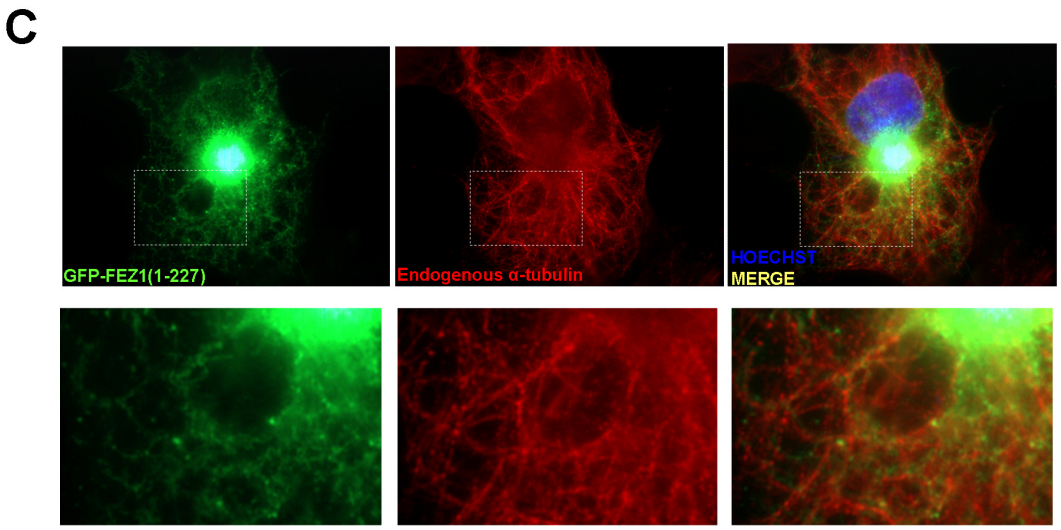
C
GFP-FEZ1(1-227)
Endogenous α-tubulin
HOECHST
MERGE

FIGURE1

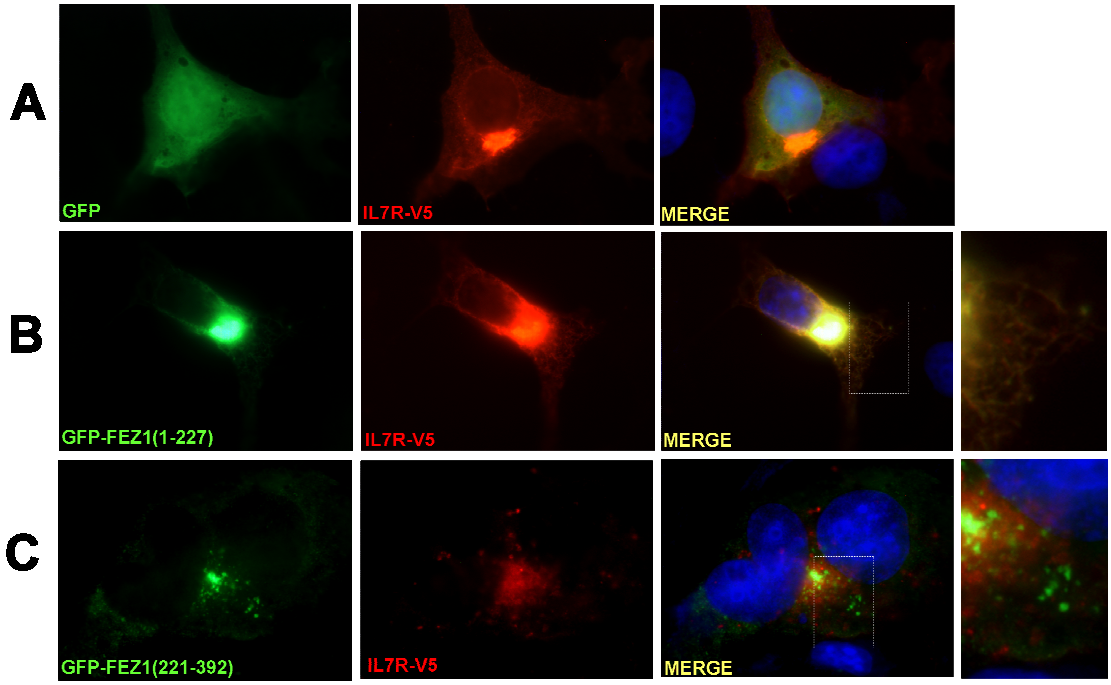
A
GFP
IL7R-V5
MERGE
B
GFP-FEZ1(1-227)
IL7R-V5
MERGE
C
GFP-FEZ1(221-392)
IL7R-V5
MERGE

FIGURE 2

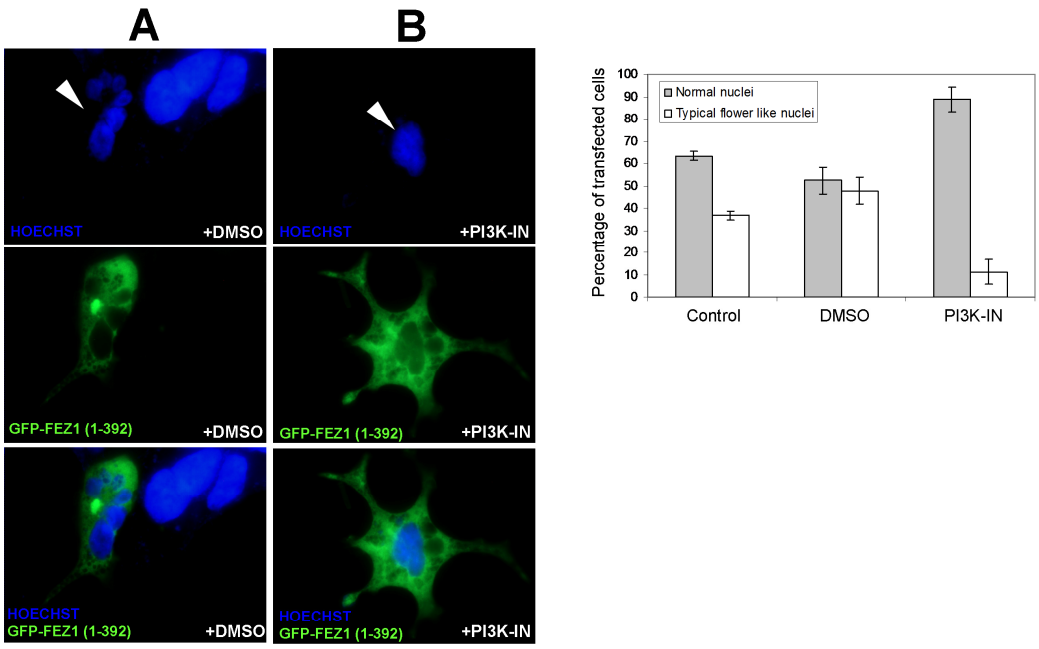
A
B
HOECHST
+DMSO
HOECHST
+PI3K-IN
GFP-FEZ1 (1-392)
+DMSO
GFP-FEZ1 (1-392)
+PI3K-IN
HOECHST
GFP-FEZ1 (1-392)
+DMSO
HOECHST
GFP-FEZ1 (1-392)
+PI3K-IN
Percentage of transfected cells
Normal nuclei
Typical flower like nuclei
100
90
80
70
60
50
40
30
20
10
0
Control
DMSO
PI3K-IN

FIGURE 3

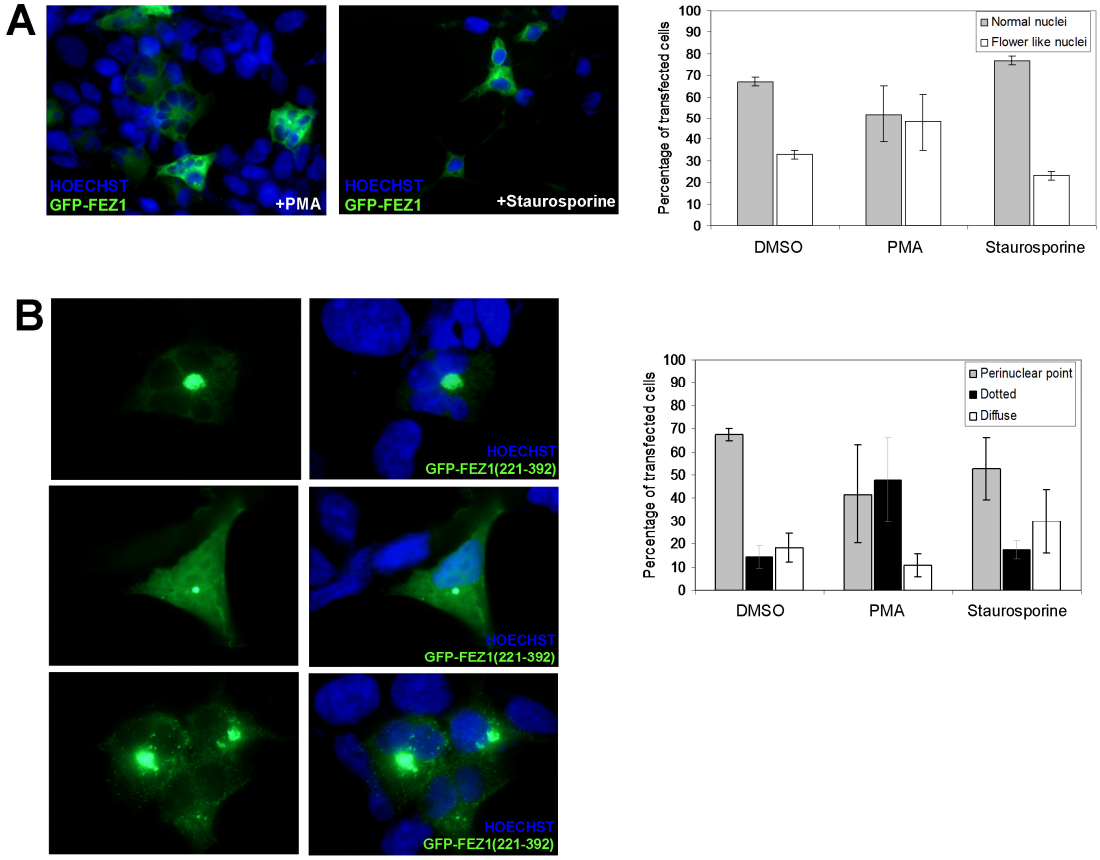
A
HOECHST
GFP-FEZ1
+PMA
HOECHST
GFP-FEZ1
+Staurosporine
Percentage of transfected cells
Normal nuclei
Flower like nuclei
DMSO
PMA
Staurosporine
B
HOECHST
GFP-FEZ1(221-392)
HOECHST
GFP-FEZ1(221-392)
HOECHST
GFP-FEZ1(221-392)
Percentage of transfected cells
Perinuclear point
Dotted
Diffuse
DMSO
PMA
Staurosporine

FIGURE 4

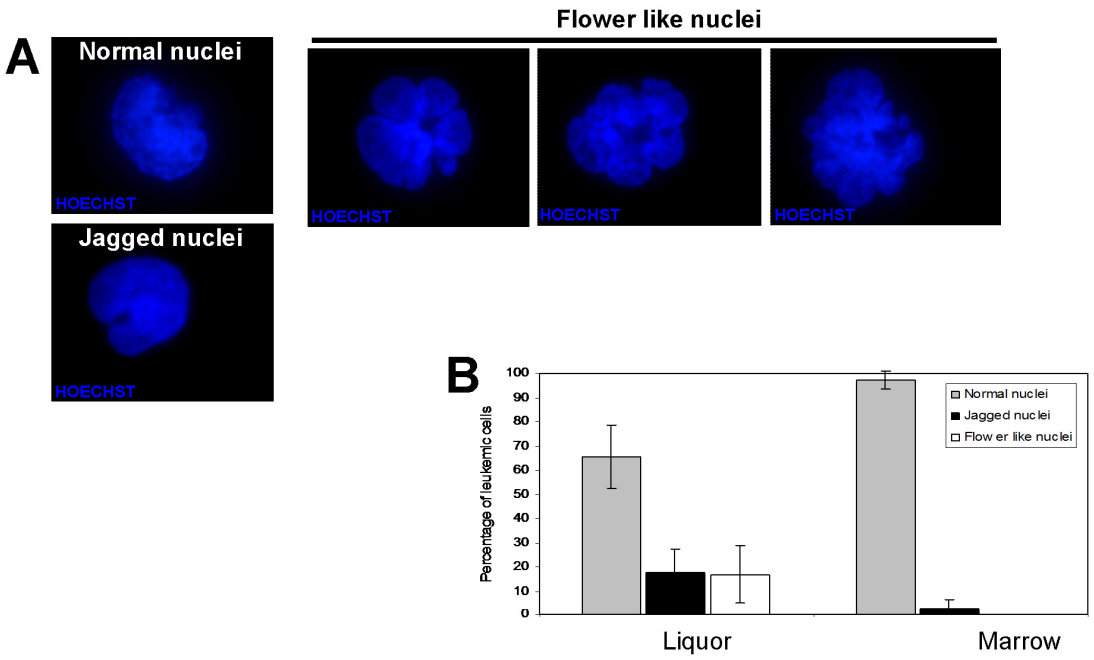
A
Normal nuclei
HOECHST
Jagged nuclei
HOECHST
Flower like nuclei
HOECHST
HOECHST
HOECHST
B
Percentage of leukemic cells
100
90
80
70
60
50
40
30
20
10
0
Normal nuclei
Jagged nuclei
Flow er like nuclei
Liquor
Marrow

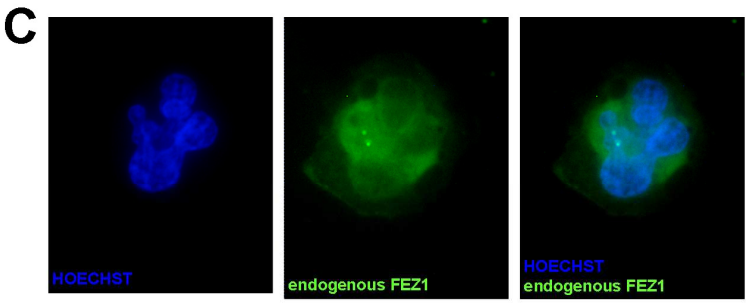
C
HOECHST
endogenous FEZ1
HOECHST
endogenous FEZ1

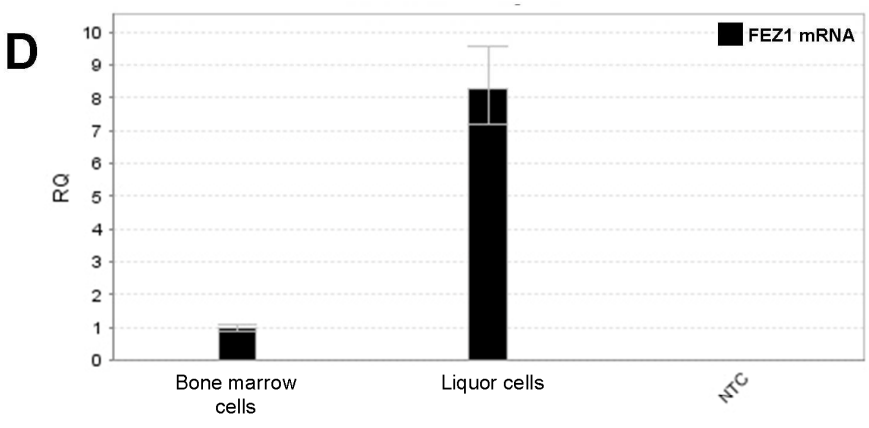
D
FEZ1 mRNA
RQ
10
9
8
7
6
5
4
3
2
1
0
Bone marrow cells
Liquor cells
NTC

FIGURE 5

4-CONCLUSÕES

ARTIGO 1

1. FEZ1 dimeriza em sua região N-terminal e apresenta uma grande região intrinsecamente desenovelada. A estrutura de FEZ1 é muito móvel.
2. O espectro de dicroísmo circular indica a existência de pequena quantidade de alfa hélice na região C-terminal da proteína. Esse resultado condiz com as predições computacionais que indicam a presença de uma região *coiled-coil* na porção C-terminal de FEZ1.
3. FEZ1 endógena é proteolizada, assim como FEZ1 recombinante, o que indica que a ausência de estrutura é uma característica da proteína em condições celulares.
4. A maioria dos sítios de fosforilação para diferentes isoformas de PKC se encontra na região C-terminal de FEZ1.
5. A dimerização de FEZ1 é independente de sua região C-terminal e do *status* de fosforilação em que a proteína se encontra.
6. A fosforilação de FEZ1 por PKCζ não causa alterações estruturais detectáveis por dicroísmo circular e espectroscopia de fluorescência.
7. A fosforilação de FEZ1 por PKCζ diminui a sua capacidade de interagir com a proteína CLASP2.

ARTIGO 2

1. FEZ1 apresenta sinais de localização nuclear e GFP-FEZ1 está presente nas frações solúvel e insolúvel do citoplasma e do núcleo celular, quando superexpressa em células HEK293.
2. A superexpressão de FEZ1 inteira causa a formação de núcleos multilobulados (*flower like*) em células humanas. O fenótipo não é observado quando o fragmento N-teminal de FEZ1 é superexpresso.
3. FEZ1 interage e colocaliza com α e γ tubulinas em células de mamífero.

4. O fenótipo *flower like* ocorre em decorrência da atuação de FEZ1 nos microtúbulos, e possivelmente é causado pela formação de *loops* de microtúbulos mediados pelo excesso de FEZ1, que comprimem o núcleo.
5. O fenótipo *flower like* não afeta as fases do ciclo celular de forma detectável em experimentos de FACS.

ARTIGO 3

1. As proteínas CLASP2 e NEK1 interagem com a região C-terminal de FEZ1 por meio de regiões *coiled-coil*.
2. CLASP2 (1192-1407) e NEK1 endógena colocalizam e interagem com γ-tubulina em uma região candidata ao centrossomo, em células HEK293.
3. FEZ1 colocaliza com NEK1 endógena e com CLASP2(1192-1407) de forma pontuada em uma região perinuclear candidata ao centrossomo em células COS-7 e HEK293 respectivamente.
4. CLASP2 (1046-1407) é fosforilada por diferentes isoformas de PKC *in vitro* e interage com diferentes isoformas de PKC ativa em nível endógeno, o que indica a fosforilação *in vivo*.

ARTIGO 4

1. Diferentes fragmentos de FEZ1 apresentam diferentes localizações sub-celulares e associação a microtúbulos, o que indica atuação em mecanismos de transporte molecular/vesicular.
2. FEZ1 colocaliza com IL7R em uma região perinuclear, em uma estrutura candidata a ser o retículo endoplasmático, o que propõe um possível mecanismo de carreamento desse receptor mediado por FEZ1 até a membrana plasmática.
3. A inibição da atividade de PI3K causa diminuição no número de células com núcleos *flower like* mediados pela superexpressão de FEZ1.

4. A ativação e a inibição da proteína PKC influencia na formação de núcleos *flower like* mediados pela superexpressão de FEZ1 indicando que o *status* de fosforilação de FEZ1 influencia na formação do fenótipo.
5. Blastos leucêmicos com núcleos *flower like* são observados no líquor de pacientes de leucemia, e não são identificados em blastos leucêmicos na medula óssea.
6. A análise de amostras celulares da medula e do líquor de um paciente revelou a expressão aumentada do mRNA de FEZ, aproximadamente oito vezes maior em blastos do líquor quando comparada a expressão de blastos da medula. Foi observado típico padrão de localização subcelular de FEZ1 em células desse mesmo paciente.

5-CONSIDERAÇÕES FINAIS

A ausência de estrutura rígida observada em FEZ1, e a dimerização na região N-terminal com liberação das duas regiões C-terminais contendo o domínio *coiled-coil* para interação com outras proteínas, condizem com resultados prévios que mostram a região C-terminal de FEZ1 como a principal região para interação com outras proteínas (ARTIGO1). A observação dos sítios de fosforilação para PKC na região C-terminal indica um dos mecanismos de regulação, pertinente com a grande quantidade de interações diferentes possíveis naquela mesma região. É interessante que o *status* de fosforilação de FEZ1 não afete de forma detectável a sua estrutura, entretanto controla sua capacidade em interagir com CLASP2.

Observamos versatilidade das interações via regiões *coiled-coil* entre FEZ1, NEK1 e CLASP2 (ARTIGO3). De forma intrigante, apenas a região correspondente a um dos *coiled-coils* preditos na C-terminal de FEZ1 é capaz de interagir com regiões *coiled-coil* de NEK1 e CLASP2. É curioso como uma região pequena e estruturalmente estável tem a versatilidade suficiente para mediar interações com proteínas diferentes. Esse fato associado à regulação por fosforilação e dimerização de FEZ1 se traduz em inúmeras possibilidades de interação, o que mais uma vez condiz com a alegação de que FEZ1 atue como *Hub*.

Sem dúvida, um dos resultados mais interessantes e inesperados desse trabalho, é a capacidade de FEZ1 em causar o fenótipo *flower like*. Os nossos resultados de SAXS e *pull down* (ARTIGO1) associados ao trabalho anterior do nosso grupo [24] indicam que FEZ1 é capaz de

interagir consigo mesma pelas regiões N e C-terminal. Confirmamos através de microscopia eletrônica (dados não mostrados) que em alta concentração FEZ1 pode formar redes e pequenos filamentos, que poderiam atuar como pontes ligando microtúbulos. Possivelmente essa ligação inespecífica afeta a organização dos microtúbulos causando o fenótipo *flower like* conforme demonstrado no ARTIGO2. Mais surpreendente, foi observar que a formação de um fenótipo tão drástico, não causa alterações detectáveis no ciclo celular. Em um primeiro momento especulamos que possivelmente ocorra um pequeno atraso, ou que células *flower like* morram em diferentes etapas do ciclo, de forma a não alterar significativamente a proporção de células em cada fase. Mas ao observarmos que esse fenótipo existe em células leucêmicas, passamos a considerar a possibilidade de uma célula *flower like* ser estável o suficiente para se dividir. As dúvidas a respeito dos fatores controladores do fenótipo motivaram estudos que irão gerar o ARTIGO4.

A existência de células *flower like* apenas no líquor de pacientes acometidos por leucemia, associada a estudos que demonstram que células *flower like* são resistentes a quimioterápicos, motivou em nós uma busca para descobrir qual o "fator causador" desse fenótipo nos pacientes. A obtenção de células do líquor para análise é um desafio, tendo-se em vista que é um evento relativamente raro e a extração via punção lombar é um procedimento doloroso para crianças, que deve ser realizado apenas para obtenção de células para diagnóstico médico. Apesar disso conseguimos amostras de um paciente, e identificamos aumento na expressão de FEZ1 em células do líquor.

Paralelamente aos estudos em pacientes, o estudo da localização celular de diferentes fragmentos de FEZ1 demonstrou que ela pode atuar em mecanismos de transporte vesicular, e possivelmente pode atuar no transporte IL7R para a membrana celular (ARTIGO4). A existência de IL7R em neurônios já é conhecida a algum tempo, entretanto, a função desse receptor em células neuronais ainda não foi elucidada.

Esses dados ficam mais interessantes ao observarmos que IL7R é um ativador da proteína PI3K. A inibição de PI3K causa regressão no fenótipo *flower like* mediado por FEZ1 (ARTIGO4), e outro trabalho demonstra que essa proteína ativa é importante para formação do *flower like* em células de pacientes acometidos por ATLL [113]. Certamente mais estudos são necessários para confirmar a atuação de FEZ1 na formação do fenótipo *flower like* em câncer, o que temos são apenas as primeiras evidências.

A nossa hipótese é que com a migração das células da medula óssea para o líquor, um microambiente tipicamente do sistema nervoso, ocorra sinalização e ativação de vias que acarretem a expressão ectópica de FEZ1 nos linfócitos. Com isso ocorre a formação das células *flower like*, que por sua vez podem ser mais resistentes a quimioterápicos, o que aumenta a agressividade do câncer. O mecanismo seria retroalimentado pelo aumento no transporte de IL7R para membrana mantendo/aumentando a viabilidade celular e a formação de núcleos multilobulados.

5-REFERÊNCIAS BIBLIOGRÁFICAS

[1] Niell CM, Smith SJ. Live optical imaging of nervous system development. Annu Rev Physiol (2004) 66:771-98.

[2] Bloom L, Horvitz HR. The Caenorhabditis elegans gene unc-76 and its human homologs define a new gene family involved in axonal outgrowth and fasciculation. Proc Natl Acad Sci USA (1997) 94:3414-9.

[3] Desai C, Garriga G, McIntire SL, Horvitz HR. A genetic pathway for the development of the Caenorhabditis elegans HSN motor neurons. Nature (1988) 336:638-46.

[4] McIntire SL, Garriga G, White J, Jacobson D, Horvitz HR. Genes necessary for directed axonal elongation or fasciculation in *C. elegans*. Neuron (1992) 8:307-22.

[5] Boguski MS, Lowe TM, Tolstoshev CM. dbEST--database for "expressed sequence tags". Nat Genet (1993) 4:332-3.

[6] Gindhart JG, Chen J, Faulkner M, Gandhi R, Doerner K, Wisniewski T, Nandlestadt A. The kinesin-associated protein UNC-76 is required for axonal transport in the Drosophila nervous system. Mol Biol Cell (2003) 14:3356-65.

[7] Brady ST. A novel brain ATPase with properties expected for the fast axonal transport motor. Nature (1985) 317:73-5.

[8] Hirokawa N, Noda Y. Intracellular transport and kinesin superfamily proteins, KIFs: structure, function, and dynamics. Physiol Rev (2008) 88:1089-118.

[9] Miyoshi K, Honda A, Baba K, Taniguchi M, Oono K, Fujita T, Kuroda S, Katayama T, Tohyama M. Disrupted-In-Schizophrenia 1, a candidate gene for schizophrenia, participates in neurite outgrowth. Mol Psychiatry (2003) 8:685-94.

[10] Honda A, Miyoshi K, Baba K, Taniguchi M, Koyama Y, Kuroda S, Katayama T, Tohyama M. Expression of fasciculation and elongation protein zeta-1 (FEZ1) in the developing rat brain. Brain Res Mol Brain Res (2004) 122:89-92.

[11] Kuroda S, Nakagawa N, Tokunaga C, Tatematsu K, Tanizawa K. Mammalian homologue of the Caenorhabditis elegans UNC-76 protein involved in axonal outgrowth is a protein kinase C zeta-interacting protein. J Cell Biol (1999) 144:403-11.

[12] Ono Y, Fujii T, Ogita K, Kikkawa U, Igarashi K, Nishizuka Y. The structure, expression, and properties of additional members of the protein kinase C family. J Biol Chem (1988) 263:6927-32.

[13] Lin D, Edwards AS, Fawcett JP, Mbamalu G, Scott JD, Pawson T. Amammalian PAR-3-PAR-6 complex implicated in Cdc42/Rac1 and aPKC signalling and cell polarity. Nat Cell Biol (2000) 2:540-7.

[14] Joberty G, Petersen C, Gao L, Macara IG. The cell-polarity protein Par6 links Par3 and atypical protein kinase C to Cdc42. Nat Cell Biol (2000) 2:531-9.

[15] Moscat J, Rennert P, Diaz-Meco MT. PKCzeta at the crossroad of NF-kappaB and Jak1/Stat6 signaling pathways. Cell Death Differ (2006) 13:702-11.

[16] Hirai T, Chida K. Protein Kinase Cζ (PKCζ): Activation Mechanisms and Cellular Functions. J Biochem (2003) 133:1-7.

[17] Sakae N, Yamasaki N, Kitaichi K, Fukuda T, Yamada M, Yoshikawa H, Hiranita T, Tatsumi Y, Kira J, Yamamoto T, Miyakawa T, Nakayama KI. Mice lacking the schizophrenia-associated protein FEZ1 manifest hyperactivity and enhanced responsiveness to psychostimulants. Hum Mol Genet (2008) 17:3191-203.

[18] Gundersen GG, Cook TA. Microtubules and signal transduction. Curr Opin Cell Biol (1999) 11:81-94.

[19] Rodriguez OC, Schaefer AW, Mandato CA, Forscher P, Bement WM, Waterman-Storer CM. Conserved microtubule-actin interactions in cell movement and morphogenesis. Nat Cell Biol (2003) 5:599-609.

[20] Kodama A, Lechler T, Fuchs E. Coordinating cytoskeletal tracks to polarize cellular movements. J Cell Biol (2004) 167:203-7.

[21] Schaefer AW, Kabir N, Forscher P. Filopodia and actin arcs guide the assembly and transport of two populations of microtubules with unique dynamic parameters in neuronal growth cones. Cell Biol (2002) 158:139-52.

[22] Huang JD, Brady ST, Richards BW, Stenolen D, Resau JH, Copeland NG, Jenkins NA. Direct interaction of microtubule and actin-based transport motors. Nature (1999) 397:267-70.

[23] Roger B, Al-Bassam J, Dehmelt L, Milligan RA, Halpain S. MAP2c, but not tau, binds and bundles F-actin via its microtubule binding domain. Curr Biol (2004) 14:363-71.

[24] Assmann EM, Alborghetti MR, Camargo ME, Kobarg J. FEZ1 dimerization and interaction with transcription regulatory proteins involves its coiled-coil region. J Biol Chem (2006) 281:9869-81.

[25] Gordon-Weeks PR. Microtubules and growth cone function. J Neurobiol. (2004) 58:70-83.

[26] Akhmanova A, Hoogenraad CC, Drabek K, Stepanova T, Dortland B, Verkerk T, Vermeulen W, Burgering BM, De Zeeuw CI, Grosveld F, Galjart N. Clasps are CLIP-115 and 170 associating proteins involved in the regional regulation of microtubule dynamics in motile fibroblasts. Cell (2001) 104:923-35.

[27] Pereira AL, Pereira AJ, Maia AR, Drabek K, Sayas CL, Hergert PJ, Lince-Faria M, Matos I, Duque C, Stepanova T, Rieder CL, Earnshaw WC, Galjart N, Maiato H. Mammalian CLASP1 and CLASP2 cooperate to ensure mitotic fidelity by regulating spindle and kinetochore function. Mol Biol Cell (2006) 17:4526-42.

[28] Liu Z, Vong QP, Zheng Y. CLASPing microtubules at the trans-Golgi network. Dev Cell (2007) 12:839-40.

[29] Tsvetkov AS, Samsonov A, Akhmanova A, Galjart N, Popov SV. Microtubule-binding proteins CLASP1 and CLASP2 interact with actin filaments. Cell Motil Cytoskeleton (2007) 64:519-30.

[30] Tang BL. Protein trafficking mechanisms associated with neurite outgrowth and polarized sorting in neurons. J Neurochem (2001) 79:923-30.

[31] Cai D, Hoppe AD, Swanson JA, Verhey KJ. Kinesin-1 structural organization and conformational changes revealed by FRET stoichiometry in live cells. J Cell Biol (2007) 176:51-63.

[32] Woźniak MJ, Allan VJ. Cargo selection by specific kinesin light chain 1 isoforms. EMBO Journal (2006) 25:5457-68.

[33] Verhey KJ, Rapoport TA. Kinesin carries the signal. Trends Biochem Sci (2001) 26(9):545-50.

[34] Hirokawa N, Takemura R. Molecular motors and mechanisms of directional transport in neurons. Nat Rev Neurosci (2005) 6:201-14.

[35] Blasius TL, Cai D, Jih GT, Toret CP, Verhey KJ. Two binding partners cooperate to activate the molecular motor Kinesin-1. J Cell Biol (2007) 176:11-7.

[36] Koushika SP. "JIP"ing along the axon: the complex roles of JIPs in axonal transport. Bioessays (2008) 30:10-4.

[37] Suzuki T, Okada Y, Semba S, Orba Y, Yamanouchi S, Endo S, Tanaka S, Fujita T, Kuroda S, Nagashima K, Sawa H. Identification of FEZ1 as a protein that interacts with JC virus agnoprotein and microtubules: role of agnoprotein-induced dissociation of FEZ1 from microtubules in viral propagation. J Biol Chem (2005) 280:24948-56.

[38] Fujita T, Maturana AD, Ikuta J, Hamada J, Walchli S, Suzuki T, Sawa H, Wooten MW, Okajima T, Tatematsu K, Tanizawa K, Kuroda S. Axonal guidance protein FEZ1 associates with tubulin and kinesin motor protein to transport mitochondria in neurites of NGF-stimulated PC12 cells. Biochem Biophys Res Commun (2007) 361:605-10.

[39] Yamazaki H, Nakata T, Okada Y, Hirokawa N. KIF3A/B: a heterodimeric kinesin superfamily protein that works as a microtubule plus end-directed motor for membrane organelle transport. J Cell Biol (1995) 130:1387-99.

[40] Manning BD, Snyder M. Drivers and passengers wanted! the role of kinesin-associated proteins. Trends Cell Biol (2000) 10:281-9.

[41] Ikuta J, Maturana A, Fujita T, Okajima T, Tatematsu K, Tanizawa K, Kuroda S. Fasciculation and elongation protein zeta-1 (FEZ1) participates in the polarization of hippocampal neuron by controlling the mitochondrial motility. Biochem Biophys Res Commun (2007) 353:127-32.

[42] Lee S, Walker CL, Karten B, Kuny SL, Tennese AA, O'Neill MA, Wevrick R. Essential role for the Prader-Willi syndrome protein necdin in axonal outgrowth. Hum Mol Genet (2005) 14:627-37.

[43] Kamiya A, Tan PL, Kubo K, Engelhard C, Ishizuka K, Kubo A, Tsukita S, Pulver AE, Nakajima K, Cascella NG, Katsanis N, Sawa A. Recruitment of PCM1 to the centrosome by the cooperative action of DISC1 and BBS4: a candidate for psychiatric illnesses. Arch Gen Psychiatry. (2008) 65:996-1006.

[44] Kuwako K, Hosokawa A, Nishimura I, Uetsuki T, Yamada M, Nada S, Okada M, Yoshikawa K. Disruption of the paternal necdin gene diminishes TrkA signaling for sensory neuron survival. J Neurosci (2005) 25:7090-9.

[45] Miller NL, Wevrick R, Mellon PL. Necdin, a Prader-Willi syndrome candidate gene, regulates gonadotropin-releasing hormone neurons during development. Hum Mol Genet (2009) 18:248-60.

[46] Taya S, Shinoda T, Tsuboi D, Asaki J, Nagai K, Hikita T, Kuroda S, Kuroda K, Shimizu M, Hirotsune S, Iwamatsu A, Kaibuchi K. DISC1 regulates the transport of the NUDEL/LIS1/14-3-3epsilon complex through kinesin-1. J Neurosci (2007) 27:15-26.

[47] Naghavi MH, Hatziioannou T, Gao G, Goff SP. Over-expression of fasciculation and elongation protein zeta-1 (FEZ1) induces a post-entry block to retroviruses in cultured cells. Genes Dev (2005) 19:1105-15.

[48] Imai A, Nashida T, Shimomura H. mRNA expression of membrane-fusion-related proteins in rat parotid gland. Arch Oral Biol (2001) 46:955-62.

[49] Gao G, Goff SP. Somatic cell mutants resistant to retrovirus replication: intracellular blocks during the early stages of infection. Mol Biol Cell (1999) 10:1705-17.

[50] Goff SP. Genetic control of retrovirus susceptibility in mammalian cells. Annu Rev Genet (2004) 38:61-85.

[51] Frisque RJ, Bream GL, Cannella MT. Human polyomavirus JC virus genome. J Virol (1984) 51:458-69.

[52] Jiang M, Abend JR, Johnson SF, Imperiale MJ. The role of polyomaviruses in human disease (2009) 384:266-73.

[53] Safak M, Barrucco R, Darbinyan A, Okada Y, Nagashima K, Khalili K. Interaction of JC virus agno protein with T antigen modulates transcription and replication of the viral genome in glial cells. J Virol (2001) 75:1476-86.

[54] Resnick J, Shenk T. Simian virus 40 agnoprotein facilitates normal nuclear location of the major capsid polypeptide and cell-to-cell spread of virus. J Virol (1986) 60:1098-106.

[55] Carswell S, Resnick J, Alwine JC. Construction and characterization of CV-1P cell lines which constitutively express the simian virus 40 agnoprotein: alteration of plaquing phenotype of viral agnogene mutants. J Virol (1986) 60:415-22.

[56] Merabova N, Kaniowska D, Kaminski R, Deshmane SL, White MK, Amini S, Darbinyan A, Khalili K. JC virus agnoprotein inhibits in vitro differentiation of oligodendrocytes and promotes apoptosis. J Virol (2008) 82:1558-69.

[57] Matoba T, Orba Y, Suzuki T, Makino Y, Shichinohe H, Kuroda S, Ochiya T, Itoh H, Tanaka S, Nagashima K, Sawa H. An siRNA against JC virus (JCV) agnoprotein inhibits JCV infection in JCV-producing cells inoculated in nude mice. Neuropathology (2008) 28:286-94.

[58] Shinohara T, Nagashima K, Major E. O Propagation of the human polyomavirus, JCV, in human human neuroblastoma cell lines. Virology (1997) 228:269-77.

[59] Stelzl U, Worm U, Lalowski M, Haenig C, Brembeck FH, Goehler H, Stroedicke M, Zenkner M, Schoenherr A, Koeppen S, Timm J, Mintzlaff S, Abraham C, Bock N, Kietzmann S, Goedde A, Toksöz E, Droege A, Krobitsch S, Korn B, Birchmeier W, Lehrach H, Wanker EE. A human protein-protein interaction network: a resource for annotating the proteome. Cell (2005) 122:957-68.

[60] Fields S, Song O. A novel genetic system to detect protein-protein interactions. Nature (1989) 340:245-6.

[61] Gavin AC, Bösche M, Krause R, Grandi P, Marzioch M, Bauer A, Schultz J, Rick JM, Michon AM, Cruciat CM, Remor M, Höfert C, Schelder M, Brajenovic M, Ruffner H, Merino A, Klein K, Hudak M, Dickson D, Rudi T, Gnau V, Bauch A, Bastuck S, Huhse B, Leutwein C, Heurtier MA, Copley RR, Edelmann A, Querfurth E, Rybin V, Drewes G, Raida M, Bouwmeester T, Bork P, Seraphin B, Kuster B, Neubauer G, Superti-Furga G. Functional organization of the yeast proteome by systematic analysis of protein complexes. Nature (2002) 415:141-7.

[62] Uetz P, Giot L, Cagney G, Mansfield TA, Judson RS, Knight JR, Lockshon D, Narayan V, Srinivasan M, Pochart P, Qureshi-Emili A, Li Y, Godwin B, Conover D, Kalbfleisch T, Vijayadamodar G, Yang M, Johnston M, Fields S, Rothberg JM. A comprehensive analysis of protein-protein interactions in Saccharomyces cerevisiae. Nature (2000) 403:623-7.

[63] Ekman D, Light S, Björklund AK, Elofsson A. What properties characterize the hub proteins of the protein-protein interaction network of Saccharomyces cerevisiae? Genome Biol (2006)7:R45.

[64] Borneman AR, Leigh-Bell JA, Yu H, Bertone P, Gerstein M, Snyder M. Target hub proteins serve as master regulators of development in yeast. Genes Dev (2006) 20:435-48.

[65] Batada NN, Hurst LD, Tyers M. Evolutionary and physiological importance of hub proteins. PLoS Comput Biol (2006) 2:e88.

[66] Jeong H, Mason SP, Barabási AL, Oltvai ZN. Lethality and centrality in protein networks. Nature (2001) 411:41-2.

[67] Gursoy A, Keskin O, Nussinov R. Topological properties of protein interaction networks from a structural perspective. Biochem Soc Trans (2008) 36:1398-403.

[68] Han JD, Bertin N, Hao T, Goldberg DS, Berriz GF, Zhang LV, Dupuy D, Walhout AJ, Cusick ME, Roth FP, Vidal M. Evidence for dynamically organized modularity in the yeast protein-protein interaction network. Nature (2004) 430:88-93.

[69] Fraser HB. Modularity and evolutionary constraint on proteins. Nat Genet (2005) 37:351-2.

[70] Fink AL. Natively unfolded proteins. Curr Opin Struct Biol (2005) 15:35-41.

[71] Dosztányi Z, Chen J, Dunker AK, Simon I, Tompa P. Disorder and sequence repeats in hub proteins and their implications for network evolution. J Proteome Res (2006) 5:2985-95.

[72] Haynes C, Oldfield CJ, Ji F, Klitgord N, Cusick ME, Radivojac P, Uversky VN, Vidal M, Iakoucheva LM. Intrinsic disorder is a common feature of hub proteins from four eukaryotic interactomes. PLoS Comput Biol (2006) 2:e100.

[73] Tompa P. Intrinsically unstructured proteins evolve by repeat expansion. Bioessays (2003) 25:847-55.

[74] Dunker AK, Obradovic Z, Romero P, Garner EC, Brown CJ. Intrinsic protein disorder in complete genomes. Genome Inform Ser Workshop Genome Inform (2000)11:161-71.

[75] Patil A, Nakamura H. Disordered domains and high surface charge confer hubs with the ability to interact with multiple proteins in interaction networks. FEBS Lett (2006) 580:2041-5.

[76] Gunasekaran K, Tsai CJ, Kumar S, Zanuy D, Nussinov R. Extended disordered proteins: targeting function with less scaffold. Trends Biochem Sci (2003) 28:81-5.

[77] Chevalier-Larsen E, Holzbaur EL. Axonal transport and neurodegenerative disease. Biochim Biophys Acta (2006) 1762:1094-108.

[78] El-Kadi AM, Soura V, Hafezparast M. Defective axonal transport in motor neuron disease. J Neurosci Res (2007) 85:2557-66.

[79] Matsuzaki S, Tohyama M. Molecular mechanism of schizophrenia with reference to disrupted-in-schizophrenia 1 (DISC1). Neurochem Int (2007) 51:165-72.

[80] Sawa A, Snyder SH Schizophrenia: diverse approaches to a complex disease. Science (2002) 296:692-5.

[81] Lewis DA, Levitt P. Schizophrenia as a disorder of neurodevelopment. Annu Rev Neurosci (2002) 25:409-32.

[82] Millar JK, Wilson-Annan JC, Anderson S, Christie S, Taylor MS, Semple CA, Devon RS, Clair DM, Muir WJ, Blackwood DH, Porteous DJ. Disruption of two novel genes by a translocation co-segregating with schizophrenia. Hum Mol Genet (2000) 9:1415-23.

[83] Blackwood DH, Fordyce A, Walker MT, St Clair DM, Porteous DJ, Muir WJ. Schizophrenia and affective disorders--cosegregation with a translocation at chromosome 1q42 that directly disrupts brain-expressed genes: clinical and P300 findings in a family. Am J Hum Genet (2001) 69:428-33.

[84] Carlsson A, Waters N, Holm-Waters S, Tedroff J, Nilsson M, Carlsson ML. Interactions between monoamines, glutamate, and GABA in schizophrenia: new evidence. Annu Rev Pharmacol Toxicol (2001) 41:237-60.

[85] Gunay-Aygun M, Schwartz S, Heeger S, O'Riordan MA, Cassidy SB. The changing purpose of Prader-Willi syndrome clinical diagnostic criteria and proposed revised criteria. Pediatrics (2001) 108:E92.

[86] Benarroch F, Hirsch HJ, Genstil L, Landau YE, Gross-Tsur V. Prader-Willi syndrome: medical prevention and behavioral challenges. Child Adolesc Psychiatr Clin N Am (2007) 16:695-708.

[87] Salehi AH, Roux PP, Kubu CJ, Zeindler C, Bhakar A, Tannis LL, Verdi JM, Barker PA.NRAGE, a novel MAGE protein, interacts with the p75 neurotrophin receptor and facilitates nerve growth factor-dependent apoptosis. Neuron (2000) 27:279-88.

[88] Lee S, Walker CL, Wevrick R. Prader-Willi syndrome transcripts are expressed in phenotypically significant regions of the developing mouse brain. Gene Expr Patterns (2003) 3:599-609.

[89] Missé D, Gajardo J, Oblet C, Religa A, Riquet N, Mathieu D, Yssel H, Veas F. Soluble HIV-1 gp120 enhances HIV-1 replication in non-dividing CD4+ T cells, mediated via cell signaling and Tat cofactor over-expression. AIDS (2005) 19:897-905.

[90] Fong YW, Zhou Q. Stimulatory effect of splicing factors on transcriptional elongation. Nature (2001) 414:929-33.

[91] Kaniowska D, Kaminski R, Amini S, Radhakrishnan S, Rappaport J, Johnson E, Khalili K, Del Valle L, Darbinyan A. Cross-interaction between JC virus agnoprotein and human immunodeficiency virus type 1 (HIV-1) Tat modulates transcription of the HIV-1 long terminal repeat in glial cells. J Virol (2006) 80:9288-99.

[92] Weber T. Progressive multifocal leukoencephalopathy. Neurol Clin (2008) 26:833-54.

[93] Darbinyan A, Darbinian N, Safak M, Radhakrishnan S, Giordano A, Khalili K. Evidence for dysregulation of cell cycle by human polyomavirus, JCV, late auxiliary protein. Oncogene (2002) 21:5574-81.

[94] Gonzalez-Duarte A, Sullivan S, Sips GJ, Naidich T, Kleinman G, Murray J, Morgello S, Germano I, Mullen M, Simpson D. Inflammatory pseudotumor associated with HIV, JCV, and immune reconstitution syndrome. Neurology (2009) 72:289-90.

[95] Thurnher MM, Thurnher SA, Mühlbauer B, Hainfellner JA, Steuer A, Fleischmann D, Trattnig S, Budka H, Schindler E. Progressive multifocal leukoencephalopathy in AIDS: initial and follow-up CT and MRI. Neuroradiology (1997) 39:611-8.

[96] Surpili MJ, Delben TM, Kobarg J. Identification of proteins that interact with the central coiled-coil region of the human protein kinase NEK1. Biochemistry (2003) 42:15369-76.

[97] Lu KP, Hunter T. Evidence for a NIMA-like mitotic pathway in vertebrate cells. Cell (1995) 81:413-24.

[98] Mahjoub MR, Trapp ML, Quarmby LM. NIMA-related kinases defective in murine models of polycystic kidney diseases localize to primary cilia and centrosomes. J Am Soc Nephrol (2005) 16:3485-9.

[99] Upadhya P, Birkenmeier EH, Birkenmeier CS, Barker JE. Mutations in a NIMA-related kinase gene, Nek1, cause pleiotropic effects including a progressive polycystic kidney disease in mice. Proc Natl Acad Sci U S A. (2000) 97:217-21.

[100] Polci R, Peng A, Chen PL, Riley DJ, Chen Y. NIMA-related protein kinase 1 is involved early in the ionizing radiation-induced DNA damage response. Cancer Res (2004) 64:8800-3.

[101] Shalom O, Shalva N, Altschuler Y, Motro B. The mammalian Nek1 kinase is involved in primary cilium formation. FEBS Lett (2008) 582:1465-70.

[102] Harris PC, Torres VE. Polycystic Kidney Disease. Annu Rev Med (2008) [Epub ahead of print]

[103] Badano JL, Katsanis N. Life without centrioles: cilia in the spotlight. Cell (2006) 125:1228-30.

[104] Marshall WF, Nonaka S. Cilia: tuning in to the cell's antenna. Curr Biol (2006) 16:604-14.

[105] Michaud EJ, Yoder BK. The primary cilium in cell signaling and cancer. Cancer Res (2006) 66:6463-7.

[106] Otto EA, Schermer B, Obara T, O'Toole JF, Hiller KS, Mueller AM, Ruf RG, Hoefele J, Beekmann F, Landau D, Foreman JW, Goodship JA, Strachan T, Kispert A, Wolf MT, Gagnadoux MF, Nivet H, Antignac C, Walz G, Drummond IA, Benzing T, Hildebrandt F. Mutations in INVS encoding inversin cause nephronophthisis type 2, linking renal cystic disease to the function of primary cilia and left-right axis determination. Nat Genet (2003) 34:413-20.

[107] Yoder BK, Hou X, Guay-Woodford LM. The polycystic kidney disease proteins, polycystin-1, polycystin-2, polaris, and cystin, are co-localized in renal cilia. J Am Soc Nephrol (2002) 13:2508-16.

[108] Pradel LC, Bonhivers M, Landrein N, Robinson DR. NIMA-related kinase TbNRKC is involved in basal body separation in Trypanosoma brucei. J Cell Sci (2006) 119:1852-63.

[109] Bradley BA, Quarmby LM. A NIMA-related kinase, Cnk2p, regulates both flagellar length and cell size in Chlamydomonas. J Cell Sci (2005) 118:3317-26.

[110] Wloga D, Camba A, Rogowski K, Manning G, Jerka-Dziadosz M, Gaertig J. Members of the NIMA-related kinase family promote disassembly of cilia by multiple mechanisms. Mol Biol Cell (2006) 17:2799-810.

[111] Whitehouse C, Chambers J, Howe K, Cobourne M, Sharpe P, Solomon E. NBR1 interacts with fasciculation and elongation protein zeta-1 (FEZ1) and calcium and integrin binding protein (CIB) and shows developmentally restricted expression in the neural tube. Eur J Biochem (2002) 269:538-45.

[112] Okumura F, Hatakeyama S, Matsumoto M, Kamura T, Nakayama KI. Functional regulation of FEZ1 by the U-box-type ubiquitin ligase E4B contributes to neuritogenesis. J Biol Chem (2004) 279:53533-43.

[113] R. Fukuda, A. Hayashi, A. Utsunomiya, Y. Nukada, R. Fukui, K. Itoh, K. Tezuka, K. Ohashi, K. Mizuno, M. Sakamoto, M. Hamanoue, T. Tsuji, Alteration of phosphatidil 3-kinase cascade in the multilobulated nuclear formation of adult T cell leukemia/lymphoma (ATLL), Proc. Natl. Acad. Sci 102 (2005) 15213–15218.